J. Plasma Phys. (2025), *vol*. 91, E111
 doi:10.1017/S0022377825100561

Mean-field dynamo as a quantum-like modulational instability

S. Jin[1,2,†] **and I.Y. Dodin**[1,2]

[1]Department of Astrophysical Sciences, Princeton University, Princeton, NJ 08543, USA
[2]Princeton Plasma Physics Laboratory, Princeton, NJ 08540, USA

Corresponding author: S. Jin, s_jin@mit.edu

(Received 28 February 2025; revision received 5 June 2025; accepted 6 June 2025)

Presented here is a novel formulation of the mean-field dynamo as a modulational instability of magnetohydrodynamic (MHD) turbulence. This formulation, termed mean-field wave kinetics (MFWK), is based on the Weyl symbol calculus and allows describing the interaction between the mean fields (magnetic field and fluid velocity) and turbulence without requiring scale separation that is commonly assumed in the literature. The turbulence is described by the Wigner–Moyal equation for the spectrum of the two-point correlation matrix (Wigner matrix) of magnetic-field and velocity fluctuations and depicts the turbulence as an effective plasma of quantum-like particles that interact via the mean fields. Eddy–eddy interactions, which serve as 'collisions' in this effective plasma, are modelled within the standard minimal tau approximation to aid comparison with existing theories. Using MFWK, the non-local electromotive force is calculated for generic turbulence from first principles, modulo the limitations of MFWK. This result is then used to study, both analytically and numerically, the modulational modes of MHD turbulence, which appear as linear instabilities of the said effective quantum-like plasma of fluctuations. The standard α^2-dynamo and other known results are reproduced as special cases. A new dynamo effect is predicted that is driven by correlations between the turbulent flow velocity and the turbulent current.

Key words: astrophysical plasmas, plasma nonlinear phenomena

1. Introduction

1.1. *Background*

The universe abounds with turbulent magnetised plasma (Schekochihin & Cowley 2007). It is now widely accepted that the observed (or inferred) strength of the magnetic fields that thread these astrophysical systems cannot be explained without invoking some kind of turbulent-dynamo process, in which the kinetic energy of the turbulent plasma flows is converted into magnetic energy (Vaĭnshteĭn & Zeldovich 1972; Brandenburg & Subramanian 2005; Federrath 2016; Subramanian 2019).

[†]A classic example is our own Sun, which exhibits a large-scale dipolar magnetic field that reverses polarity on a curious 11-year cycle (Charbonneau 2014; Jones *et al*. 2010).

These magnetic fields are often correlated on scales that are large compared with those of the underlying turbulence, and it is well established that the dynamics of these orderly fields are inextricably linked with the underlying plasma turbulence (Tobias 2021; Brandenburg *et al*. 2023).[1] Still, many aspects of this so-called 'large-scale' turbulent dynamo remain to be understood (Rädler 2014; Hughes 2018).

One of the mainstream tools for studying the large-scale turbulent dynamo has been mean-field electrodynamics (Krause & Rädler 1980; Roberts & Soward 1975; Moffatt 1978; Shukurov & Subramanian 2021). In this approach, the magnetohydrodynamic (MHD) model of interest is decomposed into a system of coupled equations for both the turbulent and mean-field components, and, ultimately, a closed equation is obtained that describes the evolution of the mean magnetic field in response to correlations of the turbulent fluctuations. Mean-field electrodynamics has now profoundly shaped much of our understanding of cosmical dynamos (Hughes 2018), and there have been many refinements to this basic framework over the years (Rädler 2014; Brandenburg 2018). However, two key aspects of the turbulent dynamo continue to pose substantial challenges for the mean-field approach.

The first of these challenges arises from the so-called small-scale dynamo. Historically, the mean-field dynamo problem was one of coherent magnetic fields emerging from a state of hydrodynamic turbulence. This original understanding of the problem justified the kinematic approximation, in which one takes the flows to be prescribed, as the magnetic fields of interest would be too weak to substantially modify these flows, at least in the initial linear growth stage. Within this approximation, one need not consider the full MHD system and can instead focus on the much simpler task of solving the induction equation for a given flow. However, it is now understood that in the astrophysically interesting regime of large magnetic Reynolds number (Rm), the small-scale dynamo generates substantial turbulent magnetic fields on time scales much shorter than those of the large-scale dynamo modes predicted by kinematic mean-field theory (Rincon 2019). It has therefore been suggested that a better-posed mean-field problem is one in which mean fields grow from the MHD turbulence aftermath of a saturated small-scale dynamo (Rincon 2019; Tobias 2021). As will be discussed extensively throughout this paper, for MHD turbulence, the mean magnetic and velocity fields can be dynamically coupled, such that the solution of the full MHD mean-field problem requires a self-consistent mean-field treatment for both the velocity and magnetic fields. Although the importance of such an approach has been recognised (Rincon 2019; Tobias 2021), and some progress has been made – analytically for simple cases as in Courvoisier *et al*. (2010*a*,*b*), and numerically with direct statistical simulations (Mondal & Bhat 2023) – the basic theory of mean-field modes for generic MHD turbulence has been lacking.

Another significant limitation of existing mean-field theories is that most of them rely on the assumption that mean fields vary on much longer scales than the turbulent fields. This assumed separation of scales is used to simplify the problem by enabling a local closure in which the turbulent electromotive force (EMF) at a given point in spacetime is expressed only in terms of the mean fields and their low-order derivatives at that same point in spacetime. However, the assumption of scale separation is often unjustified, and there has been a growing interest in understanding the impact of so-called non-local effects on mean-field dynamics (Hubbard & Brandenburg 2009; Rheinhardt & Brandenburg 2012; Rheinhardt *et al*. 2014;

[1] A classic example is our own sun, which exhibits a large-scale dipolar magnetic field that reverses polarity on a curious 11-year cycle (Jones, Thompson & Tobias 2010; Charbonneau 2014).

https://doi.org/10.1017/S0022377825100561 Published online by Cambridge University Press

Bendre & Subramanian 2022; Pipin 2023; Brandenburg *et al*., 2008; Gressel & Elstner 2020). But thus far, these effects have been studied mostly numerically, and, although some analytical calculations do exist (Rüdiger & Urpin 2001), they have been largely intractable for generic turbulence.

1.2. *Mean-field wave kinetics*

In this paper, we propose a novel approach to the dynamo problem, mean-field wave kinetics (MFWK), that is able to overcome the aforementioned limitations. The MFWK retains the dynamical independence of the turbulent correlations and treats them within the wave-kinetics framework.

To introduce the general idea of wave kinetics, let us first consider a simplified problem where the characteristic wavelength of the turbulent fluctuations is much less than the inhomogeneity scale,

$$l/L \ll 1. \tag{1.1}$$

In this 'geometrical-optics' (GO) limit, waves are much like particles in the sense that they can be described by Hamilton's ray equations (Tracy *et al*. 2014; Dodin 2022),

$$\dot{\boldsymbol{x}} = \partial_{\boldsymbol{k}}\omega, \qquad \dot{\boldsymbol{k}} = -\partial_{\boldsymbol{x}}\omega. \tag{1.2}$$

Here, $\boldsymbol{x}$ is the ray position, $\boldsymbol{k}$ is the local wavevector (which is proportional to the ray's canonical momentum) and ω is the local frequency and serves as the Hamiltonian ray. Wave kinetics therefore refers to the kinetic theory that describes the phase-space dynamics of these quasiparticles.

Turbulence can be viewed as an ensemble of such quasiparticles, with a distribution function in phase space evolving due to wave-wave collisions ('eddy-eddy' interactions) and collective effects (mean fields),

$$\partial_t f = \mathcal{C}[f] + \{H,\, f\}. \tag{1.3}$$

The situation when the collision term $\mathcal{C}[f]$ dominates over $\{H,\, f\}$ corresponds to homogeneous turbulence, where the classic subject of interest is turbulent spectra (Vedenov 1967; Nazarenko 2011). Here, though, we focus on the opposite limit, when $\mathcal{C}[f]$ is negligible compared with the collective interactions determined by $\{H,\, f\}$. This corresponds to the regime where turbulence effectively acts as a collisionless plasma. In this sense, our formulation can be viewed as 'plasma physics of turbulence' (Tsiolis, Zhou & Dodin 2020), and the resulting mean-field theory can be understood as a theory of collective effects in MHD turbulence. Although this approach has been widely used in the past (for an overview and references, see, for example Mendonca (2000), Ruiz (2017) and Zhu & Dodin (2021)), its application to MHD turbulence has been limited on the account of being technically challenging.

In particular, note that the GO approximation is typically not satisfied when the mean-field scales themselves are formed through modulational instabilities (MI) (Zakharov & Ostrovsky 2009; Tsiolis *et al*. 2020; Zhu & Dodin 2021).[2] This means that (1.3) must be replaced with a more general model that does not rely on

[2]Additional background on MI is given in Appendix A.

https://doi.org/10.1017/S0022377825100561 Published online by Cambridge University Press

scale separation. Furthermore, MHD fluctuations are inherently electromagnetic. This means that a proper quantum analogy for them is vector particles (particles with spin) and thus their distribution is a matrix rather than a scalar. The corresponding generalisation of (1.3) can be constructed using the Weyl symbol calculus (Appendix B), or more specifically, the Wigner–Moyal formalism (Weyl 1950), which will be explained in detail in § 2. This formalism provides access to regimes outside the traditional domain of the mean-field theories, yet remains analytically tractable. It depicts turbulence self-organization as a collective instability of an effective quantum-like plasma of turbulent fluctuations, in which mean fields serve as a collective field through which the fluctuations interact. The Wigner–Moyal formalism is also advantageous in that it maintains a clear connection with the GO model (1.3), namely, subsumes it as a limit.

1.3. *Outline*

This paper aims to systematically develop MFWK for MHD turbulence (§§ 2 and 3) and use this theory to study basic physics of dynamo by considering several illustrative examples (§§ 4 and 5). Rather than modelling a specific astrophysical system in detail (a pursuit that does not lack participants), we focus on developing the theoretical framework and exploring its broader implications. We find that even for the simple examples considered here, MFWK predicts qualitatively distinct features compared with previous mean-field theories.

In our first application of MFWK, we derive, from first principles, the non-local response kernel of the turbulent EMF for weak mean fields and generic MHD turbulence. We then evaluate this expression for the special cases of (i) hydrodynamic and (ii) isotropic MHD turbulence. For hydrodynamic turbulence, we find that MFWK theoretically predicts the same generic form of the non-local EMF that has been commonly assumed in the literature based on simulations (Brandenburg *et al*. 2023). For isotropic MHD turbulence, the scale-separated limit of MFWK largely reproduces the predictions of existing mean-field theories with the important exception of the dependence of the EMF on the mean flow. However, we report a qualitatively different dependence of the EMF on the mean flow compared with the only other (to our knowledge) existing calculation of this effect (Rädler & Brandenburg 2010).

In the second application of MFWK, we identify the mean-field effects associated with various statistical properties of homogeneous isotropic MHD turbulence. To do this, we first derive the general dispersion relation of modulational modes of generic MHD turbulence. We then solve the dispersion relation for the specific case of ideal isotropic MHD turbulence. Beyond the well-known α^2-dynamo driven by kinetic helicity, we predict a new dynamo effect that is driven by correlations between the fluctuating flow and current, $\langle \widetilde{\boldsymbol{v}} \cdot \widetilde{\boldsymbol{j}} \rangle$. We also predict sound-like 'correlation waves' that propagate (and, depending on the properties of turbulence, possibly grow) through plasma at speeds determined by the statistical properties of the turbulent fluctuations.

This paper is organised as follows. In § 2, we derive the main equations of MFWK. In § 3, we linearise the MFWK equations around generic turbulent equilibria and formulate mean-field effects in terms of modulational (in)stability. In § 4, we apply the MFWK to derive the non-local turbulent EMF and analyse its properties. In § 5, we derive and solve the dispersion relation of modulational modes for MHD turbulence, and we also characterise the $\langle \widetilde{\boldsymbol{v}} \cdot \widetilde{\boldsymbol{j}} \rangle$-dynamo. The main results are summarised in § 6.

https://doi.org/10.1017/S0022377825100561 Published online by Cambridge University Press

2. Derivation of mean-field wave-kinetics

2.1. *Base model: incompressible resistive MHD*

As a base model, we assume incompressible resistive MHD with homogeneous mass density $\rho = \text{const}$,

$$\partial_t \boldsymbol{v} + (\boldsymbol{v}\cdot\nabla)\boldsymbol{v} = (\boldsymbol{b}\cdot\nabla)\boldsymbol{b} - \nabla P + \nu\nabla^2\boldsymbol{v}, \tag{2.1a}$$

$$\partial_t \boldsymbol{b} = \nabla\times(\boldsymbol{v}\times\boldsymbol{b}) + \eta\nabla^2\boldsymbol{b}, \tag{2.1b}$$

$$\nabla\cdot\boldsymbol{v} = 0, \qquad \nabla\cdot\boldsymbol{b} = 0. \tag{2.1c}$$

Here, $\boldsymbol{v}$ represents the fluid velocity, $\boldsymbol{b} \doteq \boldsymbol{B}/\sqrt{4\pi\rho}$ is the local Alfvén velocity, and the normalised total pressure is defined as $P \doteq (P_{\text{kin}} + B^2/8\pi)/\rho$, with P_{kin} being the kinetic pressure (the symbol $\doteq$ denotes definitions). The viscosity, ν, and resistivity, η, are assumed to be constant. To express (2.1) in a more symmetric form, let us rewrite them in terms of the two Elsässer fields $\boldsymbol{z}^{\pm}$ (Elsasser 1950), which are also solenoidal,

$$\boldsymbol{z}^{\pm} \doteq \boldsymbol{v} \pm \boldsymbol{b}, \qquad \nabla\cdot\boldsymbol{z}^{\pm} = 0. \tag{2.2}$$

This leads to two coupled equations for $\boldsymbol{z}^{\pm}$,

$$\partial_t \boldsymbol{z}^{\pm} = -(\boldsymbol{z}^{\mp}\cdot\nabla)\boldsymbol{z}^{\pm} - \nabla P + \nu_+\nabla^2\boldsymbol{z}^{\pm} + \nu_-\nabla^2\boldsymbol{z}^{\mp}, \tag{2.3}$$

where $\nu_+ \doteq (\nu+\eta)/2$ and $\nu_- \doteq (\nu-\eta)/2$. The normalised total pressure P can be found as follows. By taking the divergence of (2.1*a*) and using (2.2), one obtains

$$\nabla^2 P = -\nabla\cdot[(\boldsymbol{z}^{\mp}\cdot\nabla)\boldsymbol{z}^{\pm}]. \tag{2.4}$$

Let us introduce the wavevector operator $\hat{\boldsymbol{k}} \doteq -\mathrm{i}\nabla$, so $\hat{k}^2 \doteq \hat{\boldsymbol{k}}^2 = -\nabla^2$. Let us also assume some appropriate (say, periodic) boundary conditions. Then, (2.4) yields

$$P = -\hat{k}^{-2}\hat{\boldsymbol{k}}\cdot[(\boldsymbol{z}^{\mp}\cdot\hat{\boldsymbol{k}})\boldsymbol{z}^{\pm}] + \text{const}, \tag{2.5}$$

whence ∇P in (2.3) can be expressed through $\boldsymbol{z}^{\pm}$.

Alternatively, ∇P can be eliminated from (2.3) by taking the curl of this equation,

$$\partial_t \boldsymbol{w}^{\pm} = -\nabla\times[(\boldsymbol{z}^{\mp}\cdot\nabla)\boldsymbol{z}^{\pm}] + \nu_+\nabla^2\boldsymbol{w}^{\pm} + \nu_-\nabla^2\boldsymbol{w}^{\mp}, \tag{2.6}$$

where the Elsässer vorticities $\boldsymbol{w}^{\pm}$ are defined as

$$\boldsymbol{w}^{\pm} \doteq \nabla\times\boldsymbol{z}^{\pm}. \tag{2.7}$$

Indeed, due to (2.2), one can express $\boldsymbol{z}^{\pm}$ using a vector potential $\boldsymbol{a}^{\pm}$ such that $\boldsymbol{z}^{\pm} = \nabla\times\boldsymbol{a}^{\pm}$. Let us assume the gauge such that $\nabla\cdot\boldsymbol{a}^{\pm} = 0$. Then,

$$\boldsymbol{w}^{\pm} = \nabla\times(\nabla\times\boldsymbol{a}^{\pm}) = -\nabla^2\boldsymbol{a}^{\pm} \equiv \hat{k}^2\boldsymbol{a}^{\pm}, \tag{2.8}$$

whence

$$\boldsymbol{z}^{\pm} = \mathrm{i}\hat{k}^{-2}(\hat{\boldsymbol{k}}\times\boldsymbol{w}^{\pm}). \tag{2.9}$$

https://doi.org/10.1017/S0022377825100561 Published online by Cambridge University Press

(Here, we assume that $\boldsymbol{z}^{\pm}$ and their first spatial derivatives have zero spatial average, so $\hat{k}^2$ is invertible.) Then, (2.3) can be expressed through $\boldsymbol{w}^{\pm}$ alone,

$$\partial_t \boldsymbol{w}^{\pm} = -\hat{\boldsymbol{k}} \times \{[(\hat{\boldsymbol{k}} \times \hat{k}^{-2}\boldsymbol{w}^{\mp}) \cdot \hat{\boldsymbol{k}}](\hat{\boldsymbol{k}} \times \hat{k}^{-2}\boldsymbol{w}^{\pm})\} - \hat{k}^2(\nu_+ \boldsymbol{w}^{\pm} + \nu_- \boldsymbol{w}^{\mp}). \tag{2.10}$$

Writing the Elsässer equations in this form has the benefit that the nonlinear term is now expressed as a product of inverse operators that act only on the Elsässer vorticities themselves, rather than an inverse operator that acts on the product of the Elsässer fields as in (2.5). As we will see shortly, this property makes (2.10) more convenient than (2.3) for the eventual formulation of MFWK. Note also that (2.10) is equivalent to (2.6) with the assumption that $\boldsymbol{z}^{\pm}$ and their first spatial derivatives have zero spatial average.

2.2. *Mean fields versus fluctuations*

As in the usual mean-field approach (Krause & Rädler 1980; Moffatt 1978), we decompose our Elsässer fields into mean and fluctuating parts,

$$\boldsymbol{z}^{\pm} = \bar{\boldsymbol{z}}^{\pm} + \widetilde{\boldsymbol{z}}^{\pm}, \qquad \boldsymbol{w}^{\pm} = \overline{\boldsymbol{w}}^{\pm} + \widetilde{\boldsymbol{w}}^{\pm}. \tag{2.11}$$

Inserting (2.11) into (2.6) and averaging yields the following equation for the mean fields:

$$\partial_t \overline{\boldsymbol{w}}^{\pm} = -\boldsymbol{\nabla} \times [(\bar{\boldsymbol{z}}^{\mp} \cdot \boldsymbol{\nabla})\bar{\boldsymbol{z}}^{\pm}] + \nu_+ \nabla^2 \overline{\boldsymbol{w}}^{\pm} + \nu_- \nabla^2 \overline{\boldsymbol{w}}^{\mp} - \langle \boldsymbol{\nabla} \times [(\widetilde{\boldsymbol{z}}^{\mp} \cdot \boldsymbol{\nabla})\widetilde{\boldsymbol{z}}^{\pm}] \rangle. \tag{2.12}$$

(Note that this is similar to (2.6), but has an additional source term due to the fluctuating fields.) Subtracting (2.12) from (2.6) yields the following equation for the fluctuations:

$$\partial_t \widetilde{\boldsymbol{w}}^{\pm} = -\boldsymbol{\nabla} \times [(\bar{\boldsymbol{z}}^{\mp} \cdot \boldsymbol{\nabla})\widetilde{\boldsymbol{z}}^{\pm} + (\widetilde{\boldsymbol{z}}^{\mp} \cdot \boldsymbol{\nabla})\bar{\boldsymbol{z}}^{\pm}] + \nu_+ \nabla^2 \widetilde{\boldsymbol{w}}^{\pm} + \nu_- \nabla^2 \widetilde{\boldsymbol{w}}^{\mp} + \boldsymbol{F}^{\pm}_{\mathrm{NL}}, \tag{2.13}$$

where the nonlinear term

$$\boldsymbol{F}^{\pm}_{\mathrm{NL}} \doteq \langle \boldsymbol{\nabla} \times [(\widetilde{\boldsymbol{z}}^{\mp} \cdot \boldsymbol{\nabla})\widetilde{\boldsymbol{z}}^{\pm}] \rangle - \boldsymbol{\nabla} \times [(\widetilde{\boldsymbol{z}}^{\mp} \cdot \boldsymbol{\nabla})\widetilde{\boldsymbol{z}}^{\pm}] \tag{2.14}$$

corresponds to eddy–eddy interactions.

Within the quasilinear approximation (QLA) (i.e. the collisionless-wave approximation of § 1.2), $\boldsymbol{F}^{\pm}_{\mathrm{NL}}$ is neglected. Although nonlinear effects are, of course, important for understanding the full picture, our present focus is on understanding mean-field formation, many aspects of which can be studied within the QLA (Tsiolis *et al*. 2020; Zhu & Dodin 2021). As discussed in the previous section, this can also be understood as retaining collective effects while neglecting pairwise interactions of the turbulent fluctuations. Deviations from the QLA are discussed extensively by Jin & Dodin (2025).

Although we will proceed with the derivation of MFWK under the QLA, in § 2.5 we will also consider a modified version of the final equations that includes a simple minimal tau approximation (MTA)-like damping term to model the effect of eddy–eddy interactions, $\boldsymbol{F}^{\pm}_{\mathrm{NL}}$.[3]

[3]One can also go beyond the QLA within the Wigner–Moyal approach in a more systematic way, as done for drift-wave turbulence by Ruiz, Glinsky & Dodin (2019).

https://doi.org/10.1017/S0022377825100561 Published online by Cambridge University Press

2.3. *Wigner–Moyal equation for the fluctuations*

2.3.1. Basic notation

Let us first introduce the state ket vectors,

$$|\widetilde{z}\rangle \doteq \begin{pmatrix} |\widetilde{z}^{+}\rangle \\ |\widetilde{z}^{-}\rangle \end{pmatrix}, \qquad |\widetilde{\boldsymbol{w}}\rangle \doteq \begin{pmatrix} |\widetilde{\boldsymbol{w}}^{+}\rangle \\ |\widetilde{\boldsymbol{w}}^{-}\rangle \end{pmatrix}. \tag{2.15}$$

The usual fields over spacetime can be understood as the spatial projections of these kets, i.e. $\langle \boldsymbol{x}|\widetilde{z}^{\pm}\rangle = \widetilde{z}^{\pm}(\boldsymbol{x})$. The fluctuation equation can then be written as a vector Schrödinger equation for $|\widetilde{\boldsymbol{w}}\rangle$,

$$i\,\partial_t|\widetilde{\boldsymbol{w}}\rangle = \hat{\boldsymbol{H}}'|\widetilde{\boldsymbol{w}}\rangle, \tag{2.16}$$

with the (generally non-Hermitian) Hamiltonian,

$$\hat{\boldsymbol{H}}' \doteq \begin{pmatrix} \hat{\boldsymbol{H}}'^{++} & \hat{\boldsymbol{H}}'^{+-} \\ \hat{\boldsymbol{H}}'^{-+} & \hat{\boldsymbol{H}}'^{--} \end{pmatrix}, \tag{2.17}$$

where we have introduced

$$\hat{H}'^{\pm\pm}_{ij} = \delta_{ij}\left(\bar{z}^{\mp}_{l}\hat{k}_l - i\bar{z}^{\mp}_{l,m}\frac{\hat{k}_l\hat{k}_m}{\hat{k}^2} - i\nu_{+}\hat{k}^2\right) + i\bar{z}^{\mp}_{l,m}\frac{\hat{k}_l\hat{k}_m}{\hat{k}^2}, \tag{2.18a}$$

$$\hat{H}'^{\pm\mp}_{ij} = \delta_{ij}\left(i\bar{z}^{\pm}_{l,m}\frac{\hat{k}_l\hat{k}_m}{\hat{k}^2} + \bar{z}^{\pm}_{l,mm}\frac{\hat{k}_l}{\hat{k}^2} - i\nu_{-}\hat{k}^2\right)$$
$$+ i\left(\bar{z}^{\pm}_{j,i} - \bar{z}^{\pm}_{j,l}\frac{\hat{k}_i\hat{k}_l}{\hat{k}^2}\right) + \left(\bar{z}^{\pm}_{j,il} - \bar{z}^{\pm}_{l,ij}\right)\frac{\hat{k}_l}{\hat{k}^2} - \bar{z}^{\pm}_{j,ll}\frac{\hat{k}_i}{\hat{k}^2}. \tag{2.18b}$$

From (2.9) and (2.7), we have

$$|\widetilde{z}\rangle = \mathrm{i}\hat{k}^{-2}\hat{\boldsymbol{k}}_{\wedge}|\widetilde{\boldsymbol{w}}\rangle, \qquad |\widetilde{\boldsymbol{w}}\rangle = \mathrm{i}\hat{\boldsymbol{k}}_{\wedge}|\widetilde{z}\rangle, \tag{2.19}$$

where

$$\hat{\boldsymbol{k}}_{\wedge} \doteq \begin{pmatrix} \hat{\boldsymbol{k}}_{\wedge} & 0 \\ 0 & \hat{\boldsymbol{k}}_{\wedge} \end{pmatrix}, \qquad \hat{\boldsymbol{k}}_{\wedge} \doteq \begin{pmatrix} 0 & -\hat{k}_z & \hat{k}_y \\ \hat{k}_z & 0 & -\hat{k}_x \\ -\hat{k}_y & \hat{k}_x & 0 \end{pmatrix}. \tag{2.20}$$

Using (2.19) and (2.13), (2.16) can then be put in a simpler form for the state vector $|z\rangle$, with Hamiltonian $\hat{\boldsymbol{H}} \doteq \mathrm{i}\hat{k}^{-2}\hat{\boldsymbol{k}}_{\wedge}\hat{\boldsymbol{H}}'\hat{\boldsymbol{k}}_{\wedge}$. Specifically, (2.16) becomes

$$\mathrm{i}\partial_t|\widetilde{z}\rangle = \hat{\boldsymbol{H}}|\widetilde{z}\rangle, \tag{2.21}$$

where $\hat{\boldsymbol{H}}$ is a matrix operator given by

$$\hat{\boldsymbol{H}} = \begin{pmatrix} \hat{\boldsymbol{H}}^{++} & \hat{\boldsymbol{H}}^{+-} \\ \hat{\boldsymbol{H}}^{-+} & \hat{\boldsymbol{H}}^{--} \end{pmatrix}, \tag{2.22}$$

https://doi.org/10.1017/S0022377825100561 Published online by Cambridge University Press

and we have also introduced

$$\hat{H}_{ij}^{\pm\pm} = \delta_{ij}\left(\bar{z}_l^{\mp}\hat{k}_l - \mathrm{i}\nu_+\hat{k}^2\right) + \mathrm{i}\frac{\hat{k}_i}{\hat{k}^2}\bar{z}_{l,j}^{\mp}\hat{k}_l, \tag{2.23a}$$

$$\hat{H}_{ij}^{\pm\mp} = -\delta_{ij}\mathrm{i}\nu_-\hat{k}^2 - \mathrm{i}\bar{z}_{i,j}^{\pm} + \mathrm{i}\frac{\hat{k}_i}{\hat{k}^2}\bar{z}_{l,j}^{\pm}\hat{k}_l. \tag{2.23b}$$

Note that the Hamiltonian $\hat{\boldsymbol{H}}$ is generally not Hermitian (even in the ideal-MHD limit) and is highly non-trivial. Also, because $|\boldsymbol{z}\rangle$ is a multicomponent vector, one can think of the quasiparticles as quantum-like particles with spin, and the 'spin-up' and 'spin-down' components are strongly coupled in the presence of inhomogeneous mean fields.

For homogeneous $\bar{\boldsymbol{z}}^{\pm}$ and vanishing $\nu_{\pm}$, the Hamiltonian (2.22) is diagonal, so $|\tilde{\boldsymbol{z}}^{\pm}\rangle$ decouple. In principle, it can also be diagonalised for two-dimensional (2-D) dynamics when $|\bar{\boldsymbol{b}}| \gg |\bar{\boldsymbol{v}}|$ (Appendix D), such that the corresponding dynamics can be understood in terms of the resulting phase-space trajectories available to quasiparticles. A more detailed investigation of the properties of the Hamiltonian (2.22) may be of interest for future work and may reveal ways to make greater use of the quasiparticle analogy.[4] However, such an exploration is beyond the scope of this paper. Also, for three-dimensional dynamics that is of interest in the context of the dynamo problem, a diagonalisation of $\hat{\boldsymbol{H}}$ does not seem possible.

2.3.2. Wigner–Moyal equation

Right-multiplying (2.16) by $\langle\tilde{\boldsymbol{z}}|$ and subtracting the adjoint of the resulting equation yields the von Neumann equation for the density operator of Alfvénic fluctuations, $\hat{\boldsymbol{W}} \doteq |\tilde{\boldsymbol{z}}\rangle\langle\tilde{\boldsymbol{z}}|$,

$$\mathrm{i}\partial_t\hat{\boldsymbol{W}} = \hat{\boldsymbol{H}}\hat{\boldsymbol{W}} - \hat{\boldsymbol{W}}\hat{\boldsymbol{H}}^{\dagger}. \tag{2.24}$$

Applying the Wigner–Weyl transform (Appendix B) to (2.24) yields the Wigner–Moyal equation (WME), which governs the dynamics of Alfvénic fluctuations in the phase space $(\boldsymbol{x}, \boldsymbol{k})$,

$$\mathrm{i}\partial_t\boldsymbol{W} = \boldsymbol{H}\star\boldsymbol{W} - \boldsymbol{W}\star\boldsymbol{H}^{\dagger}. \tag{2.25}$$

Here, $\boldsymbol{H}$ is the symbol of the Hamiltonian $\hat{\boldsymbol{H}}$,

$$\boldsymbol{H} = \begin{pmatrix} \boldsymbol{H}^{++} & \boldsymbol{H}^{+-} \\ \boldsymbol{H}^{-+} & \boldsymbol{H}^{--} \end{pmatrix}, \tag{2.26}$$

and the individual components are given by

$$H_{ij}^{\pm\pm} = \delta_{ij}\left(\bar{z}_l^{\mp}\star k_l - \mathrm{i}\nu_+k^2\right) + \mathrm{i}\frac{k_i}{k^2}\star\bar{z}_{l,j}^{\mp}\star k_l, \tag{2.27a}$$

$$H_{ij}^{\pm\mp} = -\delta_{ij}\mathrm{i}\nu_-k^2 - \mathrm{i}\bar{z}_{i,j}^{\pm} + \mathrm{i}\frac{k_i}{k^2}\star\bar{z}_{l,j}^{\mp}\star k_l, \tag{2.27b}$$

[4]For example, the topology of phase-space trajectories available to drift-wave quasiparticles has been used to explain the nonlinear saturation dynamics of zonal flows by Zhu, Zhou & Dodin (2019).

https://doi.org/10.1017/S0022377825100561 Published online by Cambridge University Press

the Moyal star product $\star$ (B.8) is defined in Appendix B, and $\boldsymbol{W}$ is the symbol of $\hat{\boldsymbol{W}}$, also known as the Wigner matrix. The latter can be expressed as

$$\boldsymbol{W} = \begin{pmatrix} \boldsymbol{W}^{++} & \boldsymbol{W}^{+-} \\ \boldsymbol{W}^{-+} & \boldsymbol{W}^{--} \end{pmatrix}, \tag{2.28}$$

where

$$W_{ij}^{\sigma_1\sigma_2} = \int \mathrm{d}\boldsymbol{s}\, \mathrm{e}^{-\mathrm{i}\boldsymbol{k}\cdot\boldsymbol{s}} \widetilde{z}_i^{\sigma_1}(\boldsymbol{x}+\boldsymbol{s}/2)\widetilde{z}_j^{\sigma_2}(\boldsymbol{x}-\boldsymbol{s}/2). \tag{2.29}$$

Note that the Wigner matrix $\boldsymbol{W}$ is Hermitian, i.e.

$$W_{ij}^{\sigma_1\sigma_2}(t,\boldsymbol{x},\boldsymbol{k}) = W_{ji}^{\sigma_2\sigma_1 *}(t,\boldsymbol{x},\boldsymbol{k}). \tag{2.30}$$

Additionally, since the Elsässer fields are real, we also have that

$$W_{ij}^{\sigma_1\sigma_2}(t,\boldsymbol{x},\boldsymbol{k}) = W_{ji}^{\sigma_2\sigma_1}(t,\boldsymbol{x},-\boldsymbol{k}). \tag{2.31}$$

2.3.3. Average Wigner matrix and the GO expansion

By averaging (2.25) with the same averaging operation used to define the mean fields, we obtain the averaged WME,

$$\mathrm{i}\partial_t \overline{\boldsymbol{W}} = \overline{\boldsymbol{H}} \star \overline{\boldsymbol{W}} - \overline{\boldsymbol{W}} \star \overline{\boldsymbol{H}}^\dagger. \tag{2.32}$$

Here, $\overline{\boldsymbol{H}} = \boldsymbol{H}$, since $\boldsymbol{H}$ is independent of the fluctuating fields, and the averaged Wigner matrix is the average of $\boldsymbol{W}$,

$$\overline{\boldsymbol{W}} \equiv \langle \boldsymbol{W} \rangle = \begin{pmatrix} \overline{\boldsymbol{W}}^{++} & \overline{\boldsymbol{W}}^{+-} \\ \overline{\boldsymbol{W}}^{-+} & \overline{\boldsymbol{W}}^{--} \end{pmatrix}, \tag{2.33}$$

where

$$\overline{W}_{ij}^{\sigma_1\sigma_2} = \int \mathrm{d}\boldsymbol{s}\, \mathrm{e}^{-\mathrm{i}\boldsymbol{k}\cdot\boldsymbol{s}} \left\langle \widetilde{z}_i^{\sigma_1}(\boldsymbol{x}+\boldsymbol{s}/2)\widetilde{z}_j^{\sigma_2}(\boldsymbol{x}-\boldsymbol{s}/2) \right\rangle. \tag{2.34}$$

Notice that the average Wigner matrix (2.33) can be understood as the Fourier transform of the symmetrised two-point correlation tensor of the Elsässer fields.

Below, the original Wigner matrix (2.28) will not be needed, so we will call (2.33) 'the' Wigner matrix and omit the bar in $\overline{\boldsymbol{W}}$ to simplify notation. The properties (2.30) and (2.31) hold for this averaged matrix as well. Also, the trace of $\boldsymbol{W}$, to some extent,[5] can be interpreted as the phase-space density of turbulent quasiparticles. In this sense, the WME can be considered as a generalisation of the Liouville equation. Its interpretation as a quantum extension of kinetic theory becomes clearer when we consider the series expansion of the Moyal star,

$$\begin{aligned} \mathrm{i}\partial_t \boldsymbol{W} &= \boldsymbol{H}\mathrm{e}^{\mathrm{i}\hat{\mathcal{L}}/2}\boldsymbol{W} - \boldsymbol{W}\mathrm{e}^{\mathrm{i}\hat{\mathcal{L}}/2}\boldsymbol{H}^\dagger \\ &= \boldsymbol{H}(1+\mathrm{i}\hat{\mathcal{L}}/2+\cdots)\boldsymbol{W} - \boldsymbol{W}(1+\mathrm{i}\hat{\mathcal{L}}/2+\cdots)\boldsymbol{H}^\dagger, \end{aligned} \tag{2.35}$$

where the Janus operator $\hat{\mathcal{L}}$ (B.9) is defined in Appendix B, and, basically, stands for the canonical Poisson bracket in the $(\boldsymbol{x},\boldsymbol{k})$ space, $A\hat{\mathcal{L}}B = \{A, B\}$. Note that

[5] As discussed in § 2.3.1, the quasiparticle analogy for MHD in the absence of a strong guide field has its limitations due to the lack of a general diagonalisation for $\hat{\boldsymbol{H}}$.

https://doi.org/10.1017/S0022377825100561 Published online by Cambridge University Press

$\hat{\mathcal{L}}$ effectively scales as the GO parameter l/L, so the higher-order terms (denoted '. . .' in (2.35)) can be omitted. Furthermore, this equation can be further simplified when W and H are scalar functions (as can be the case, for example, in drift-wave turbulence (Zhu & Dodin 2021)). In this case, (2.35) becomes the familiar 'classical' wave kinetic equation when $l/L \to 0$,

$$\partial_t W \approx \{H_{\mathrm{H}}, W\} + 2H_{\mathrm{A}} W, \tag{2.36}$$

where H_{H} and H_{A} are the real (Hermitian) and the imaginary (anti-Hermitian) parts of the Hamiltonian. However, keep in mind that, for MHD turbulence, $\boldsymbol{W}$ and $\boldsymbol{H}$ are non-commuting matrices. Furthermore, when L is determined by MI, it is often the case that $l \sim L$, so the GO approximation of the WME is inapplicable.

2.4. *Turbulent source term for the mean field*

As with any quadratic functional of the fluctuating field (Dodin 2022), the turbulent source term for the mean field,

$$\boldsymbol{S}^{\pm} \doteq -\langle \boldsymbol{\nabla} \times [(\widetilde{\boldsymbol{z}}^{\mp} \cdot \boldsymbol{\nabla})\widetilde{\boldsymbol{z}}^{\pm}] \rangle, \tag{2.37}$$

can be expressed through the Wigner matrix $\boldsymbol{W}$,

$$\begin{aligned} S_i^{\pm} &= -\left\langle \epsilon_{ijk} \partial_j \left(\widetilde{z}_l^{\mp} \partial_l \widetilde{z}_k^{\pm} \right) \right\rangle \\ &= -\epsilon_{ijk} \left\langle \left(\langle \boldsymbol{x}| \mathrm{i}\hat{k}_j |\widetilde{z}_l^{\mp}\rangle \langle \boldsymbol{x}| \mathrm{i}\hat{k}_l |\widetilde{z}_k^{\pm}\rangle - \langle \boldsymbol{x}| \widetilde{z}_l^{\mp}\rangle \langle \boldsymbol{x}| \hat{k}_j \hat{k}_l |\widetilde{z}_k^{\pm}\rangle \right) \right\rangle \\ &= -\epsilon_{ijk} \left\langle \left(\langle \boldsymbol{x}| \hat{k}_j |\widetilde{z}_l^{\mp}\rangle \langle \widetilde{z}_k^{\pm}| \hat{k}_l |\boldsymbol{x}\rangle - \langle \boldsymbol{x}| \widetilde{z}_l^{\mp}\rangle \langle \widetilde{z}_k^{\pm}| \hat{k}_j \hat{k}_l |\boldsymbol{x}\rangle \right) \right\rangle \\ &= \epsilon_{ijk} \int \frac{\mathrm{d}\boldsymbol{k}}{(2\pi)^3} \left(k_l k_j \star W_{kl}^{\pm\mp} - k_l \star W_{kl}^{\pm\mp} \star k_j \right), \end{aligned} \tag{2.38}$$

where ϵ_{ijk} is the Levi–Civita symbol and the transition from the third line to the fourth line uses (B.4).

Note that the source term involves only the off-diagonal blocks of the Wigner matrix, $\boldsymbol{W}^{\pm\mp}$, i.e. mean fields are generated only by correlations between $\widetilde{\boldsymbol{z}}^{+}$ and $\widetilde{\boldsymbol{z}}^{-}$. This can also be expected from the original Elsässer equations (2.3), where the nonlinear term vanishes if either $\boldsymbol{z}^{+}$ or $\boldsymbol{z}^{-}$ is zero.

2.5. *Summary of the main equations*

In summary, our mean-field wave-kinetics model is as follows:

$$\partial_t \overline{\boldsymbol{w}}^{\pm} = -\hat{\boldsymbol{k}} \times \left\{ \left[\left(\frac{\hat{\boldsymbol{k}}}{\hat{k}^2} \times \overline{\boldsymbol{w}}^{\mp} \right) \cdot \hat{\boldsymbol{k}} \right] \left(\frac{\hat{\boldsymbol{k}}}{\hat{k}^2} \times \overline{\boldsymbol{w}}^{\pm} \right) \right\} - \hat{k}^2 (\nu_+ \overline{\boldsymbol{w}}^{\pm} + \nu_- \overline{\boldsymbol{w}}^{\mp}) + \boldsymbol{S}^{\pm}, \tag{2.39a}$$

$$\mathrm{i}\partial_t \boldsymbol{W} = \boldsymbol{H} \star \boldsymbol{W} - \boldsymbol{W} \star \boldsymbol{H}^{\dagger}, \tag{2.39b}$$

where

$$S_i^{\pm} = \epsilon_{ijk} \int \frac{\mathrm{d}\boldsymbol{k}}{(2\pi)^3} \left(k_l k_j \star W_{kl}^{\pm\mp} - k_l \star W_{kl}^{\pm\mp} \star k_j \right), \tag{2.40}$$

https://doi.org/10.1017/S0022377825100561 Published online by Cambridge University Press

and the matrix

$$\boldsymbol{H} = \begin{pmatrix} \boldsymbol{H}^{++} & \boldsymbol{H}^{+-} \\ \boldsymbol{H}^{-+} & \boldsymbol{H}^{--} \end{pmatrix} \tag{2.41}$$

consists of

$$H_{ij}^{\pm\pm} = \delta_{ij}\left(\bar{z}_l^{\mp} \star k_l - \mathrm{i}\nu_+ k^2\right) + \mathrm{i}\frac{k_i}{k^2} \star \bar{z}_{l,j}^{\mp} \star k_l, \tag{2.42a}$$

$$H_{ij}^{\pm\mp} = -\delta_{ij}\mathrm{i}\nu_- k^2 - \mathrm{i}\bar{z}_{i,j}^{\pm} + \mathrm{i}\frac{k_i}{k^2} \star \bar{z}_{l,j}^{\pm} \star k_l. \tag{2.42b}$$

Note that (2.39) are equivalent to the original MHD system within the QLA and do not assume scale separation between the fluctuations and mean fields, which is typically done in the literature (Brandenburg 2018; Hughes 2018). As we show in Appendix C, (2.39) conserve the total energy and cross-helicity, while allowing for the transfer of these invariants between the mean and fluctuating fields.

To aid comparisons with existing theories, we will also often work with the following *ad hoc* modification of (2.39b):

$$\mathrm{i}\partial_t \boldsymbol{W} = \boldsymbol{H} \star \boldsymbol{W} - \boldsymbol{W} \star \boldsymbol{H}^{\dagger} - \mathrm{i}\tau_c^{-1}\boldsymbol{W} + \boldsymbol{T}, \tag{2.43}$$

where τ_c is the correlation time that determines the damping of fluctuations through wave–wave collisions. Such a damping term is used in the popular MTA closure (Blackman & Field 2002; Brandenburg & Subramanian 2005). The forcing term $\boldsymbol{T}$, which is yet to specified, is added to allow for turbulent equilibria at non-zero dissipation (§ 3).

3. Linear modulational dynamics within MFWK

Let us now consider small mean-field perturbations to an otherwise homogeneous turbulent background.[6] This corresponds to

$$\boldsymbol{W} = (2\pi)^3[\boldsymbol{F}(\boldsymbol{k}) + \boldsymbol{f}(t, \boldsymbol{x}, \boldsymbol{k})], \tag{3.1}$$

where $\boldsymbol{F}(\boldsymbol{k})$ is the Wigner matrix of the homogeneous turbulent equilibrium, and $\boldsymbol{f}(t, \boldsymbol{x}, \boldsymbol{k})$ is the first-order response of the turbulence to the mean fields. (The factor $(2\pi)^3$ is introduced to shorten notation in some formulae below.) Similarly, the Hamiltonian will be of the form

$$\boldsymbol{H} = \boldsymbol{H}_0(\boldsymbol{k}) + \boldsymbol{h}(t, \boldsymbol{x}, \boldsymbol{k}), \tag{3.2}$$

where $\boldsymbol{H}_0$ captures viscous dissipation and resistivity, and $\boldsymbol{h}$ is the perturbed Hamiltonian due to the mean fields.

[6]While we assume a homogeneous background at this stage (and we will also generally assume isotropy for explicit examples presented later) for simplicity, note that the approach here could in principle be extended to inhomogeneous and anisotropic backgrounds (e.g. in the case of background shear that is of interest for $\alpha - \Omega$ dynamos (Krause & Rädler, 1980), the magnetic shear-current effect (Squire & Bhattacharjee 2016) and the shear–driven α-effect (Ebrahimi & Blackman 2019)). Such inhomogeneities would be most conveniently incorporated by assuming a sinusoidal profile for the background fields, such that the MI of the corresponding Floquet modes can be treated with the Wigner–Moyal formalism presented here.

https://doi.org/10.1017/S0022377825100561 Published online by Cambridge University Press

3.1. *Properties of statistically homogeneous turbulent equilibria*

3.1.1. Equilibrium condition

In the absence of zeroth-order mean fields, (2.39) give the following equations for the equilibrium:

$$0 = \boldsymbol{S}_0^{\pm}, \tag{3.3a}$$

$$0 = (2\pi)^3\big(\boldsymbol{H}_0\boldsymbol{F} - \boldsymbol{F}\boldsymbol{H}_0^{\dagger} - \mathrm{i}\tau_c^{-1}\boldsymbol{F}\big) + \boldsymbol{T}, \tag{3.3b}$$

$$S_{0i}^{\pm} = \epsilon_{ijk}\int \mathrm{d}\boldsymbol{k}\big(k_l k_j \star F_{kl}^{\pm\mp} - k_l \star F_{kl}^{\pm\mp} \star k_j\big), \tag{3.3c}$$

$$\boldsymbol{H}_0^{\pm\pm} = -\mathrm{i}\nu_+ k^2 \mathbf{1}_3, \qquad \boldsymbol{H}_0^{\pm\mp} = -\mathrm{i}\nu_- k^2 \mathbf{1}_3, \tag{3.3d}$$

where $\mathbf{1}_3$ is the 3×3 identity matrix. Thus, for a given $\boldsymbol{F}$, the matrix $\boldsymbol{T}$ must satisfy

$$\boldsymbol{T}^{\sigma_1\sigma_2} = \mathrm{i}(2\pi)^3\big[\big(2\nu_+ k^2 + \tau_c^{-1}\big)\boldsymbol{F}^{\sigma_1\sigma_2} + \nu_- k^2\big(\boldsymbol{F}^{\sigma_1\bar{\sigma}_2} + \boldsymbol{F}^{\bar{\sigma}_1\sigma_2}\big)\big], \tag{3.4}$$

where $\sigma_{1/2} = +/-$ and $\bar{\sigma} \doteq -\sigma$.

Note that in the absence of dissipation ($\tau_c^{-1} = 0$ and $\nu_\pm = 0$), (3.4) gives $\boldsymbol{T} = 0$; i.e. any such homogeneous turbulent background is quasilinearly self-consistent without external driving. Also note that the consistency of the mean-field equation, $\boldsymbol{S}_0 = 0$, follows directly from the background homogeneity, $\boldsymbol{F}(\boldsymbol{x},\boldsymbol{k}) = \boldsymbol{F}(\boldsymbol{k})$,

$$\begin{aligned} S_{0i}^{\pm} &= \epsilon_{ijk}\int \mathrm{d}\boldsymbol{k}\,\big(k_l k_j \star F_{kl}^{\pm\mp} - k_l \star F_{kl}^{\pm\mp} \star k_j\big) \\ &= \epsilon_{ijk}\int \mathrm{d}\boldsymbol{k}\,(k_l k_j - k_l k_j) F_{kl}^{\pm\mp} \\ &= 0. \end{aligned} \tag{3.5}$$

3.1.2. Wigner matrix of isotropic MHD turbulence

For a homogeneous turbulent background, we have

$$\begin{aligned} F_{ij}^{\sigma_1\sigma_2}(\boldsymbol{k}) &= \frac{1}{(2\pi)^3}\int \mathrm{d}\boldsymbol{s}\,\mathrm{e}^{-\mathrm{i}\boldsymbol{k}\cdot\boldsymbol{s}}\left\langle \widetilde{z}_i^{\sigma_1}\left(\boldsymbol{x}+\frac{\boldsymbol{s}}{2}\right)\widetilde{z}_j^{\sigma_2}\left(\boldsymbol{x}-\frac{\boldsymbol{s}}{2}\right)\right\rangle \\ &= R_{ij}^{\sigma_1\sigma_2}(-\boldsymbol{k}), \end{aligned} \tag{3.6}$$

where $\boldsymbol{R}^{\sigma_1\sigma_2}(\boldsymbol{k})$ is the Fourier transform of the two-point correlation tensor,

$$R_{ij}^{\sigma_1\sigma_2}(\boldsymbol{r}) = \big\langle \widetilde{z}_i^{\sigma_1}(\boldsymbol{x}-\boldsymbol{r}/2)\widetilde{z}_j^{\sigma_2}(\boldsymbol{x}+\boldsymbol{r}/2)\big\rangle. \tag{3.7}$$

If we further assume that the turbulence is isotropic (Oughton, Rädler & Matthaeus 1997), then

$$R_{ij}^{\sigma_1\sigma_2}(\boldsymbol{k}) = \left(\delta_{ij} - \frac{k_i k_j}{k^2}\right)\frac{E^{\sigma_1\sigma_2}(k)}{4\pi k^2} + \mathrm{i}\epsilon_{ijk}\frac{k_k}{k^2}\frac{H^{\sigma_1\sigma_2}(k)}{8\pi k^2}, \tag{3.8}$$

where $\boldsymbol{R}^{\sigma_1\sigma_2} = \boldsymbol{R}^{\sigma_2\sigma_1}$, $k \doteq |\boldsymbol{k}|$ and the $H^{\sigma_1\sigma_2}$ are zero for non-helical turbulence. Note that $E^{\sigma_1\sigma_2}(k)$ and $H^{\sigma_1\sigma_2}(k)$ are the spectra of energy-like and helicity-like quantities, respectively, in the following sense:

$$\big\langle z_1^{\sigma}\cdot z_2^{\sigma}\big\rangle = 2\int \mathrm{d}k\; E^{\sigma_1\sigma_2}(k), \qquad \big\langle z_1^{\sigma}\cdot\big(\nabla\times z_2^{\sigma}\big)\big\rangle = \int \mathrm{d}k\; H^{\sigma_1\sigma_2}(k). \tag{3.9}$$

https://doi.org/10.1017/S0022377825100561 Published online by Cambridge University Press

In other words, isotropic MHD turbulence corresponds to

$$\boldsymbol{F} = \begin{pmatrix} \boldsymbol{F}^{+} & \boldsymbol{F}^{C} \\ \boldsymbol{F}^{C} & \boldsymbol{F}^{-} \end{pmatrix},$$

$$F_{ij}^{\chi}(\boldsymbol{k}) = \left(\delta_{ij} - \frac{k_i k_j}{k^2}\right) \frac{E^{\chi}(k)}{4\pi k^2} - \mathrm{i}\epsilon_{ijk} \frac{k_k}{k^2} \frac{H^{\chi}(k)}{8\pi k^2} \tag{3.10}$$

with $\chi = +,\ -,\ C$. It will also be convenient to work with the symmetric and anti-symmetric combinations $\boldsymbol{F}^{S} \doteq (\boldsymbol{F}^{+} + \boldsymbol{F}^{-})/2$ and $\boldsymbol{F}^{A} \doteq (\boldsymbol{F}^{+} - \boldsymbol{F}^{-})/2$, and we also extend this notation to E and H. Then,

$$\begin{aligned}
\int_0^\infty \mathrm{d}k\ E^{S}(k) &= \frac{1}{2}\langle \widetilde{\boldsymbol{v}} \cdot \widetilde{\boldsymbol{v}} + \widetilde{\boldsymbol{b}} \cdot \widetilde{\boldsymbol{b}} \rangle, \\
\int_0^\infty \mathrm{d}k\ E^{C}(k) &= \frac{1}{2}\langle \widetilde{\boldsymbol{v}} \cdot \widetilde{\boldsymbol{v}} - \widetilde{\boldsymbol{b}} \cdot \widetilde{\boldsymbol{b}} \rangle, \\
\int_0^\infty \mathrm{d}k\ E^{A}(k) &= \langle \widetilde{\boldsymbol{v}} \cdot \widetilde{\boldsymbol{b}} \rangle, \\
\int_0^\infty \mathrm{d}k\ H^{S}(k) &= \langle \widetilde{\boldsymbol{v}} \cdot \widetilde{\boldsymbol{w}} + \widetilde{\boldsymbol{b}} \cdot \widetilde{\boldsymbol{j}} \rangle, \\
\int_0^\infty \mathrm{d}k\ H^{C}(k) &= \langle \widetilde{\boldsymbol{v}} \cdot \widetilde{\boldsymbol{w}} - \widetilde{\boldsymbol{b}} \cdot \widetilde{\boldsymbol{j}} \rangle, \\
\int_0^\infty \mathrm{d}k\ H^{A}(k) &= 2\langle \widetilde{\boldsymbol{v}} \cdot \widetilde{\boldsymbol{j}} \rangle = 2\langle \widetilde{\boldsymbol{w}} \cdot \widetilde{\boldsymbol{b}} \rangle,
\end{aligned} \tag{3.11}$$

where $\widetilde{\boldsymbol{w}} \doteq \boldsymbol{\nabla} \times \widetilde{\boldsymbol{v}}$ and $\widetilde{\boldsymbol{j}} \doteq \boldsymbol{\nabla} \times \widetilde{\boldsymbol{b}}$.

3.2. *Linear modulational dynamics*

3.2.1. Linearised equations

The perturbed quantities are governed by the following linearised MFWK equations:

$$\partial_t \overline{\boldsymbol{w}}^{\pm} = -\hat{k}^2(\nu_{+}\overline{\boldsymbol{w}}^{\pm} + \nu_{-}\overline{\boldsymbol{w}}^{\mp}) + \boldsymbol{s}^{\pm}, \tag{3.12a}$$

$$\mathrm{i}\partial_t \boldsymbol{f} = \boldsymbol{H_0} \star \boldsymbol{f} - \boldsymbol{f} \star \boldsymbol{H_0}^{\dagger} + \boldsymbol{h} \star \boldsymbol{F} - \boldsymbol{F} \star \boldsymbol{h}^{\dagger} - \mathrm{i}\tau_c^{-1}\boldsymbol{f}, \tag{3.12b}$$

$$s_i^{\pm} = \epsilon_{ijk} \int \mathrm{d}\boldsymbol{k} \left(k_l k_j \star f_{kl}^{\pm\mp} - k_l \star f_{kl}^{\pm\mp} \star k_j\right), \tag{3.12c}$$

$$\begin{aligned}
h_{ij}^{\pm\pm} &= \delta_{ij}\left(\bar{z}_l^{\mp} \star k_l\right) + \mathrm{i}\,\frac{k_i}{k^2} \star \bar{z}_{l,j}^{\mp} \star k_l, \\
h_{ij}^{\pm\mp} &= -\mathrm{i}\bar{z}_{i,j}^{\pm} + \mathrm{i}\,\frac{k_i}{k^2} \star \bar{z}_{l,j}^{\pm} \star k_l.
\end{aligned} \tag{3.12d}$$

Note that this model is fundamentally different from the commonly used kinematic approximation (Krause & Rädler 1980). The kinematic approximation assumes that all magnetic fields (that is, both turbulent and mean components) are sufficiently

https://doi.org/10.1017/S0022377825100561 Published online by Cambridge University Press

weak such that the flow (again, both mean and turbulent parts) can be taken as prescribed. The momentum equation is then never invoked, and the resulting mean-field theory is built on the induction equation alone. It has already been pointed out in the literature (Courvoisier *et al*. 2010*a*,*b*) that such an approach, which artificially privileges the magnetic field over the flow, is fundamentally inconsistent in the presence of substantial magnetic field fluctuations (which are to be expected in MHD turbulence), but the general theory for this case has been lacking. Our approach fixes this problem in that it is formulated in terms of the Elsässer fields and thus treats velocity and magnetic fields on the same footing.

3.2.2. Eikonal perturbations

Let us now look for the linear eigenmodes of (3.12). For that, let us consider perturbed quantities of the following form:

$$\bar{\boldsymbol{z}}^{\pm} = \mathrm{Re}\left(\boldsymbol{z}^{\pm}\mathrm{e}^{\mathrm{i}\Theta}\right), \tag{3.13a}$$

$$\overline{\boldsymbol{w}}^{\pm} = \mathrm{Re}\left(\boldsymbol{w}^{\pm}\mathrm{e}^{\mathrm{i}\Theta}\right), \tag{3.13b}$$

$$\boldsymbol{f} = \left(\boldsymbol{f}(\boldsymbol{k})\mathrm{e}^{\mathrm{i}\Theta}\right)_{\mathrm{H}}, \tag{3.13c}$$

$$\boldsymbol{h} = \frac{1}{2}\left(\boldsymbol{h}_{(+)}(\boldsymbol{k})\mathrm{e}^{i\Theta} + \boldsymbol{h}^{\dagger}_{(-)}(\boldsymbol{k})\mathrm{e}^{-i\Theta^{*}}\right), \tag{3.13d}$$

with

$$\Theta = -\Omega t + \boldsymbol{K}\cdot\boldsymbol{x}, \tag{3.14}$$

where Ω and $\boldsymbol{K}$ are the modulational frequency and wavevector, respectively, and $\boldsymbol{w}^{\pm} = \mathrm{i}\boldsymbol{K}\times\boldsymbol{z}^{\pm}$. (The index H denotes the Hermitian part.) We will use the convention that the modulational wavevector $\boldsymbol{K}$ is real, while the modulational frequency Ω may be complex. Note that the mean-field polarisations, $\boldsymbol{z}^{\pm}$ and $\boldsymbol{w}^{\pm}$, are constants, while $\boldsymbol{h}_{(\pm)}$ and $\boldsymbol{f}$ are functions of $\boldsymbol{k}$. We also use the convention that the argument of a function will only be explicitly written when it is first defined, not obvious from the context, or judged to provide helpful information.

3.2.3. Equations for the polarisations

Using (B.11), we can write the following equations for the polarisations $\boldsymbol{z}^{\pm}$ and $\boldsymbol{f}$:

$$\Omega\boldsymbol{z}^{\pm} = -\mathrm{i}K^{2}(\nu_{+}\boldsymbol{z}^{\pm} + \nu_{-}\boldsymbol{z}^{\mp}) - \frac{\boldsymbol{K}}{K^{2}}\times\boldsymbol{s}^{\pm}, \tag{3.15}$$

$$\Omega'\boldsymbol{f} - \boldsymbol{H}_{0}(\boldsymbol{k}_{+})\boldsymbol{f} + \boldsymbol{f}\boldsymbol{H}_{0}^{\dagger}(\boldsymbol{k}_{-}) = \boldsymbol{h}_{(+)}\boldsymbol{F}(\boldsymbol{k}_{-}) - \boldsymbol{F}(\boldsymbol{k}_{+})\boldsymbol{h}_{(-)}, \tag{3.16}$$

where

$$-\left(\frac{\boldsymbol{K}}{K^{2}}\times\boldsymbol{s}^{\pm}\right)_{i} = \int \mathrm{d}\boldsymbol{k}\left(K_{n}\mathrm{f}^{\pm\mp}_{in} - \frac{K_{i}K_{m}K_{n}}{K^{2}}\mathrm{f}^{\pm\mp}_{mn}\right), \tag{3.17}$$

and

$$\boldsymbol{h}_{(\pm)} = \begin{pmatrix} \boldsymbol{h}^{++}_{(\pm)} & \boldsymbol{h}^{+-}_{(\pm)} \\ \boldsymbol{h}^{-+}_{(\pm)} & \boldsymbol{h}^{--}_{(\pm)} \end{pmatrix}, \tag{3.18}$$

https://doi.org/10.1017/S0022377825100561 Published online by Cambridge University Press

where

$$\mathrm{h}^{\pm\pm}_{(+)ij} = (\boldsymbol{z}^{\mp}\cdot\boldsymbol{k})\left(\delta_{ij} - \frac{k_{+i}K_j}{k_+^2}\right), \tag{3.19a}$$

$$\mathrm{h}^{\pm\mp}_{(+)ij} = \mathrm{z}^{\mp}_i K_j - (\boldsymbol{z}^{\mp}\cdot\boldsymbol{k})\frac{k_{+i}K_j}{k_+^2}, \tag{3.19b}$$

$$\mathrm{h}^{\pm\pm}_{(-)ij} = (\boldsymbol{z}^{\mp}\cdot\boldsymbol{k})\left(\delta_{ij} + \frac{K_i k_{-j}}{k_-^2}\right), \tag{3.19c}$$

$$\mathrm{h}^{\pm\mp}_{(-)ij} = -\mathrm{z}^{\pm}_j K_i + (\boldsymbol{z}^{\pm}\cdot\boldsymbol{k})\frac{K_i k_{-j}}{k_-^2}. \tag{3.19d}$$

Also, $\Omega' \doteq \Omega + \mathrm{i}\tau_c^{-1}$, $\boldsymbol{k}_\pm \doteq \boldsymbol{k} \pm \boldsymbol{K}/2$ and $k_{\pm i}$ refers to the ith element of $\boldsymbol{k}_\pm$. We study applications of these equations in § 4 and § 5.

4. Non-local turbulent EMF

Much of mean-field dynamo theory is concerned with the calculation of the turbulent EMF (Rogachevskii & Kleeorin 2003; Rädler 2007; Rädler & Brandenburg, 2010; Squire & Bhattacharjee 2015; Yokoi 2018). One of the primary limitations of traditional mean-field theories is that they assume scale separation, i.e. the existing analytical closures are local in the sense that the EMF at a given point in spacetime is expressed purely in terms of the magnetic field and its low-order derivatives at that same point.

Scale separation is often unjustified, and non-locality may play an important role in astrophysical systems of interest (Käpylä *et al*. 2006; Brandenburg 2018). In such cases, the local formulation of the EMF must be replaced with the non-local response kernel,

$$\boldsymbol{\mathcal{E}}(t,\boldsymbol{x}) = \int \mathrm{d}t' \int \mathrm{d}\boldsymbol{x}'\, \boldsymbol{G}(t,\boldsymbol{x};t',\boldsymbol{x}')\,\bar{\boldsymbol{b}}(t',\boldsymbol{x}'). \tag{4.1}$$

When considering small mean-field based departures from an otherwise homogeneous turbulent equilibrium, such that $\boldsymbol{G}(t,\boldsymbol{x};t',\boldsymbol{x}') = \boldsymbol{G}(t-t',\boldsymbol{x}-\boldsymbol{x}')$, this leads to a simple formula for the corresponding Fourier images,

$$\boldsymbol{\mathcal{E}}(\Omega,\boldsymbol{K}) = \boldsymbol{G}(\Omega,\boldsymbol{K})\bar{\boldsymbol{b}}(\Omega,\boldsymbol{K}). \tag{4.2}$$

Note that we only explicitly included the dependence of the EMF on the mean magnetic field in the discussion above, as this is the case that has been considered in the literature. As we shall see shortly, neglecting contributions from the mean velocity field is valid only for purely hydrodynamic turbulent backgrounds.

Determining $\boldsymbol{G}(\Omega,\boldsymbol{K})$ is the key to incorporating non-locality in mean-field models and is the subject of ongoing research (Brandenburg *et al*. 2008; Hubbard & Brandenburg 2009; Rheinhardt & Brandenburg 2012; Rheinhardt *et al*. 2014; Gressel & Elstner 2020; Bendre & Subramanian 2022; Pipin 2023).[7] Current efforts to probe non-locality typically use the 'test-field method' (Schrinner *et al*. 2005,

[7]The Green's function approach in the context of the two-scale direct interaction approximation is a powerful analytical approach to incorporating non-locality into mean-field models, but does not provide explicit expressions for the response kernels (Yoshizawa 1984, 1990; Yokoi 2013, 2023).

https://doi.org/10.1017/S0022377825100561 Published online by Cambridge University Press

2007), in which various test mean fields are imposed on some turbulent background, and the induction equation for the fluctuating magnetic field is solved, allowing for transport coefficients to be inferred numerically. Such efforts have deduced the following approximate form for the non-local response kernel:

$$G_{ij}(\Omega, \boldsymbol{K}) \approx \frac{\alpha + \mathrm{i}\epsilon_{ijk} K_k \beta}{1 - \mathrm{i}\tau\Omega + l^2 K^2}, \tag{4.3}$$

where

$$\alpha = -\frac{\tau_c}{3}\langle \widetilde{\boldsymbol{v}} \cdot \boldsymbol{\nabla} \times \widetilde{\boldsymbol{v}} \rangle, \qquad \beta = \frac{\tau_c}{3}\langle \widetilde{\boldsymbol{v}} \cdot \widetilde{\boldsymbol{v}} \rangle \tag{4.4}$$

are the local turbulent transport coefficients corresponding to the α-effect and turbulent diffusivity, respectively. The coefficients τ and l are fitting parameters that represent the degree of non-locality, and while τ is consistently found to be of the order of the eddy-turnover time, there is less, if any, agreement in the literature on how to understand and model l (Rheinhardt & Brandenburg 2012; Brandenburg 2018). Advancing our understanding of this non-locality requires an analytical prediction for the non-local response kernel, which is not possible with the traditional local mean-field formalism.

The MFWK enables an analytic calculation of the non-local response kernel from first principles (within the QLA), and in the weakly inhomogeneous limit. This result serves as a first step in providing physical motivation for the form of the non-local response kernel. By comparisons with test-field methods (Schrinner *et al*. 2005; Rheinhardt & Brandenburg 2012), it can help isolate which aspects of non-locality can be fully described within mean-field effects, and which are fundamentally nonlinear. In the remainder of this section, we outline the calculation and highlight main results.

4.1. *Derivation*

The generic non-local linear response of the turbulent EMF $\boldsymbol{\mathcal{E}}$ to the mean fields $\bar{\boldsymbol{b}}$ and $\bar{\boldsymbol{v}}$ can be written as follows:

$$\boldsymbol{\mathcal{E}}(t, \boldsymbol{x}) = \int \mathrm{d}t' \int \mathrm{d}\boldsymbol{x}' \big(\boldsymbol{G}^{(b)}(t, \boldsymbol{x}; t', \boldsymbol{x}')\, \bar{\boldsymbol{b}}(t', \boldsymbol{x}') + \boldsymbol{G}^{(v)}(t, \boldsymbol{x}; t', \boldsymbol{x}')\, \bar{\boldsymbol{v}}(t', \boldsymbol{x}') \big). \tag{4.5}$$

Note that we are allowing for a possible dependence on the mean flow, which is often neglected. (Since the mean flow is generally inhomogeneous, for example, as in (3.13*a*), it cannot be removed by a Galilean transformation.) For the remainder of our calculation of the turbulent EMF, we will also work with the traditional velocity and magnetic fields, as opposed to the Elsässer fields, in order to aid comparisons with existing theories.

We now assume weakly inhomogeneous turbulence, such that $\bar{\boldsymbol{z}}^{\pm}$ and $\overline{\boldsymbol{w}}^{\pm}$ are perturbations to an otherwise homogeneous turbulent background. In this case, we can take $\boldsymbol{G}^{(b,v)}(t, \boldsymbol{x}; t', \boldsymbol{x}') = \boldsymbol{G}^{(b,v)}(t - t', \boldsymbol{x} - \boldsymbol{x}')$ such that in Fourier space we have

$$\boldsymbol{\mathcal{E}}(\Omega, \boldsymbol{K}) = \boldsymbol{G}^{(b)}(\Omega, \boldsymbol{K})\bar{\boldsymbol{b}}(\Omega, \boldsymbol{K}) + \boldsymbol{G}^{(v)}(\Omega, \boldsymbol{K})\bar{\boldsymbol{v}}(\Omega, \boldsymbol{K}). \tag{4.6}$$

(For the remainder of our calculation of the turbulent EMF, we will also work with the traditional velocity and magnetic fields, as opposed to the Elsässer fields, in order to aid comparisons with existing theories.) An expression relating the Fourier

https://doi.org/10.1017/S0022377825100561 Published online by Cambridge University Press

coefficients of $\boldsymbol{\mathcal{E}}$, $\bar{\boldsymbol{b}}$ and $\bar{\boldsymbol{v}}$ at frequency Ω and wavenumber $\boldsymbol{K}$ therefore yields the non-local response kernel $\boldsymbol{G}(\Omega, \boldsymbol{K})$.

To do this, we first note that the EMF can be directly written in terms of our Wigner matrix as follows:

$$\begin{aligned}\mathcal{E}_i &= -\frac{1}{2}\langle \tilde{\boldsymbol{z}}^{+} \times \tilde{\boldsymbol{z}}^{-} \rangle_i \\ &= -\frac{1}{2}\int \frac{\mathrm{d}\boldsymbol{k}}{(2\pi)^3}\, \epsilon_{ijk} W^{+-}_{jk}.\end{aligned} \tag{4.7}$$

Curiously, (4.7) can be expressed even more concisely as

$$\boldsymbol{\mathcal{E}} = \bigstar \int \frac{\mathrm{d}\boldsymbol{k}}{(2\pi)^3}\, \boldsymbol{W}^{-+}, \tag{4.8}$$

where $\bigstar$ is the Hodge star, $(\bigstar \boldsymbol{A})_i \doteq \epsilon_{ijk} A_{jk}/2$. The desired expression can therefore be obtained with the modulational mode analysis described in § 3, by solving the WME to obtain the Wigner matrix in terms of the mean fields (which enter the WME through $\boldsymbol{H}$).

We can immediately see that there may, in principle, be some contribution to the turbulent EMF from $\boldsymbol{F}$, which has nothing to do with the mean fields,

$$\begin{aligned}\mathcal{E}_{0i} &= -\frac{\epsilon_{ijk}}{2}\int \mathrm{d}\boldsymbol{k}\, F^{+-}_{jk} \\ &= -\frac{\epsilon_{ijk}}{4}\int \mathrm{d}\boldsymbol{k}\, \left(F^{+-}_{jk} + F^{-+}_{kj}\right) \\ &= -\frac{\epsilon_{ijk}}{4}\int \mathrm{d}\boldsymbol{k}\, \left(F^{+-}_{jk} - F^{-+}_{jk}\right).\end{aligned} \tag{4.9}$$

It can be easily shown that such a background EMF $\boldsymbol{\mathcal{E}}_0$ vanishes for a broad class of turbulent backgrounds. For example, isotropy is a sufficient but not necessary condition for $\boldsymbol{F}^{+-} = \boldsymbol{F}^{-+}$. We henceforth understand $\boldsymbol{\mathcal{E}}$ to refer to the mean-field contribution alone and will not discuss $\boldsymbol{\mathcal{E}}_0$ further.

The mean-field contribution to the turbulent EMF is captured by the perturbed Wigner matrix,

$$\mathcal{E}_i = -\epsilon_{ijk}\int \mathrm{d}\boldsymbol{k}\, f^{+-}_{jk}. \tag{4.10}$$

As in § 3, we now take our perturbed quantities to be of the following form:

$$\begin{gathered}\bar{\boldsymbol{v}}^{\pm} = \mathrm{Re}\left(\boldsymbol{v}^{\pm}\mathrm{e}^{\mathrm{i}\Theta}\right), \qquad \bar{\boldsymbol{b}}^{\pm} = \mathrm{Re}\left(\boldsymbol{b}^{\pm}\mathrm{e}^{\mathrm{i}\Theta}\right), \qquad \boldsymbol{\mathcal{E}} = \mathrm{Re}\left(\boldsymbol{\mathfrak{E}}\mathrm{e}^{\mathrm{i}\Theta}\right), \\ \boldsymbol{f} = \left(\boldsymbol{f}(\boldsymbol{k})\mathrm{e}^{\mathrm{i}\Theta}\right)_{\mathrm{H}}, \qquad \boldsymbol{h} = \frac{1}{2}\left(\boldsymbol{h}_{+}(\boldsymbol{k})\mathrm{e}^{i\Theta} + \boldsymbol{h}^{\dagger}_{-}(\boldsymbol{k})\mathrm{e}^{-i\Theta^{*}}\right),\end{gathered} \tag{4.11}$$

with $\Theta = -\Omega t + \boldsymbol{K}\cdot\boldsymbol{x}$, where Ω and $\boldsymbol{K}$ are the modulational frequency and wavevector, respectively. In terms of the notation of (4.6), one has

$$\boldsymbol{\mathcal{E}}(\Omega, \boldsymbol{K}) = \boldsymbol{\mathfrak{E}}, \qquad \bar{\boldsymbol{b}}(\Omega, \boldsymbol{K}) = \boldsymbol{b}, \qquad \bar{\boldsymbol{v}}(\Omega, \boldsymbol{K}) = \boldsymbol{v}. \tag{4.12}$$

Therefore, our relevant equations are

$$\mathfrak{E}_i = -\frac{1}{2}\int \mathrm{d}\boldsymbol{k}\, \epsilon_{ijk} \mathfrak{f}^{+-}_{jk}, \tag{4.13}$$

https://doi.org/10.1017/S0022377825100561 Published online by Cambridge University Press

along with (3.16), $\boldsymbol{v} = (\boldsymbol{z}^+ + \boldsymbol{z}^-)/2$ and $\boldsymbol{b} = (\boldsymbol{z}^+ - \boldsymbol{z}^-)/2$.

Solving (3.16) for the off-diagonal blocks of the perturbed Wigner matrix yields

$$\begin{aligned}\boldsymbol{f}^{\pm\mp} = {}& \frac{C_1(\boldsymbol{k})}{C(\boldsymbol{k})}\left[\boldsymbol{h}_{(+)}^{\pm+}\boldsymbol{F}^{+\mp}(\boldsymbol{k}_-) + \boldsymbol{h}_{(+)}^{\pm-}\boldsymbol{F}^{-\mp}(\boldsymbol{k}_-) - \boldsymbol{F}^{\pm+}(\boldsymbol{k}_+)\boldsymbol{h}_{(-)}^{+\mp} - \boldsymbol{F}^{\pm-}(\boldsymbol{k}_+)\boldsymbol{h}_{(-)}^{-\mp}\right] \\ & + \frac{C_2(\boldsymbol{k})}{C(\boldsymbol{k})}\left[\boldsymbol{h}_{(+)}^{\mp+}\boldsymbol{F}^{+\pm}(\boldsymbol{k}_-) + \boldsymbol{h}_{(+)}^{\mp-}\boldsymbol{F}^{-\pm}(\boldsymbol{k}_-) - \boldsymbol{F}^{\mp+}(\boldsymbol{k}_+)\boldsymbol{h}_{(-)}^{+\pm} - \boldsymbol{F}^{\mp-}(\boldsymbol{k}_+)\boldsymbol{h}_{(-)}^{-\pm}\right] \\ & + \frac{C_3(\boldsymbol{k})}{C(\boldsymbol{k})}\left[\boldsymbol{h}_{(+)}^{\mp+}\boldsymbol{F}^{+\mp}(\boldsymbol{k}_-) + \boldsymbol{h}_{(+)}^{\mp-}\boldsymbol{F}^{-\mp}(\boldsymbol{k}_-) - \boldsymbol{F}^{\mp+}(\boldsymbol{k}_+)\boldsymbol{h}_{(-)}^{+\mp} - \boldsymbol{F}^{\mp-}(\boldsymbol{k}_+)\boldsymbol{h}_{(-)}^{-\mp}\right] \\ & + \frac{C_4(\boldsymbol{k})}{C(\boldsymbol{k})}\left[\boldsymbol{h}_{(+)}^{\pm+}\boldsymbol{F}^{+\pm}(\boldsymbol{k}_-) + \boldsymbol{h}_{(+)}^{\pm-}\boldsymbol{F}^{-\pm}(\boldsymbol{k}_-) - \boldsymbol{F}^{\pm+}(\boldsymbol{k}_+)\boldsymbol{h}_{(-)}^{+\pm} - \boldsymbol{F}^{\pm-}(\boldsymbol{k}_+)\boldsymbol{h}_{(-)}^{-\pm}\right],\end{aligned} \tag{4.14}$$

where

$$\begin{aligned} C(\boldsymbol{k}) &= [\mathcal{W}^2(\Omega, \boldsymbol{K}, \boldsymbol{k}) + \nu_-^2(k_+^4 + k_-^4)]^2 - 4\nu_-^4 k_+^4 k_-^4, \\ C_1(\boldsymbol{k}) &= \mathcal{W}(\Omega, \boldsymbol{K}, \boldsymbol{k})[\mathcal{W}^2(\Omega, \boldsymbol{K}, \boldsymbol{k}) + \nu_-^2(k_+^4 + k_-^4)], \\ C_2(\boldsymbol{k}) &= -2\nu_-^2 k_+^2 k_-^2 \mathcal{W}(\Omega, \boldsymbol{K}, \boldsymbol{k}), \\ C_3(\boldsymbol{k}) &= -\mathrm{i}\nu_- k_+^2[\mathcal{W}^2(\Omega, \boldsymbol{K}, \boldsymbol{k}) + \nu_-^2(k_+^4 + k_-^4)] + 2\mathrm{i}\nu_-^3 k_-^4 k_+^2, \\ C_4(\boldsymbol{k}) &= -\mathrm{i}\nu_- k_-^2[\mathcal{W}^2(\Omega, \boldsymbol{K}, \boldsymbol{k}) + \nu_-^2(k_+^4 + k_-^4)] + 2\mathrm{i}\nu_-^3 k_+^4 k_-^2, \\ \mathcal{W}(\Omega, \boldsymbol{K}, \boldsymbol{k}) &\doteq \Omega' + \mathrm{i}\nu_+\left(k_+^2 + k_-^2\right), \end{aligned} \tag{4.15}$$

and, as before, $\boldsymbol{k}_\pm = \boldsymbol{k} \pm \boldsymbol{K}/2$. Noting that

$$\begin{aligned} D_1(\boldsymbol{k}) &\doteq \frac{C_1(\boldsymbol{k}_+)}{C(\boldsymbol{k}_+)} = \frac{C_1(-\boldsymbol{k}_+)}{C(-\boldsymbol{k}_+)}, \qquad & D_2(\boldsymbol{k}) &\doteq \frac{C_2(\boldsymbol{k}_+)}{C(\boldsymbol{k}_+)} = \frac{C_2(-\boldsymbol{k}_+)}{C(-\boldsymbol{k}_+)}, \\ D_3(\boldsymbol{k}) &\doteq \frac{C_3(\boldsymbol{k}_+)}{C(\boldsymbol{k}_+)} = \frac{C_4(-\boldsymbol{k}_+)}{C(-\boldsymbol{k}_+)}, \qquad & D_4(\boldsymbol{k}) &\doteq \frac{C_4(\boldsymbol{k}_+)}{C(\boldsymbol{k}_+)} = \frac{C_3(-\boldsymbol{k}_+)}{C(-\boldsymbol{k}_+)}, \end{aligned} \tag{4.16}$$

let us define

$$\boldsymbol{h}(\boldsymbol{k}) \doteq \boldsymbol{h}_{(+)}(\boldsymbol{k}_+) = -\boldsymbol{h}_{(-)}^{\intercal}(-\boldsymbol{k}_+), \tag{4.17}$$

where $^\intercal$ denotes transposition and

$$\begin{aligned} \mathrm{h}_{ij}^{\pm\pm}(\boldsymbol{k}) &= (\boldsymbol{z}^\mp \cdot \boldsymbol{k})\left[\delta_{ij} - \frac{(k_i + K_i)K_j}{(\boldsymbol{k} + \boldsymbol{K})^2}\right], \\ \mathrm{h}_{ij}^{\pm\mp}(\boldsymbol{k}) &= \mathrm{z}_i^\mp K_j - (\boldsymbol{z}^\mp \cdot \boldsymbol{k})\frac{(k_i + K_i)K_j}{(\boldsymbol{k} + \boldsymbol{K})^2}. \end{aligned} \tag{4.18}$$

Substituting (4.14) into (4.13) yields

$$\begin{aligned}\mathfrak{E}_i = -\frac{1}{2}\int \boldsymbol{dk}\,\epsilon_{ijk}\big\{ & -\left[\Delta_1(\boldsymbol{k})\mathrm{h}_{jl}^{-+}(\boldsymbol{k}) + \Delta_2(\boldsymbol{k})\mathrm{h}_{jl}^{++}(\boldsymbol{k})\right]F_{lk}^{++}(\boldsymbol{k}) \\ & + \left[\Delta_1(\boldsymbol{k})\mathrm{h}_{jl}^{+-}(\boldsymbol{k}) + \Delta_2(\boldsymbol{k})\mathrm{h}_{jl}^{--}(\boldsymbol{k})\right]F_{lk}^{--}(\boldsymbol{k}) \\ & + \left[\Delta_1(\boldsymbol{k})\mathrm{h}_{jl}^{++}(\boldsymbol{k}) + \Delta_2(\boldsymbol{k})\mathrm{h}_{jl}^{-+}(\boldsymbol{k})\right]F_{lk}^{+-}(\boldsymbol{k}) \\ & - \left[\Delta_1(\boldsymbol{k})\mathrm{h}_{jl}^{--}(\boldsymbol{k}) + \Delta_2(\boldsymbol{k})\mathrm{h}_{jl}^{+-}(\boldsymbol{k})\right]F_{lk}^{-+}(\boldsymbol{k})\big\},\end{aligned} \tag{4.19}$$

https://doi.org/10.1017/S0022377825100561 Published online by Cambridge University Press

where

$$\Delta_1(\boldsymbol{k}) = D_1 - D_2 = \frac{\mathcal{V}(\Omega, \boldsymbol{K}, \boldsymbol{k})}{\mathcal{V}^2(\Omega, \boldsymbol{K}, \boldsymbol{k}) + \nu_-^2\kappa^4(\boldsymbol{K}, \boldsymbol{k})},$$

$$\Delta_2(\boldsymbol{k}) = D_3 - D_4 = -\frac{\mathrm{i}\nu_-\kappa^2}{\mathcal{V}^2(\Omega, \boldsymbol{K}, \boldsymbol{k}) + \nu_-^2\kappa^4(\boldsymbol{K}, \boldsymbol{k})},$$

$$\mathcal{V}(\Omega, \boldsymbol{K}, \boldsymbol{k}) \doteq \Omega' + \mathrm{i}\nu_+[k^2 + (\boldsymbol{k}+\boldsymbol{K})^2],$$

$$\kappa^2(\boldsymbol{K}, \boldsymbol{k}) \doteq (\boldsymbol{k}+\boldsymbol{K})^2 - k^2. \tag{4.20}$$

Finally, noting that

$$\mathrm{h}_{ij}^{\pm\pm}(\boldsymbol{k}) = M_{ijk}(\boldsymbol{k})\mathrm{z}_k^{\mp}, \qquad \mathrm{h}_{ij}^{\pm\mp}(\boldsymbol{k}) = N_{ijk}(\boldsymbol{k})\mathrm{z}_k^{\mp}, \tag{4.21}$$

where

$$M_{ijk} = \left(\delta_{ij} - \frac{(k_i + K_i)K_j}{(\boldsymbol{k}+\boldsymbol{K})^2}\right)k_k, \qquad N_{ijk} = \delta_{ik}K_j - \frac{(k_i + K_i)K_j}{(\boldsymbol{k}+\boldsymbol{K})^2}k_k, \tag{4.22}$$

we have

$$G_{ij}^{(\boldsymbol{v})}(\Omega, \boldsymbol{K}) = \frac{\epsilon_{imn}}{2}\int \mathrm{d}\boldsymbol{k}\big\{M_{mlj}\big[\Delta_1\big(F_{ln}^{-+} - F_{ln}^{+-}\big) + \Delta_2\big(F_{ln}^{++} - F_{ln}^{--}\big)\big] + N_{mlj}\big[\Delta_1\big(F_{ln}^{++} - F_{ln}^{--}\big) + \Delta_2\big(F_{ln}^{-+} - F_{ln}^{+-}\big)\big]\big\}, \tag{4.23}$$

$$G_{ij}^{(\boldsymbol{b})}(\Omega, \boldsymbol{K}) = \frac{\epsilon_{imn}}{2}\int \mathrm{d}\boldsymbol{k}\big\{M_{mlj}\big[\Delta_1\big(F_{ln}^{-+} + F_{ln}^{+-}\big) - \Delta_2\big(F_{ln}^{++} + F_{ln}^{--}\big)\big] + N_{mlj}\big[\Delta_1\big(F_{ln}^{++} + F_{ln}^{--}\big) - \Delta_2\big(F_{ln}^{-+} + F_{ln}^{+-}\big)\big]\big\}. \tag{4.24}$$

Equations (4.23) and (4.24) are the exact (within the QLA) forms of the linear non-local response kernel of the turbulent EMF to mean velocity and magnetic fields, respectively. We emphasise that, in deriving them, we have made no additional approximations, such as scale separation or any particular symmetries of the turbulence (e.g. isotropy). It is immediately evident from (4.23) that the contribution to the EMF from the mean flow vanishes if $\boldsymbol{F}^{++} = \boldsymbol{F}^{--}$ and $\boldsymbol{F}^{+-} = \boldsymbol{F}^{-+}$, that is, if $\widetilde{\boldsymbol{z}}^+$ and $\widetilde{\boldsymbol{z}}^-$ have the same two-point correlations. This condition is somewhat trivially satisfied by hydrodynamic turbulence (in which $\widetilde{\boldsymbol{b}} = 0$ such that $\widetilde{\boldsymbol{z}}^+ = \widetilde{\boldsymbol{z}}^-$) but can also be satisfied by more general MHD turbulence, as will be discussed shortly.

In the remainder of this section, we examine (4.23) and (4.24) for specific turbulent backgrounds. We also compare them with traditional mean-field theories and the numerically inferred form of the non-local response kernel $\boldsymbol{G}^{(\boldsymbol{b})}$ used in the literature.

4.2. *Hydrodynamic turbulence*

Consider homogeneous hydrodynamic turbulence, where $\widetilde{\boldsymbol{z}}^+ = \widetilde{\boldsymbol{z}}^-$ and thus $\boldsymbol{F} \doteq \boldsymbol{F}^{\pm\pm} = \boldsymbol{F}^{\pm\mp}$. Then (4.19) becomes simply

$$\mathfrak{E}_i = \epsilon_{ijk}\int \mathrm{d}\boldsymbol{k}\,\Delta(\boldsymbol{k})[(\boldsymbol{b}\cdot\boldsymbol{k})\delta_{jl} - \mathrm{b}_j K_l]F_{lk}, \tag{4.25}$$

https://doi.org/10.1017/S0022377825100561 Published online by Cambridge University Press

where

$$\Delta(\boldsymbol{k}) \doteq \Delta_1(\boldsymbol{k}) - \Delta_2(\boldsymbol{k}) = \frac{1}{\Omega' + \mathrm{i}\nu k^2 + \mathrm{i}\eta(\boldsymbol{k}+\boldsymbol{K})^2}. \tag{4.26}$$

This is the generic answer for hydrodynamic turbulence for general $\boldsymbol{F}(\boldsymbol{k})$. Notably, the EMF is entirely independent of $\bar{\boldsymbol{v}}$ in this case.

If we further assume that the turbulent flow is isotropic (3.10), we have

$$F_{lp}(\boldsymbol{k}) = \left(\delta_{lp} - \frac{k_l k_p}{k^2}\right)\frac{E(k)}{4\pi k^2} - \mathrm{i}\epsilon_{lpq}\frac{k_q}{k^2}\frac{H(k)}{8\pi k^2}, \tag{4.27}$$

where $E(k)$ and $H(k)$ are the energy and helicity spectra, respectively,

$$\frac{1}{2}\langle v^2\rangle = \int_0^\infty \mathrm{d}k\, E(k), \qquad \langle \boldsymbol{v}\cdot(\boldsymbol{\nabla}\times\boldsymbol{v})\rangle = \int_0^\infty \mathrm{d}k\, H(k). \tag{4.28}$$

We now assume sufficiently weak dissipation, such that $\tau_c \nu_\pm k^2 \ll 1$ and $\tau_c \nu_\pm k K \ll 1$ over the range where $E(k)$ and $H(k)$ substantially contribute to the integrals over $\boldsymbol{k}$. In this case, we can use the following approximation for Δ:

$$\Delta(\boldsymbol{k}) \approx \frac{1}{\Omega' + \mathrm{i}\eta K^2}\left(1 - \frac{2\mathrm{i}(\nu_+ k^2 + \eta \boldsymbol{k}\cdot\boldsymbol{K})}{\Omega' + \mathrm{i}\eta K^2}\right). \tag{4.29}$$

Note that we have assumed dissipation to be weak, so that the terms $\nu_+ k^2$ and $\eta\boldsymbol{k}\cdot\boldsymbol{K}$ could be taken out of the denominator of Δ. (The ηK^2 terms are retained for reasons that will become evident shortly.) With (4.29), the integration over $\boldsymbol{k}$ in (4.25) can be performed without assuming any particular form of the spectra $E(k)$ and $H(k)$, and one obtains the relatively familiar form

$$\mathfrak{E} = \mathcal{A}(\Omega, \boldsymbol{K})\boldsymbol{b} - \mathcal{B}(\Omega, \boldsymbol{K})(\mathrm{i}\boldsymbol{K}\times\boldsymbol{b}), \tag{4.30a}$$

$$\mathcal{A}(\Omega, \boldsymbol{K}) = \frac{\alpha}{N(\Omega, \boldsymbol{K})} + \frac{2}{3}\frac{\nu_+\tau_c^2\langle\widetilde{\boldsymbol{w}}\cdot\boldsymbol{\nabla}\times\widetilde{\boldsymbol{w}}\rangle}{N^2(\Omega, \boldsymbol{K})}, \tag{4.30b}$$

$$\mathcal{B}(\Omega, \boldsymbol{K}) = \frac{\beta}{N(\Omega, \boldsymbol{K})} - \frac{2}{3}\frac{\nu_+\tau_c^2\langle\widetilde{\boldsymbol{v}}\cdot\boldsymbol{\nabla}\times\widetilde{\boldsymbol{w}}\rangle}{N^2(\Omega, \boldsymbol{K})}, \tag{4.30c}$$

where

$$N(\Omega, \boldsymbol{K}) \doteq 1 - \mathrm{i}\tau_c\Omega + \tau_c\eta K^2, \tag{4.31}$$

α and β are the local transport coefficients defined in (4.4),

$$\langle\widetilde{\boldsymbol{w}}\cdot\boldsymbol{\nabla}\times\widetilde{\boldsymbol{w}}\rangle = \int_0^\infty \mathrm{d}k\, k^2 H(k), \qquad \langle\widetilde{\boldsymbol{v}}\cdot\boldsymbol{\nabla}\times\widetilde{\boldsymbol{w}}\rangle = \int_0^\infty \mathrm{d}k\, k^2 E(k), \tag{4.32}$$

and the corresponding response kernel is given by

$$G_{ij}^{(\boldsymbol{b})}(\Omega, \boldsymbol{K}) = \mathcal{A}(\Omega, \boldsymbol{K})\delta_{ij} + \mathrm{i}\mathcal{B}(\Omega, \boldsymbol{K})\epsilon_{ijk}K_k. \tag{4.33}$$

The first terms in the expressions for $\mathcal{A}$ and $\mathcal{B}$ are exactly the empirical non-local response kernel (4.3), with $\tau = \tau_c$ and

$$l^2 = \tau_c\eta. \tag{4.34}$$

https://doi.org/10.1017/S0022377825100561 Published online by Cambridge University Press

The second terms are viscous and resistive corrections. In particular, note that in the ideal limit ($\nu_\pm \to 0$) and for short correlation times ($\tau_c \Omega \ll 1$), we recover the original local statement of the α-effect, that is, $\mathcal{A} \to \alpha$ and $\mathcal{B} \to \beta$.

These results are consistent with reports of the non-locality parameter τ being of the order of the turnover time across multiple simulations with different values of the magnetic Reynolds number. In contrast, the inferred value of l varies more widely in the literature (Rheinhardt & Brandenburg 2012; Brandenburg 2018), and (4.34) can be considered the first actual calculation of l from first principles (modulo the fact that we rely on the QLA and introduce τ_c in (2.43) *ad hoc*, as usual).

4.3. *Isotropic MHD turbulence*

The non-local turbulent EMF for isotropic MHD turbulence (3.10) can be written as follows:

$$\boldsymbol{\mathfrak{E}} = \mathcal{A}(\Omega, \boldsymbol{K})\boldsymbol{b} - \mathcal{B}(\Omega, \boldsymbol{K})(\mathrm{i}\boldsymbol{K} \times \boldsymbol{b}) + \mathcal{C}(\Omega, \boldsymbol{K})\boldsymbol{v} - \mathcal{D}(\Omega, \boldsymbol{K})(\mathrm{i}\boldsymbol{K} \times \boldsymbol{v}), \tag{4.35}$$

where

$$\mathcal{A}(\Omega, \boldsymbol{K}) = \mathrm{i}\int \mathrm{d}\boldsymbol{k}\, \frac{k_b^2}{k^2}\left[\frac{\boldsymbol{k}\cdot\boldsymbol{K} + K^2}{(\boldsymbol{k}+\boldsymbol{K})^2}(\Delta_1 + \Delta_2)\left(\frac{H^C(k)}{8\pi k^2} - \frac{H^S(k)}{8\pi k^2}\right)\right.$$
$$\left. +2\left(\Delta_2 \frac{H^S(k)}{8\pi k^2} - \Delta_1 \frac{H^C(k)}{8\pi k^2}\right)\right], \tag{4.36a}$$

$$\mathcal{B}(\Omega, \boldsymbol{K}) = \mathrm{i}\int \mathrm{d}\boldsymbol{k}\left[\frac{k_b^2}{k^2}\frac{k^2 + \boldsymbol{k}\cdot\boldsymbol{K}}{(\boldsymbol{k}+\boldsymbol{K})^2}(\Delta_1 + \Delta_2)\left(\frac{E^C(k)}{4\pi k^2} - \frac{E^S(k)}{4\pi k^2}\right)\right.$$
$$\left. +\frac{k^2 - k_K^2}{k^2}\left(\Delta_1 \frac{E^S(k)}{4\pi k^2} - \Delta_2 \frac{E^C(k)}{4\pi k^2}\right)\right], \tag{4.36b}$$

$$\mathcal{C}(\Omega, \boldsymbol{K}) = \mathrm{i}\int \mathrm{d}\boldsymbol{k}\, \frac{k_v^2}{k^2}\left[\frac{\boldsymbol{k}\cdot\boldsymbol{K} + K^2}{(\boldsymbol{k}+\boldsymbol{K})^2}(\Delta_1 + \Delta_2) - 2\Delta_2\right]\frac{H^A(k)}{8\pi k^2}, \tag{4.36c}$$

$$\mathcal{D}(\Omega, \boldsymbol{K}) = \mathrm{i}\int \mathrm{d}\boldsymbol{k}\left[\frac{k_v^2}{k^2}\frac{k^2 + \boldsymbol{k}\cdot\boldsymbol{K}}{(\boldsymbol{k}+\boldsymbol{K})^2}(\Delta_1 - \Delta_2) + \frac{k_K^2 - k^2}{k^2}\Delta_1\right]\frac{E^A(k)}{4\pi k^2}, \tag{4.36d}$$

$k_\xi \doteq (\boldsymbol{k}\cdot\boldsymbol{\xi})/\xi$ denotes the component of $\boldsymbol{k}$ along a given vector $\boldsymbol{\xi}$ and the functions $E^\chi(k)$ and $H^\chi(k)$ are defined in (3.11). In particular, for ideal MHD in the commonly assumed GO limit, the above coefficients acquire a more familiar form,

$$\mathcal{A}(\Omega, \boldsymbol{K}) \approx -\frac{\mathrm{i}}{3\Omega'}\langle\widetilde{\boldsymbol{v}}\cdot\nabla\times\widetilde{\boldsymbol{v}} - \widetilde{\boldsymbol{b}}\cdot\nabla\times\widetilde{\boldsymbol{b}}\rangle, \tag{4.37a}$$

$$\mathcal{B}(\Omega, \boldsymbol{K}) \approx \frac{\mathrm{i}}{3\Omega'}\langle\widetilde{\boldsymbol{v}}\cdot\widetilde{\boldsymbol{v}}\rangle, \tag{4.37b}$$

$$\mathcal{C}(\Omega, \boldsymbol{K}) \approx 0, \tag{4.37c}$$

$$\mathcal{D}(\Omega, \boldsymbol{K}) = \frac{\mathrm{i}}{3\Omega'}\langle\widetilde{\boldsymbol{v}}\cdot\widetilde{\boldsymbol{b}}\rangle. \tag{4.37d}$$

https://doi.org/10.1017/S0022377825100561 Published online by Cambridge University Press

Let us now discuss each of these contributions to the non-local EMF and their relationship to the results of local mean-field theories. As established in the previous discussion for hydrodynamic turbulence (§ 4.2), the transport coefficients $\mathcal{A}$ and $\mathcal{B}$ correspond to the usual α-effect driven by kinetic helicity and turbulent diffusivity, respectively. Note that for MHD turbulence, the MFWK framework captures the cancellation of kinetic helicity by current helicity, i.e. the magnetic α-effect, also known as the Pouquet effect (Pouquet, Frisch & Léorat 1976). The coefficient $\mathcal{A}$ is therefore qualitatively in agreement with previous theories, up to non-local corrections (the difference between (4.36*a*) and (4.37*a*)). Notably, it is commonly stated that the magnetic α-effect is captured only beyond the QLA, as done in the eddy-damped quasinormal Markovian (Orszag 1970) or MTA (Blackman & Field 2002) closures. However, as can be seen from our calculation, this is not the case. Although we included an MTA-like *ad hoc* damping term in (2.43), this modification to the QLA is inessential for capturing the magnetic α-effect in (4.37a), and taking $\tau_c \to \infty$ results only in replacing Ω' with Ω. The coefficient $\mathcal{B}$ also agrees with the vast majority of previous mean-field theories in that it contains no contribution to the turbulent diffusivity from magnetic fluctuations (Vainshtein & Kichatinov 1983; Rädler *et al*. 2002; Squire & Bhattacharjee 2015), although such a contribution was found with the two-scale direct interaction approximation in Yoshizawa (1990).

The contribution to the turbulent EMF proportional to the mean-flow vorticity, as determined by $\mathcal{D}$, is known as the Yoshizawa effect (Yoshizawa 1990; Yokoi 2013) and is related to the cross-helicity $\langle \widetilde{\boldsymbol{v}} \cdot \widetilde{\boldsymbol{b}} \rangle$. As with the α-effect term, the coefficient $\mathcal{D}$ agrees exactly with previous mean-field theories in the GO limit ($lK \ll 1$) and for short correlation times ($\tau_c \Omega \ll 1$).

In contrast, the effect of $\mathcal{C}$ predicted by the MFWK framework is qualitatively new. The term in the EMF that is proportional to the mean flow has received limited attention in the literature. Typically, Galilean invariance is invoked to argue that any term proportional to the mean flow should vanish. This is, of course, true if the flow is homogeneous, and, indeed, the contribution from $\bar{\boldsymbol{v}}$ vanishes in the limit of negligible K; i.e. $\mathcal{C} \to 0$ as $K \to 0$. However, the contribution of $\bar{\boldsymbol{v}}$ at non-negligible K is non-zero. To the best of our knowledge, the only other work where this subject is discussed is Rädler & Brandenburg (2010). Using our notation, the result of Rädler & Brandenburg (2010) can be expressed as follows:

$$\mathcal{E} = \ldots + C\bar{\boldsymbol{v}}, \tag{4.38a}$$

$$C = \frac{1}{3}\int \mathrm{d}\tau \int \mathrm{d}\boldsymbol{\xi}\, [\mathcal{G}^{(v)}(\tau,\xi) - \mathcal{G}^{(\eta)}(\tau,\xi)]\langle \widetilde{\boldsymbol{v}}(t,\boldsymbol{x}) \cdot \widetilde{\boldsymbol{j}}(t-\tau, \boldsymbol{x}-\boldsymbol{\xi})\rangle, \tag{4.38b}$$

$$\mathcal{G}^{(\gamma)}(\tau,\xi) \doteq \begin{cases} (4\pi\gamma\tau)^{-3/2}\exp(-\xi^2/4\gamma\tau), & \tau > 0, \\ 0, & \tau \leqslant 0. \end{cases} \tag{4.38c}$$

The ellipsis indicates the additional contributions to the EMF that are not relevant to the present discussion.

Although (4.38) and (4.36*c*) are in agreement in that the basic effect is driven by flow–current alignment $\langle \widetilde{\boldsymbol{v}} \cdot \widetilde{\boldsymbol{j}} \rangle$, they differ in several significant ways beyond what can be attributed to non-local corrections. Firstly, (4.38) predicts a finite contribution to the non-local EMF even for constant mean flows. In Rädler & Brandenburg (2010), it is argued that this does not violate Galilean invariance because the frame of reference is fixed by the assumption of isotropic turbulence, i.e. that shifting from

https://doi.org/10.1017/S0022377825100561 Published online by Cambridge University Press

a frame with a constant mean flow and isotropic turbulence to the frame where the mean flow is zero would render the turbulence anisotropic. However, because the constant shift to the total velocity $\boldsymbol{v} = \bar{\boldsymbol{v}} + \widetilde{\boldsymbol{v}}$ that would be introduced by a change in reference frame would be absorbed by the mean flow $\bar{\boldsymbol{v}}$ and not contribute to the fluctuating fields $\widetilde{\boldsymbol{v}}$ that comprise the turbulence. In contrast, (4.36*c*) has the correct limiting behaviour for constant mean flows, as the transport coefficient $\mathcal{C}$ vanishes as $K \to 0$.

Although the violation of Galilean invariance alone indicates that (4.38) is unphysical, let us also mention other ways in which it disagrees with our theory. Equation (4.38) predicts that the mean-flow contribution to the EMF vanishes when $\nu = \eta$, and, in particular, in the ideal limit $\nu_\pm \to 0$. In contrast, (4.36*c*) at $\nu = \eta$ (i.e. $\nu_- = 0$) predicts non-zero C,

$$\mathcal{C}(\Omega, \boldsymbol{K}) = \mathrm{i} \int \mathrm{d}\boldsymbol{k}\, \frac{k_v^2}{k^2} \frac{\boldsymbol{k}\cdot\boldsymbol{K} + K^2}{(\boldsymbol{k}+\boldsymbol{K})^2[\Omega' + \mathrm{i}\nu_+(k^2 + (\boldsymbol{k}+\boldsymbol{K})^2]} \frac{H^A(k)}{8\pi k^2}, \tag{4.39}$$

or, in the ideal limit,

$$\mathcal{C}(\Omega, \boldsymbol{K}) = \frac{\mathrm{i}}{\Omega'} \int \mathrm{d}\boldsymbol{k}\, \frac{k_v^2}{k^2} \frac{\boldsymbol{k}\cdot\boldsymbol{K} + K^2}{(\boldsymbol{k}+\boldsymbol{K})^2} \frac{H^A(k)}{8\pi k^2}, \tag{4.40}$$

both of which are generally non-zero. These discrepancies may be related to the treatment of the mean flow as an externally prescribed field, as opposed to a self-consistent field.

Note that flow–current correlations have also been found to produce additional contributions to the α-effect in the case of non-stationary and (or) inhomogeneous turbulence, or when the correlation time scales of the magnetic and velocity fluctuations are not equal (Mizerski, Yokoi & Brandenburg 2023; Yokoi 2023; Hughes, Mason & Proctor 2024). However, that effect is different from the one we discuss here. In our case, the flow–current effect manifests as a contribution to the EMF proportional to the mean flow rather than the mean magnetic field, is found for stationary and homogeneous turbulent backgrounds, and does not depend on the correlation times of the turbulent fields.

In the following section, we will see that this little-known contribution to the EMF couples the mean magnetic fields and flows in such a way that enables a previously unknown $\langle\widetilde{\boldsymbol{v}}\cdot\widetilde{\boldsymbol{j}}\rangle$-driven dynamo effect.

5. Modulational modes of MHD turbulence

Perhaps some of the most basic questions that can be asked regarding mean-field generation from turbulence are as follows: What properties of turbulence make it susceptible to spontaneously generating mean fields, what do these unstable mean fields look like and how fast do they grow? These questions lie within the purview of the modulational-mode analysis presented in this section, which therefore encapsulates some of the most fundamental predictions of MFWK as a theoretical framework. We will also compare and contrast the predictions of MFWK with those of existing mean-field theories.

5.1. *Derivation*

The dispersion relation of modulational modes follows directly from the linearised MFWK equations written in terms of the polarisations of the perturbed quantities

https://doi.org/10.1017/S0022377825100561 Published online by Cambridge University Press

(3.15) and (3.16). Let us first rewrite (3.15) in a form that aids the eventual dispersion matrix formulation,

$$\begin{pmatrix} (\mathrm{i}\Omega - \nu_+ K^2)\mathbf{1}_3 & -\nu_- K^2 \mathbf{1}_3 \\ -\nu_- K^2 \mathbf{1}_3 & (\mathrm{i}\Omega - \nu_+ K^2)\mathbf{1}_3 \end{pmatrix} \boldsymbol{z} = \mathrm{i} \begin{pmatrix} \boldsymbol{\mathcal{S}}^+ \\ \boldsymbol{\mathcal{S}}^- \end{pmatrix}, \tag{5.1}$$

where $\boldsymbol{z} \doteq (\boldsymbol{z}^+, \boldsymbol{z}^-)^\intercal$ and

$$\begin{aligned} \mathcal{S}_i^\pm &= \int \mathrm{d}\boldsymbol{k}\, K_n \left(\mathrm{f}_{in}^{\pm\mp} - \frac{K_i K_m}{K^2} \mathrm{f}_{mn}^{\pm\mp} \right) \\ &= K_n \left(\delta_{im} - \frac{K_i K_m}{K^2} \right) \int \mathrm{d}\boldsymbol{k}\, \mathrm{f}_{mn}^{\pm\mp}. \end{aligned} \tag{5.2}$$

To find the dispersion matrix, we must express $\boldsymbol{\mathcal{S}}$ in terms of the mean fields $\boldsymbol{z}^\pm$. To do this, the integral of the perturbed Wigner matrix (4.14) can be simplified by shifting and flipping integration variables as done in § 4.1,

$$\begin{aligned} \int \mathrm{d}\boldsymbol{k}\, \mathrm{f}_{mn}^{\pm\mp} = &\Bigg[\int \mathrm{d}\boldsymbol{k}\, M_{mpj} \left(D_2 F_{pn}^{\mp\pm} + D_3 F_{pn}^{\mp\mp} \right) + N_{mpj} \left(D_2 F_{pn}^{\pm\pm} + D_3 F_{pn}^{\pm\mp} \right) \\ &+ M_{npj} \left(D_1 F_{pm}^{\mp\pm} + D_4 F_{pm}^{\mp\mp} \right) + N_{npj} \left(D_1 F_{pm}^{\pm\pm} + D_4 F_{pm}^{\pm\mp} \right) \Bigg] \mathrm{z}_j^\pm \\ &+ \Bigg[\int \mathrm{d}\boldsymbol{k}\, M_{mpj} \left(D_1 F_{pn}^{\pm\mp} + D_4 F_{pn}^{\pm\pm} \right) + N_{mpj} \left(D_1 F_{pn}^{\mp\mp} + D_4 F_{pn}^{\mp\pm} \right) \\ &+ M_{npj} \left(D_2 F_{pm}^{\pm\mp} + D_3 F_{pm}^{\pm\pm} \right) + N_{npj} \left(D_2 F_{pm}^{\mp\mp} + D_3 F_{pm}^{\mp\pm} \right) \Bigg] \mathrm{z}_j^\mp, \end{aligned} \tag{5.3}$$

where the matrices M_{ijk} and N_{ijk} are defined in (4.22) and the functions D_n are defined as follows:

$$\begin{aligned} D_1 &= \frac{\mathcal{W}\left(\mathcal{W}^2 + \nu_-^2 \kappa_1^4\right)}{\left(\mathcal{W}^2 + \nu_-^2 \kappa_1^4\right)^2 - 4\nu_-^4 \kappa_2^8}, \\ D_2 &= \frac{-2\nu_-^2 \kappa_2^4 \mathcal{W}}{\left(\mathcal{W}^2 + \nu_-^2 \kappa_1^4\right)^2 - 4\nu_-^4 \kappa_2^8}, \\ D_3 &= \frac{-\mathrm{i}\nu_- (\boldsymbol{k}+\boldsymbol{K})^2 \left(\mathcal{W}^2 + \nu_-^2 \kappa_1^4\right) + 2\mathrm{i}\nu_-^3 k^2 \kappa_2^4}{\left(\mathcal{W}^2 + \nu_-^2 \kappa_1^4\right)^2 - 4\nu_-^4 \kappa_2^8}, \\ D_4 &= \frac{-\mathrm{i}\nu_- k^2 \left(\mathcal{W}^2 + \nu_-^2 \kappa_1^4\right) + 2\mathrm{i}\nu_-^3 (\boldsymbol{k}+\boldsymbol{K})^2 \kappa_2^4}{\left(\mathcal{W}^2 + \nu_-^2 \kappa_1^4\right)^2 - 4\nu_-^4 \kappa_2^8}, \end{aligned} \tag{5.4}$$

and $\mathcal{W} \doteq \Omega' + \mathrm{i}\nu_+ \kappa_0^2$, $\kappa_0^2 \doteq k^2 + (\boldsymbol{k}+\boldsymbol{K})^2$, $\kappa_1^4 \doteq k^4 + (\boldsymbol{k}+\boldsymbol{K})^4$ and $\kappa_2^4 \doteq k^2 (\boldsymbol{k}+\boldsymbol{K})^2$.

After extensive but straightforward calculation, one can rewrite this as follows:

$$\mathrm{i}\boldsymbol{S}^\pm = \boldsymbol{P}^\pm \boldsymbol{z}^\pm + \boldsymbol{Q}^\pm \boldsymbol{z}^\mp, \tag{5.5}$$

https://doi.org/10.1017/S0022377825100561 Published online by Cambridge University Press

where the matrices $\boldsymbol{P}^{\pm}$ and $\boldsymbol{Q}^{\pm}$ are given by

$$P_{ij}^{\pm} = \mathrm{i}K_n \int \mathrm{d}\boldsymbol{k} \left[\frac{K_p}{K^2} F_{pn}^{\mp\mp} \mathcal{M}_{ij}(D_{12}, D_1, D_{34}, D_{13}) - F_{in}^{\mp\mp} D_3 k_j \right.$$
$$+ \frac{K_p}{K^2} F_{pn}^{\mp\pm} \mathcal{M}_{ij}(D_{34}, D_4, D_{12}, D_{24}) - F_{in}^{\mp\pm} D_2 k_j$$
$$\left. - F_{ni}^{\mp\mp} \mathcal{N}_j(D_2, D_4, D_{24}) - F_{ni}^{\mp\pm} \mathcal{N}_j(D_3, D_1, D_{13}) \right], \tag{5.6a}$$

$$Q_{ij}^{\pm} = \mathrm{i}K_n \int \mathrm{d}\boldsymbol{k} \left[\frac{K_p}{K^2} F_{pn}^{\pm\pm} \mathcal{M}_{ij}(D_{12}, D_2, D_{34}, D_{24}) - F_{in}^{\pm\pm} D_4 k_j \right.$$
$$+ \frac{K_p}{K^2} F_{pn}^{\pm\mp} \mathcal{M}_{ij}(D_{34}, D_3, D_{12}, D_{13}) - F_{in}^{\pm\mp} D_1 k_j$$
$$\left. - F_{ni}^{\pm\pm} \mathcal{N}_j(D_1, D_3, D_{13}) - F_{ni}^{\pm\mp} \mathcal{N}_j(D_4, D_2, D_{24}) \right], \tag{5.6b}$$

where

$$\mathcal{M}_{ij}(f_1, f_2, f_3, f_4) \doteq f_1 K_i K_j - f_2 K^2 \delta_{ij} + \left(f_3 - D \frac{\boldsymbol{K} \cdot (\boldsymbol{k} + \boldsymbol{K})}{(\boldsymbol{k} + \boldsymbol{K})^2} \right) K_i k_j$$
$$+ f_4 \frac{K^2}{(\boldsymbol{k} + \boldsymbol{K})^2} (k_i + K_i) K_j, \tag{5.7}$$

$$\mathcal{N}_j(f_1, f_2, f_3) \doteq f_1 K_j + \left(f_2 - f_3 \frac{\boldsymbol{K} \cdot (\boldsymbol{k} + \boldsymbol{K})}{(\boldsymbol{k} + \boldsymbol{K})^2} \right) k_j, \tag{5.8}$$

and we use the shorthand $D \doteq D_1 + D_2 + D_3 + D_4$ and $D_{mn} \doteq D_m + D_n$.

5.2. *Dispersion relation*

The general dispersion relation and polarisations for the modulational modes of MHD turbulence are given by

$$\det \boldsymbol{\Pi} = 0, \qquad \boldsymbol{\Pi} \boldsymbol{z} = 0, \tag{5.9}$$

where $\boldsymbol{z} \doteq (\boldsymbol{z}^+, \boldsymbol{z}^-)^{\intercal}$, $\bar{\boldsymbol{z}}^{\pm} = \boldsymbol{z}^{\pm} \exp(-\mathrm{i}\Omega t + \mathrm{i}\boldsymbol{K} \cdot \boldsymbol{x})$ and the dispersion matrix $\boldsymbol{\Pi}$ is given by

$$\boldsymbol{\Pi} = \begin{pmatrix} \boldsymbol{\Pi}^{++} & \boldsymbol{\Pi}^{+-} \\ \boldsymbol{\Pi}^{-+} & \boldsymbol{\Pi}^{--} \end{pmatrix}, \tag{5.10}$$

where

$$\boldsymbol{\Pi}^{\pm\pm} = (\mathrm{i}\Omega - \nu_+ K^2) \boldsymbol{1}_3 - \boldsymbol{P}^{\pm}, \tag{5.11a}$$

$$\boldsymbol{\Pi}^{\pm\mp} = -\nu_- K^2 \boldsymbol{1}_3 - \boldsymbol{Q}^{\pm}, \tag{5.11b}$$

and $\boldsymbol{P}^{\pm}$ and $\boldsymbol{Q}^{\pm}$ are defined in (5.6*a*) and (5.6*b*), respectively. Equation (5.9) is the general dispersion relation of modulational modes of generic incompressible resistive MHD turbulence within the MTA closure (which reduces to the QLA in the limit $\tau_c \to \infty$). We emphasise that no particular properties of the turbulence, e.g. isotropy or scale-separation, have been assumed to derive these equations.

https://doi.org/10.1017/S0022377825100561 Published online by Cambridge University Press

5.3. *Examples*

Although (5.9) is powerful in its generality, the intricate dependence of the integrands in (5.6*a*) and (5.6*b*) on Ω and $\boldsymbol{K}$ means that obtaining the solutions to (5.9) is challenging in its own right. In the remainder of this section, we make a series of simplifying assumptions to obtain explicit solutions of (5.9) that allow us to compare the predictions of MFWK with those of traditional mean-field theories.

5.3.1. Isotropic turbulence

For isotropic turbulent backgrounds (3.10), we can, without loss of generality, let the modulational wavevector $\boldsymbol{K}$ lie along $\boldsymbol{e}_z$ ($\boldsymbol{K} = K\boldsymbol{e}_z$). By incompressibility, we then have $z_z^{\pm} = 0$, so we may consider the following reduced system:

$$\underline{\boldsymbol{\Pi}}\,\underline{\boldsymbol{z}} = 0, \qquad \det \underline{\boldsymbol{\Pi}} = 0, \tag{5.12}$$

where $\underline{\boldsymbol{z}} \doteq (z_x^+, z_y^+, z_x^-, z_y^-)$ and the dispersion matrix $\underline{\boldsymbol{\Pi}}$ can be written as

$$\underline{\boldsymbol{\Pi}} \doteq \begin{pmatrix} M_S + M_A & m_S + m_A & N_S + N_A & n_S + n_A \\ -m_S - m_A & M_S + M_A & -n_S - n_A & N_S + N_A \\ N_S - N_A & n_S - n_A & M_S - M_A & m_S - m_A \\ -n_S + n_A & N_S - N_A & -m_S + m_A & M_S - M_A \end{pmatrix}. \tag{5.13}$$

Here,

$$M_S \doteq \mathrm{i}\Omega - \nu_+ K^2 + \mathrm{i}K \int \mathrm{d}\boldsymbol{k} \frac{k_x^2}{k^2} \left[\frac{E_S}{4\pi k^2} \underline{\mathcal{M}}(D_1, D_{13}, D_{34}, D_{24}) + \frac{E_C}{4\pi k^2} \underline{\mathcal{M}}(D_4, D_{24}, D_{12}, D_{13}) \right], \tag{5.14a}$$

$$N_S \doteq -\nu_- K^2 + \mathrm{i}K \int \mathrm{d}\boldsymbol{k} \frac{k_x^2}{k^2} \left[\frac{E_S}{4\pi k^2} \underline{\mathcal{M}}(D_2, D_{24}, D_{34}, D_{13}) + \frac{E_C}{4\pi k^2} \underline{\mathcal{M}}(D_3, D_{13}, D_{12}, D_{24}) \right], \tag{5.14b}$$

$$M_A \doteq -\mathrm{i}K \int \mathrm{d}\boldsymbol{k} \frac{E_A}{4\pi k^2} \frac{k_x^2}{k^2} \underline{\mathcal{M}}(D_1, D_{13}, D_{34}, D_{24}), \tag{5.14c}$$

$$N_A \doteq \mathrm{i}K \int \mathrm{d}\boldsymbol{k} \frac{E_A}{4\pi k^2} \frac{k_x^2}{k^2} \underline{\mathcal{M}}(D_2, D_{24}, D_{34}, D_{13}), \tag{5.14d}$$

$$m_S \doteq K \int \mathrm{d}\boldsymbol{k} \frac{k_x^2}{k^2} \left[\frac{H_S}{8\pi k^2} \underline{\mathcal{N}}(D_3, D_4, D_{24}) + \frac{H_C}{8\pi k^2} \underline{\mathcal{N}}(D_2, D_1, D_{13}) \right], \tag{5.14e}$$

$$n_S \doteq K \int \mathrm{d}\boldsymbol{k} \frac{k_x^2}{k^2} \left[\frac{H_S}{8\pi k^2} \underline{\mathcal{N}}(D_4, D_3, D_{13}) + \frac{H_C}{8\pi k^2} \underline{\mathcal{N}}(D_1, D_2, D_{24}) \right], \tag{5.14f}$$

https://doi.org/10.1017/S0022377825100561 Published online by Cambridge University Press

$$m_A \doteq -K \int \mathrm{d}\boldsymbol{k} \frac{k_x^2}{k^2} \frac{H_A}{8\pi k^2} \underline{\mathcal{N}}(D_3, D_4, D_{24}), \tag{5.14g}$$

$$n_A \doteq K \int \mathrm{d}\boldsymbol{k} \frac{k_x^2}{k^2} \frac{H_A}{8\pi k^2} \underline{\mathcal{N}}(D_4, D_3, D_{13}), \tag{5.14h}$$

where

$$\underline{\mathcal{M}}(f_1, f_2, f_3, f_4) \doteq 2K \left(-f_1 + f_2 \frac{k_x^2}{(\boldsymbol{k}+\boldsymbol{K})^2} \right) + k_z \left(f_3 - f_4 \frac{K(k_z+K)}{(\boldsymbol{k}+\boldsymbol{K})^2} \right), \tag{5.15}$$

$$\underline{\mathcal{N}}(f_1, f_2, f_3) \doteq f_1 - \left(f_2 - f_3 \frac{K(k_z+K)}{(\boldsymbol{k}+\boldsymbol{K})^2} \right). \tag{5.16}$$

The dispersion relation can then be factored as follows:

$$\begin{aligned} \det \underline{\boldsymbol{\Pi}} &= (a + \mathrm{i}b)(a - \mathrm{i}b), \\ a &\doteq M_S^2 - M_A^2 - N_S^2 + N_A^2 - m_S^2 + m_A^2 + n_S^2 - n_A^2, \\ b &\doteq 2(M_s m_s - N_s n_s - M_A m_A + N_A n_A). \end{aligned} \tag{5.17}$$

In the remainder of the section, we focus on solving (5.17) for isotropic backgrounds as an example.

5.3.2. Ideal limit

The dispersion matrix (5.13) takes a particularly simple form in the ideal limit $\nu_\pm \to 0$. In this limit, one has $D_1 \to 1/\Omega'$ and all of the $D_{n\neq 1}$ are zero, so the modulational frequency Ω can be pulled outside of the integrals in (5.14a). Then, we have

$$\begin{aligned} M_S = \mathrm{i}\Omega + \frac{\mathrm{i}K}{\Omega'} \int \mathrm{d}\boldsymbol{k} \left\{ \frac{E_S}{4\pi k^2} \frac{k_x^2}{k^2} \left[2K \left(-1 + \frac{k_x^2}{(\boldsymbol{k}+\boldsymbol{K})^2} \right) \right] \right. \\ \left. - \frac{E_C}{4\pi k^2} \frac{k_x^2}{k^2} \left[k_z \left(\frac{K(k_z+K)}{(\boldsymbol{k}+\boldsymbol{K})^2} \right) \right] \right\}, \end{aligned} \tag{5.18a}$$

$$\begin{aligned} N_S = \frac{\mathrm{i}K}{\Omega'} \int \mathrm{d}\boldsymbol{k} \left\{ \frac{E_S}{4\pi k^2} \frac{k_x^2}{k^2} \left[k_z \left(-\frac{K(k_z+K)}{(\boldsymbol{k}+\boldsymbol{K})^2} \right) \right] \right. \\ \left. + \frac{E_C}{4\pi k^2} \frac{k_x^2}{k^2} \left[2K \left(\frac{k_x^2}{(\boldsymbol{k}+\boldsymbol{K})^2} \right) \right] \right\}, \end{aligned} \tag{5.18b}$$

$$M_A = -\frac{\mathrm{i}K}{\Omega'} \int \mathrm{d}\boldsymbol{k} \frac{E_A}{4\pi k^2} \frac{k_x^2}{k^2} \left[2K \left(-1 + \frac{k_x^2}{(\boldsymbol{k}+\boldsymbol{K})^2} \right) \right], \tag{5.18c}$$

$$N_A = \frac{\mathrm{i}K}{\Omega'} \int \mathrm{d}\boldsymbol{k} \frac{E_A}{4\pi k^2} \frac{k_x^2}{k^2} \left[k_z \left(-\frac{K(k_z+K)}{(\boldsymbol{k}+\boldsymbol{K})^2} \right) \right], \tag{5.18d}$$

https://doi.org/10.1017/S0022377825100561 Published online by Cambridge University Press

$$m_S = \frac{K}{\Omega'} \int \mathrm{d}\boldsymbol{k} \frac{k_x^2}{k^2} \left\{ \frac{H_C}{8\pi k^2} \left[-1 + \frac{K(k_z + K)}{(\boldsymbol{k} + \boldsymbol{K})^2} \right] \right\}, \tag{5.18e}$$

$$n_S = \frac{K}{\Omega'} \int \mathrm{d}\boldsymbol{k} \frac{k_x^2}{k^2} \left\{ \frac{H_S}{8\pi k^2} \left[\frac{K(k_z + K)}{(\boldsymbol{k} + \boldsymbol{K})^2} \right] + \frac{H_C}{8\pi k^2} \right\}, \tag{5.18f}$$

$$m_A = 0, \tag{5.18g}$$

$$n_A = \frac{K}{\Omega'} \int \mathrm{d}\boldsymbol{k} \frac{k_x^2}{k^2} \frac{H_A}{8\pi k^2} \left[\frac{K(k_z + K)}{(\boldsymbol{k} + \boldsymbol{K})^2} \right]. \tag{5.18h}$$

Hence, the dispersion relation (5.17) becomes the product of two quadratic polynomials in $\Omega\Omega'$. It can then be easily solved, yielding eight total solutions $\Omega(\boldsymbol{K})$. The solutions obtained in this manner are what will be presented throughout this section. Also, unless explicitly stated otherwise, we will assume the limit $St \to \infty$, i.e. $\Omega' \approx \Omega$, for clarity.

Although the Rm, $St \to \infty$ limit is formally outside of the QLA applicability domain, we believe this to be a worthwhile approach nonetheless, for the following reasons. Firstly, it is often the case that equations derived in a certain asymptotic limit qualitatively hold outside of that same limit. In particular, the accuracy of the QLA for the modulational dynamics of MHD is a rather complicated issue, and the conventional validity criterion $\min\{St, Rm\} \ll 1$ can be understood as a sufficient, but not necessary condition (Jin & Dodin 2025). Secondly, the simplified picture that emerges in the QLA can serve as a stepping stone towards a more complex future theory that will contain quasilinear dynamics as a limiting case.

In addition, we will also supplement qualitatively novel predictions of MFWK with a study of their dependence on St within the MTA-like closure used in (2.43), i.e. retaining the τ_c^{-1} term in $\Omega' = \Omega + \mathrm{i}\tau_c^{-1}$. This is, of course, a highly simplified model of the effect of the higher-order correlations neglected in the QLA, the results of which must therefore be taken with a grain of salt. Nevertheless, establishing the dependence on St within this limited approach can serve as a tentative predictor of the robustness of the collective effects found in the ideal limit ($St \gg 1$) to eddy–eddy interactions.

5.4. *Parametrization of isotropic helical background*

As discussed in § 3.1, the Wigner matrix of a generic isotropic turbulent background is fully determined by the six spectra that characterise the total energy $E_S(k)$, residual energy $E_C(k)$, cross-helicity $E_A(k)$, total (kinetic + current) helicity $H_S(k)$, residual (kinetic − current) helicity $H_C(k)$ and flow–current alignment $H_A(k)$. Solving (5.17) for different background spectra will therefore allow us to determine how the modulational dynamics of the system depend on the properties of the turbulent equilibrium.

For simplicity, we assume Gaussian test spectra:

$$\frac{E_S}{4\pi k^2} = \frac{\langle \widetilde{\boldsymbol{v}} \cdot \widetilde{\boldsymbol{v}} \rangle + \langle \widetilde{\boldsymbol{b}} \cdot \widetilde{\boldsymbol{b}} \rangle}{(\sqrt{2\pi})^3} \frac{l^3}{2} \exp\left(-\frac{l^2 k^2}{2} \right), \tag{5.19a}$$

$$\frac{E_C}{4\pi k^2} = \frac{\langle \widetilde{\boldsymbol{v}} \cdot \widetilde{\boldsymbol{v}} \rangle - \langle \widetilde{\boldsymbol{b}} \cdot \widetilde{\boldsymbol{b}} \rangle}{(\sqrt{2\pi})^3} \frac{l^3}{2} \exp\left(-\frac{l^2 k^2}{2} \right), \tag{5.19b}$$

https://doi.org/10.1017/S0022377825100561 Published online by Cambridge University Press

$$\frac{E_A}{4\pi k^2} = \frac{2\langle \widetilde{\boldsymbol{v}} \cdot \widetilde{\boldsymbol{b}} \rangle}{(\sqrt{2\pi})^3} \frac{l^3}{2} \exp\left(-\frac{l^2 k^2}{2}\right), \tag{5.19c}$$

$$\frac{H_S}{8\pi k^2} = \frac{\langle \widetilde{\boldsymbol{v}} \cdot \nabla \times \widetilde{\boldsymbol{v}} \rangle + \langle \widetilde{\boldsymbol{b}} \cdot \nabla \times \widetilde{\boldsymbol{b}} \rangle}{(\sqrt{2\pi})^3} \frac{l^3}{2} \exp\left(-\frac{l^2 k^2}{2}\right), \tag{5.19d}$$

$$\frac{H_C}{8\pi k^2} = \frac{\langle \widetilde{\boldsymbol{v}} \cdot \nabla \times \widetilde{\boldsymbol{v}} \rangle - \langle \widetilde{\boldsymbol{b}} \cdot \nabla \times \widetilde{\boldsymbol{b}} \rangle}{(\sqrt{2\pi})^3} \frac{l^3}{2} \exp\left(-\frac{l^2 k^2}{2}\right), \tag{5.19e}$$

$$\frac{H_A}{8\pi k^2} = \frac{\langle \widetilde{\boldsymbol{v}} \cdot \nabla \times \widetilde{\boldsymbol{b}} \rangle + \langle \widetilde{\boldsymbol{b}} \cdot \nabla \times \widetilde{\boldsymbol{v}} \rangle}{(\sqrt{2\pi})^3} \frac{l^3}{2} \exp\left(-\frac{l^2 k^2}{2}\right). \tag{5.19f}$$

Such spectra correspond to two-point correlations of the form

$$\langle \widetilde{\boldsymbol{v}}(\boldsymbol{x} + \boldsymbol{r}/2) \cdot \widetilde{\boldsymbol{v}}(\boldsymbol{x} - \boldsymbol{r}/2) \rangle = \langle \widetilde{\boldsymbol{v}} \cdot \widetilde{\boldsymbol{v}} \rangle \exp\left(-\frac{r^2}{2l^2}\right) \tag{5.20}$$

and are a convenient and popular choice in the mean-field dynamo literature (Rädler & Stepanov 2006; Squire & Bhattacharjee 2015). Note that we have assumed the same Gaussian form and same characteristic correlation length l for all spectra. Although this is surely a simplification, it enables a minimal parametrization of the properties of the turbulent background in terms of the single-point statistics. Although six spectra are needed to fully define the isotropic Wigner matrix, we need only five parameters to capture physical properties of the turbulent equilibria that have the potential to qualitatively impact the modulational dynamics, since

$$\tau \doteq l / v_{\mathrm{rms}} \tag{5.21}$$

simply serves to set the characteristic time scale of the problem.[8] In the following section, we will normalise all modulational frequencies, Ω to τ^{-1} and all modulational wavevectors $\boldsymbol{K}$ to l^{-1}. Then, our turbulent equilibria (after the Gaussian spectral ansatz) can be fully characterised by the five dimensionless parameters,

$$m \doteq b_{\mathrm{rms}}^2 / v_{\mathrm{rms}}^2, \tag{5.22a}$$

$$a \doteq \langle \widetilde{\boldsymbol{v}} \cdot \widetilde{\boldsymbol{b}} \rangle / v_{\mathrm{rms}} b_{\mathrm{rms}}, \tag{5.22b}$$

$$h_v \doteq l \langle \widetilde{\boldsymbol{v}} \cdot \nabla \times \widetilde{\boldsymbol{v}} \rangle / v_{\mathrm{rms}}^2, \tag{5.22c}$$

$$h_b \doteq l \langle \widetilde{\boldsymbol{b}} \cdot \nabla \times \widetilde{\boldsymbol{b}} \rangle / b_{\mathrm{rms}}^2, \tag{5.22d}$$

$$h_c \doteq l \langle \widetilde{\boldsymbol{v}} \cdot \nabla \times \widetilde{\boldsymbol{b}} \rangle / v_{\mathrm{rms}} b_{\mathrm{rms}}, \tag{5.22e}$$

where $\langle \widetilde{\boldsymbol{v}} \cdot \widetilde{\boldsymbol{v}} \rangle = v_{\mathrm{rms}}^2$ and $\langle \widetilde{\boldsymbol{b}} \cdot \widetilde{\boldsymbol{b}} \rangle = b_{\mathrm{rms}}^2$. The relative strength of magnetic fluctuations is captured by the parameter m, with $m = 0$ corresponding to hydrodynamic

[8] In general, the turbulent velocity and magnetic fields will have different characteristic time scales (Yokoi 2023; Hughes et al. 2024), and this will be an important assumption to relax in future work.

https://doi.org/10.1017/S0022377825100561 Published online by Cambridge University Press

turbulence and $m = 1$ corresponding to equipartition. The parameter a is the normalised cross-helicity, which is non-zero only in the case of 'imbalanced' MHD turbulence, i.e. when energy is unevenly distributed between $\widetilde{\boldsymbol{z}}^{+}$ and $\widetilde{\boldsymbol{z}}^{-}$. (Note that $\langle \widetilde{\boldsymbol{z}}^{+} \cdot \widetilde{\boldsymbol{z}}^{+} \rangle - \langle \widetilde{\boldsymbol{z}}^{-} \cdot \widetilde{\boldsymbol{z}}^{-} \rangle = 2\langle \widetilde{\boldsymbol{v}} \cdot \widetilde{\boldsymbol{b}} \rangle$.) The parameters h_v and h_b are the normalised kinetic and current helicities, respectively. The parameter h_c captures flow–current alignment and can be understood as the 'helical counterpart' to the cross-helicity a in that it captures the imbalance of the Elsässer-fields helicities ($\langle \widetilde{\boldsymbol{z}}^{+} \cdot \boldsymbol{\nabla} \times \widetilde{\boldsymbol{z}}^{+} \rangle - \langle \widetilde{\boldsymbol{z}}^{+} \cdot \boldsymbol{\nabla} \times \widetilde{\boldsymbol{z}}^{+} \rangle = 2\langle \widetilde{\boldsymbol{v}} \cdot \widetilde{\boldsymbol{j}} \rangle$).

Note that the parameters are scaled such that their values lie between zero and one for 'realistic' turbulence, which we define to include turbulence that can be feasibly obtained in numerical simulations with the appropriate choice of forcing functions. For example, $h_v = 1$ is commonly referred to as 'maximally helical turbulence' in the literature, and, understandably, it is a popular scenario for numerical studies of the α-effect (Brandenburg 2001; Sur, Brandenburg & Subramanian 2008; Mitra *et al*. 2009), although such turbulence is indeed highly stylised and not realistic in the usual sense of the word.

The mean-field effects associated with h_v, h_b and m are relatively well understood, since the kinetic-helicity-driven α-effect and its quenching by current helicity are arguably the central results of traditional mean-field theory for homogeneous MHD turbulence and have been the subject of much numerical investigation. Furthermore, these effects alone can be accommodated within the usual mean-field treatment where only the dynamics of the mean magnetic field are considered, since the mean induction equation decouples from the momentum equation in the absence of cross-helicity or flow–current alignment, as discussed in § 4.

For cases where $a = 0$ and $h_c = 0$, we therefore expect MFWK to largely corroborate the results of previous mean-field theories. In contrast, the mean-field dynamics associated with cross-helicity (as parametrised by a) and flow–current alignment (parametrised by h_c) have not yet been fully analysed. As discussed in § 4, cross-helicity and flow–current alignment couple the mean induction and momentum equations such that the usual kinematic approach cannot be applied. Determining the mean-field modes associated with these effects has therefore, until now, been intractable in the general case.[9] In particular, we report a new dynamo effect driven by correlations between the fluctuating velocity and current, $\langle \widetilde{\boldsymbol{v}} \cdot \widetilde{\boldsymbol{j}} \rangle$.

5.5. *Benchmark example: the α^2-dynamo*

We first benchmark the modulational dynamics obtained with the MFWK formalism by reproducing the expected α-effect and associated α^2-dynamo, i.e. solve (5.17) for $a = h_c = 0$.

5.5.1. Hydrodynamic turbulence

Figure 1 shows the modulational modes obtained from MFWK for hydrodynamic helical turbulence. As expected, the kinetic helicity supports a stationary ($\mathrm{Re}\Omega = 0$) unstable solution that is helically $\boldsymbol{b}$-polarised ($\mathrm{b}_x = \mathrm{i}\mathrm{b}_y$, $\mathrm{v}_x = \mathrm{v}_y = 0$), with a growth rate that is maximised at relatively large modulational wavelengths ($lK < 1$). To further confirm that the unstable $\boldsymbol{b}$-polarised mode is indeed the expected α^2-dynamo, figure 2 shows that the growth rate of the unstable $\boldsymbol{b}$-polarised mode indeed

[9] However, see Courvoisier et al. (2010*a*,b) for a different approach to this problem for simple cases.

https://doi.org/10.1017/S0022377825100561 Published online by Cambridge University Press

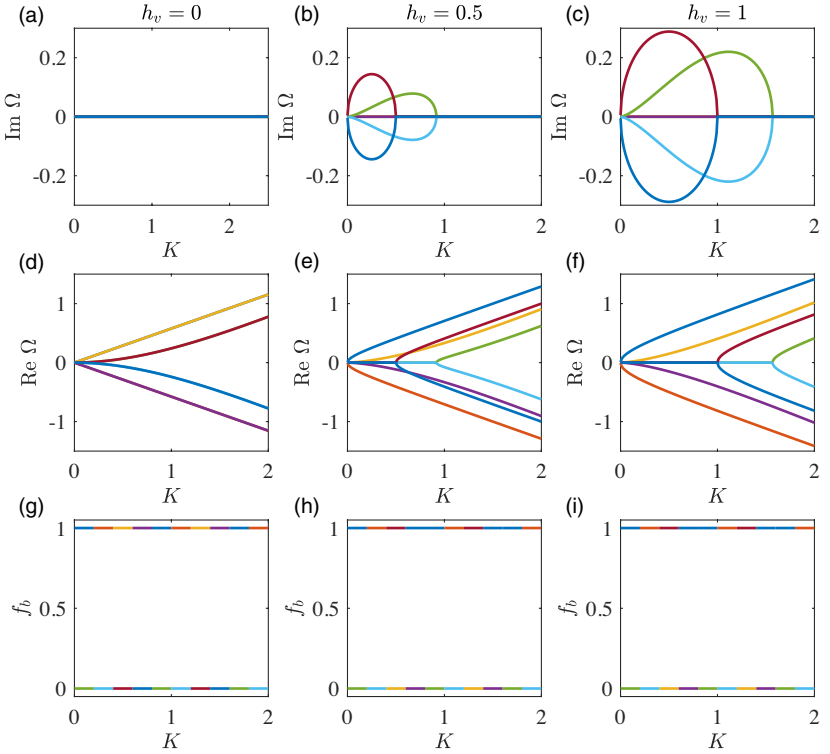

FIGURE 1. The imaginary (*a–c*) and real (*d–f*) parts of modulational frequency Ω versus modulational wavevector K at $m = a = h_b = h_c = 0$ and $St = 10^5$ for $h_v = 0$ (*a*,*d*), $h_v = 0.5$ (*b*,*e*) and $h_v = 1$ (*c*,*f*). The magnetic-energy fraction $f_b \doteq b^2/(v^2 + b^2)$ of the corresponding eigenmodes are given in panels (*g*)–(*i*). The frequencies are given in units of the inverse turnover time τ^{-1} and wavevectors are given in units of the inverse characteristic eddy size l^{-1}.

converges to the local α^2-dynamo growth rate,

$$\Gamma = \alpha K - (\eta + \beta) K^2, \tag{5.23}$$

in the $St \ll 1$ limit, and still qualitatively agrees with (5.23) for larger values of St in that it is unstable strictly for $K < 1$ and is stabilised by current helicity.

Note that in the ideal limit ($\nu_\pm \to 0$), and unless driven unstable by helicity, the modulational perturbations obtained from the MFWK framework are damped at the rate $\tau_c^{-1}/2$, irrespective of the modulational wavenumber K. In this sense, the interpretation of β in the local expansion of the EMF (also, $\mathcal{B}$ in (4.35)) as a turbulent diffusivity relies on the assumption of short correlation times, and the analogy must therefore be applied with caution. A true dissipation such as viscosity ν would damp the modulational perturbations at the rate νK^2. Figure 1 also shows another (less) unstable stationary mode that is helically $\boldsymbol{v}$-polarised ($\mathrm{i}v_x = v_y$, $b_x = b_y = 0$; note the opposite handedness relative to the $\boldsymbol{b}$-polarised mode) and is unstable for relatively larger values of K. It may seem, at first glance, that this is simply the hydrodynamic α-effect, also known as the Hα-effect (Moiseev *et al*. 1983); however, it has been argued that the latter vanishes in incompressible turbulence (Khomenko, Moiseev & Tur 1991). The incompressible analogue is known as the anisotropic kinetic alpha instability (Frisch, She & Sulem 1987); however, as the name might

https://doi.org/10.1017/S0022377825100561 Published online by Cambridge University Press

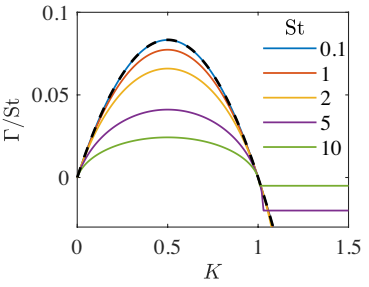

FIGURE 2. The growth rate $\Gamma \doteq \mathrm{Im}\,\Omega$ versus modulational wavenumber K for various $St \doteq \tau_c/\tau$. The classic α^2-dynamo dispersion relation (5.23) is shown in the black dashed line. The frequencies are given in units of the inverse turnover time τ^{-1} and wavevectors are given in units of the inverse characteristic eddy size l^{-1}.

suggest, this effect requires anisotropy, while our figure 1 is for an incompressible, isotropic turbulent background. Therefore, this mode remains to be interpreted. Although the generation of mean flows from hydrodynamic turbulence has received considerable attention (Rüdiger 1980; Yokoi & Yoshizawa 1993; Elperin, Kleeorin & Rogachevskii 2003; Yokoi & Brandenburg 2016), our focus is on the turbulent dynamo problem. We therefore do not discuss this hydrodynamic mode further, except to note that it is stabilised by magnetic fluctuations and vanishes entirely for $m \gtrsim 0.2$. Instead, we invite future investigations that may resolve this mystery.

5.6. *Dynamo driven by flow–current alignment*

Let us now examine the effect of flow–current alignment by solving (5.17) for non-zero values of the parameter h_c. As discussed in § 4, flow–current alignment (equivalently, an imbalance in the helicities of the Elsässer fields) couples the mean momentum and induction equations, and the fundamental modulational dynamics associated with this property have not yet been established. Let us therefore first isolate the influence of flow–current alignment by removing all other potential effects ($a = h_v = h_b = 0$). The resulting modes are shown in figure 3.

It can be seen that the flow–current alignment h_c indeed drives a strange and novel dynamo effect, the properties of which we shall discuss at length in the remainder of this section. Let us first highlight that this effect is emphatically not one that can be captured under the assumption of scale separation, as the mode is stable for $lK \lessapprox 1$. Moreover, in the absence of viscosity or resistivity, the growth rate asymptotes to a constant non-zero value as $K \to \infty$, although we will show in Appendix E that this property is limited to the case $a = 0$.

In contrast to the stationary α^2-dynamo, the unstable modes driven by flow–current alignment propagate as they grow. The propagation speed of these 'correlation waves' is given by

$$v_{\mathrm{ph}}^{\pm} = \sqrt{\langle \widetilde{\boldsymbol{z}}^{\mp} \cdot \widetilde{\boldsymbol{z}}^{\mp} \rangle / 3} \tag{5.24}$$

for $\bar{\boldsymbol{z}}^{\pm}$ polarised modes, and they are further discussed in Appendix E. Furthermore, for $a = 0$ these modes are polarised such that the associated energy is split evenly between the mean flow and magnetic fields, or equivalently, between $\bar{\boldsymbol{z}}^{+}$ and $\bar{\boldsymbol{z}}^{-}$. Note that this means that a $\langle \widetilde{\boldsymbol{v}} \cdot \widetilde{\boldsymbol{j}} \rangle$-dynamo drives a net conversion of kinetic energy

https://doi.org/10.1017/S0022377825100561 Published online by Cambridge University Press

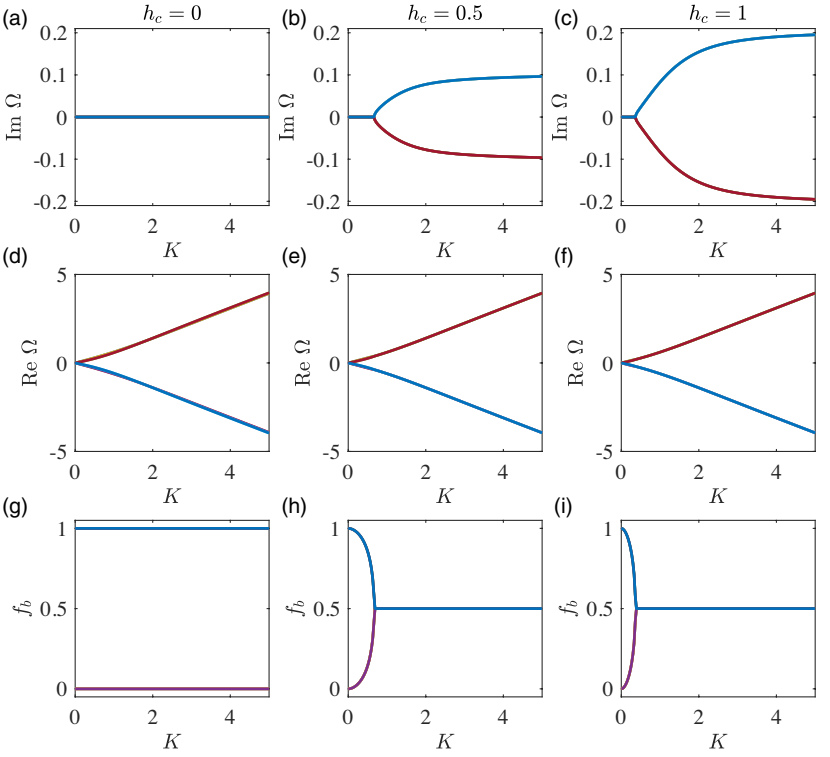

FIGURE 3. The imaginary (*a–c*) and real (*d–f*) parts of modulational frequency Ω normalised to τ^{-1} at $m = 1$, $a = h_b = h_v = 0$ and $St = 10^5$ for $h_c = 0$ (*a*,*d*), $h_c = 0.5$ (*b*, *e*) and $h_c = 1$ (*c*,*f*). The magnetic energy fraction $f_b \doteq b^2/(v^2 + b^2)$ of the corresponding eigenmodes is presented in panels (*g*)–(*i*). The frequencies are given in units of the inverse turnover time τ^{-1} and wavevectors are given in units of the inverse characteristic eddy size l^{-1}.

to magnetic energy as long as the turbulent magnetic energy is below equipartition ($m < 1$). As will be discussed shortly, the energy balance for the $a \neq 0$ case is more complicated, but the ultimate consequence of dynamo action is the same.

5.6.1. Interaction with kinetic helicity

Although the EMF for isotropic MHD turbulence can be neatly split into the sum of separate 'effects' (for example, the term proportional to the mean flow that arises from $\langle \widetilde{\boldsymbol{v}} \cdot \widetilde{\boldsymbol{j}} \rangle$), these additive contributions to the EMF certainly do not guarantee additive contributions to the solutions of (5.17), and the various statistical properties of the turbulence can interact in non-obvious ways. To illustrate this, figure 4 shows the dependence of the maximum growth rate of the $\langle \widetilde{\boldsymbol{v}} \cdot \widetilde{\boldsymbol{j}} \rangle$-dynamo on the kinetic and current helicities. This figure also compares the said maximum growth rate with that of the α^2-dynamo, particularly in how it depends on flow–current alignment and the current helicity.

It can be seen that although flow–current alignment has almost no effect on the α^2-dynamo (as opposed to current helicity, which can exactly cancel the destabilising drive for $h_v = mh_b$), kinetic helicity partially suppresses the $\langle \widetilde{\boldsymbol{v}} \cdot \widetilde{\boldsymbol{j}} \rangle$-dynamo. Interestingly, the $\langle \widetilde{\boldsymbol{v}} \cdot \widetilde{\boldsymbol{j}} \rangle$-dynamo is not perceptibly affected by current helicity. Let us therefore, in the remainder of this section, take $h_v = mh_b$, so that the α^2-dynamo

https://doi.org/10.1017/S0022377825100561 Published online by Cambridge University Press

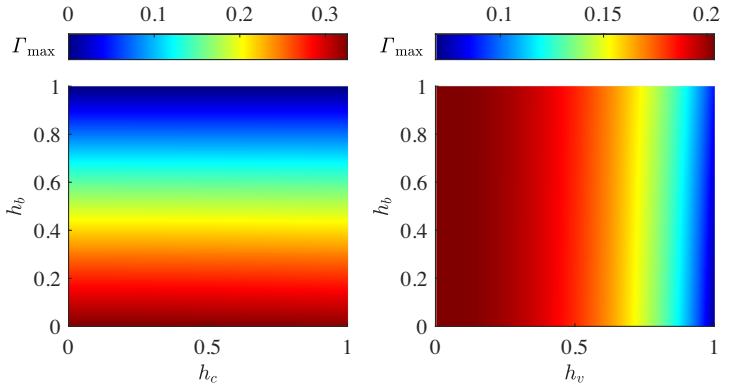

FIGURE 4. The maximum growth rate $\Gamma_{\max}$ (colourbars) of the (*a*) α^2-dynamo versus flow–current alignment (h_c) and current helicity (h_b); (*b*) $\langle\widetilde{\boldsymbol{v}}\cdot\widetilde{\boldsymbol{j}}\rangle$-dynamo versus the dimensionless kinetic (h_v) and current (h_b) helicities. The growth rates are given in units of the inverse turnover time τ^{-1} and wavevectors are given in units of the inverse characteristic eddy size l^{-1}.

is completely stabilised. This will allow us to focus on the $\langle\widetilde{\boldsymbol{v}}\cdot\widetilde{\boldsymbol{j}}\rangle$-dynamo and pin down the dimension of the parameter space that is irrelevant for the dynamics of interest.

Beyond a simple suppression of the maximum growth rate, kinetic helicity can qualitatively impact the $\langle\widetilde{\boldsymbol{v}}\cdot\widetilde{\boldsymbol{j}}\rangle$-driven mode properties shown in figure 3. As seen in figure 5, kinetic helicity breaks the degeneracy of the modes shown in figure 3, shifting one unstable branch towards higher K and the other towards lower K. For brevity, let us refer to the former mode as M_1 and the latter as M_2 (each mode label refers to two separate solutions of (5.17) with opposite signs of Re Ω). As shown in figure 5, at sufficiently high values of h_v, M_2 splits into two unstable K regions at low and high K. The modes are both circularly polarised in both z^+ and z^-, but with opposite handedness ($\mathrm{z}_x^\pm = \mathrm{i}\mathrm{z}_y^\pm$ for M_1 and $\mathrm{i}\mathrm{z}_x^\pm = \mathrm{z}_y^\pm$ for M_2).

5.6.2. Cross-helicity interaction

Let us now examine the impact of cross-helicity on the $\langle\widetilde{\boldsymbol{v}}\cdot\widetilde{\boldsymbol{j}}\rangle$-dynamo. As can be seen in figure 6, the overall effect of cross-helicity is to suppress the $\langle\widetilde{\boldsymbol{v}}\cdot\widetilde{\boldsymbol{j}}\rangle$-dynamo and shift the instability range to smaller K, for both M_1 and M_2.

At first, this may seem like bad news for the $\langle\widetilde{\boldsymbol{v}}\cdot\widetilde{\boldsymbol{j}}\rangle$-dynamo, since cross-helicity is a measure of the imbalance between the Elsässer fields ($\langle\widetilde{\boldsymbol{z}}^+\cdot\widetilde{\boldsymbol{z}}^+\rangle - \langle\widetilde{\boldsymbol{z}}^-\cdot\widetilde{\boldsymbol{z}}^-\rangle = 2\langle\widetilde{\boldsymbol{v}}\cdot\widetilde{\boldsymbol{b}}\rangle$), and flow–current alignment is a measure of the imbalance between the Elsässer helicities ($\langle\widetilde{\boldsymbol{z}}^+\cdot\widetilde{\boldsymbol{w}}^+\rangle - \langle\widetilde{\boldsymbol{z}}^-\cdot\widetilde{\boldsymbol{w}}^-\rangle = 2\langle\widetilde{\boldsymbol{v}}\cdot\widetilde{\boldsymbol{j}}\rangle$). Although they both capture some form of imbalance between the Elsässer fields, cross-helicity and flow–current alignment are entirely independent properties of MHD turbulence (determined by the spectra E_A and H_A, respectively). Whether such turbulence is realised in astrophysical environments or other environments of interest is a question that we leave to future work.

5.6.3. Dependence on St

The results presented in this section thus far are truly quasilinear, in that they are obtained in the $St \to \infty$ limit of (2.43). For 'realistic' large-Rm turbulence, St is

https://doi.org/10.1017/S0022377825100561 Published online by Cambridge University Press

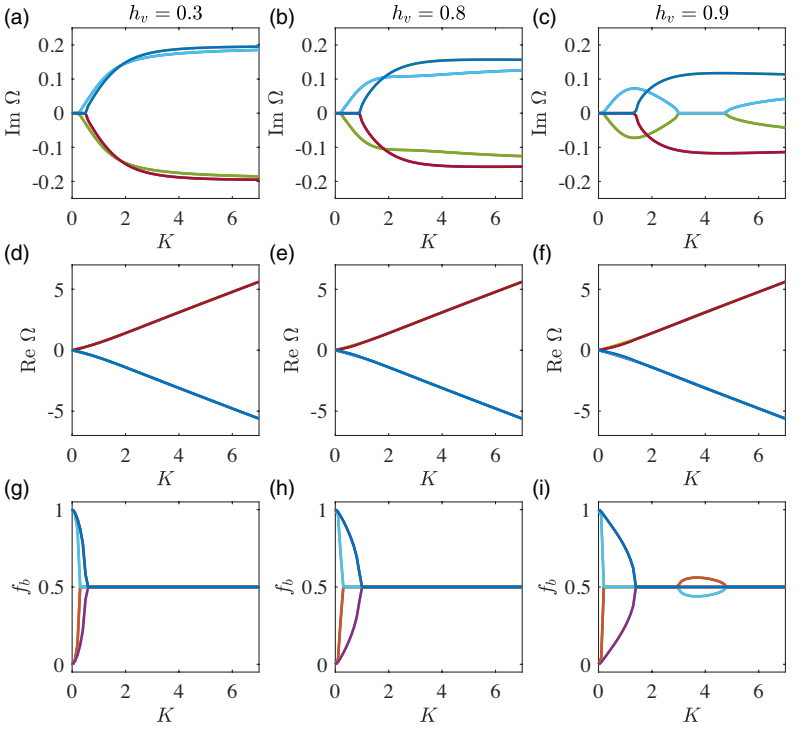

FIGURE 5. The imaginary (*a–c*) and real (*d–f*) parts of modulational frequency Ω at $m = h_c = 1$, $a = 0$ and $St = 10^5$ for $h_v = h_b = 0.3$ (*a*,*d*), $h_v = h_b = 0.8$ (*b*, *e*) and $h_v = h_b = 0.9$ (*c*,*f*). The magnetic energy fraction $f_b \doteq \mathrm{b}^2/(\mathrm{v}^2 + \mathrm{b}^2)$ of the corresponding eigenmodes are given in panels (*g–i*). The frequencies are given in units of the inverse turnover time τ^{-1} and wavevectors are given in units of the inverse characteristic eddy size l^{-1}.

expected to be order-one. Let us therefore explore how strongly damped the $\langle \widetilde{\boldsymbol{v}} \cdot \widetilde{\boldsymbol{j}} \rangle$-dynamo is by eddy–eddy collisions, at least within the simple MTA-type model used in (2.43). Figure 7(*a*) shows the maximum growth rate of the $\langle \widetilde{\boldsymbol{v}} \cdot \widetilde{\boldsymbol{j}} \rangle$-dynamo over the (m, h_c) parameter space, and figure 7(*b*) shows the critical St below which the fastest growing $\langle \widetilde{\boldsymbol{v}} \cdot \widetilde{\boldsymbol{j}} \rangle$-mode is completely stabilised. It can be seen that although the $\langle \widetilde{\boldsymbol{v}} \cdot \boldsymbol{j} \rangle$-dynamo can still be unstable at $St \sim 1$, it is, in general, far less robust to the damping effect of decorrelations than the α^2-dynamo, whose growth rate scales linearly with τ_c in the $St \to 0$ limit.

5.6.4. Discussion

In summary, we have shown that correlations between the turbulent flow and current, $\langle \widetilde{\boldsymbol{v}} \cdot \widetilde{\boldsymbol{j}} \rangle$, support a previously unknown mechanism of mean-field dynamo. The curious properties of this dynamo warrant further investigation in a number of directions that we leave to future research.

Firstly, as we have shown, the $\langle \widetilde{\boldsymbol{v}} \cdot \widetilde{\boldsymbol{j}} \rangle$-dynamo is notably less robust to the effect of eddy–eddy interactions than the classic kinetic-helicity-driven α-effect, at least within the simple MTA-type closure (2.43). Targeted direct numerical simulations (DNS) with the Elsässer fields helically driven with opposite handedness could clarify if these effects persists beyond this simple closure. There is then the separate question of whether such an imbalance in Elsässer helicities naturally occurs in astrophysical

https://doi.org/10.1017/S0022377825100561 Published online by Cambridge University Press

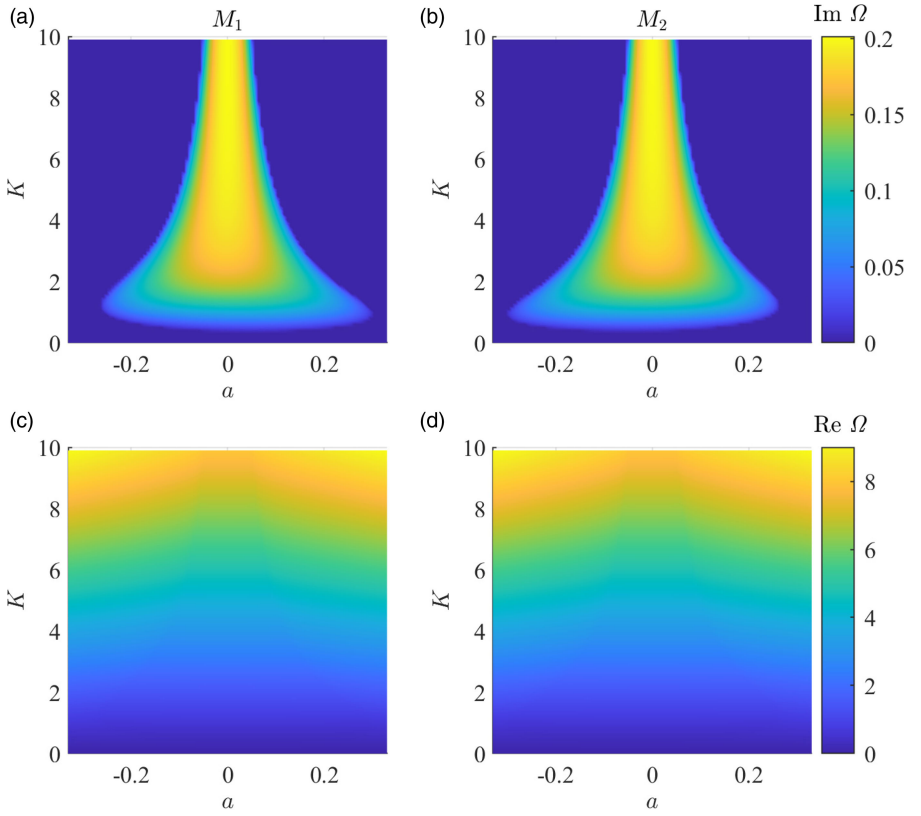

FIGURE 6. The imaginary (*a*,*b*) and real (*c*,*d*) parts of modulational frequency Ω versus K and a at $m = h_v = h_b = h_c = 1$ and $St = 10^5$, for both $\langle \widetilde{\boldsymbol{v}} \cdot \widetilde{\boldsymbol{j}} \rangle$-driven modes M_1 (*a*,*c*) and M_2 (*b*,*d*). The frequencies are given in units of the inverse turnover time τ^{-1} and wavevectors are given in units of the inverse characteristic eddy size l^{-1}.

systems, e.g. through instability-driven turbulence in the presence of a magnetic field. For instance, magnetoconvection or the Tayler instability with rotation – where the unstable eigenmodes are helical – could plausibly generate such an imbalance (Tayler 1973; Chatterjee *et al*. 2011; Bonanno *et al*. 2012). The relevance and broader significance of the $\langle \widetilde{\boldsymbol{v}} \cdot \widetilde{\boldsymbol{j}} \rangle$-dynamo, beyond being a curious collective effect that emerges in the quasilinear limit, hinges on such further investigations.

Although whether it is anything more remains to be seen, the $\langle \widetilde{\boldsymbol{v}} \cdot \widetilde{\boldsymbol{j}} \rangle$-dynamo is certainly an interesting and previously unrecognised collective effect of isotropic MHD turbulence, and it is worth pondering its properties further. Perhaps most notably, although it is a mean-field dynamo in the sense that it is a mode of the mean-field system, it is clearly not a large-scale dynamo. For the ideal balanced case shown in figure 3, the $\langle \widetilde{\boldsymbol{v}} \cdot \widetilde{\boldsymbol{j}} \rangle$-modes do not have a K at which the growth rate is maximised, instead asymptoting to its maximum growth rate as $K \to \infty$. (This, of course, would be cut off by dissipation in practice.) What kind of physical phenomenon does such a solution describe? As the growth rate is mostly insensitive to K at large K, perhaps this describes the system's propensity to form coherent structures, as any initial perturbation would roughly retain its shape while getting steeper (due to the effective high-pass filter) and growing exponentially in the linear stage. Perhaps this is some

https://doi.org/10.1017/S0022377825100561 Published online by Cambridge University Press

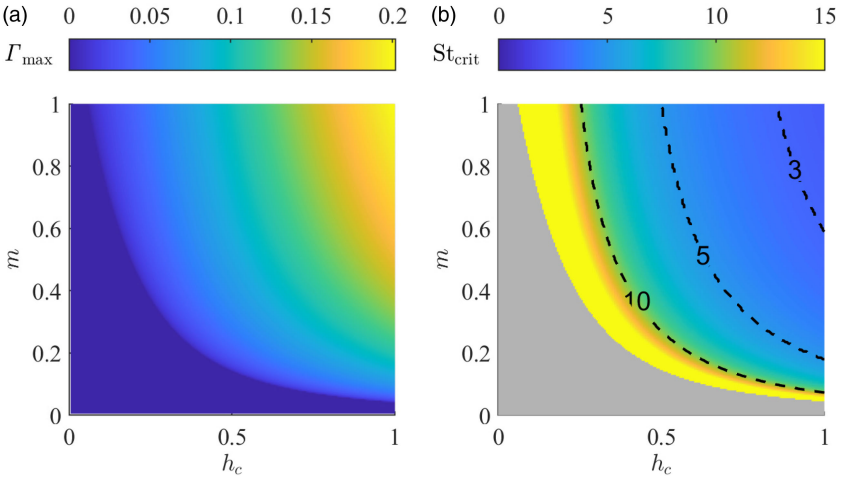

FIGURE 7. (*a*) The maximum growth rate $\Gamma_{\max}$ normalised to τ^{-1} of $\langle\widetilde{\boldsymbol{v}}\cdot\widetilde{\boldsymbol{b}}\rangle$-dynamo, at $St = 10^5$ and (*b*) critical St, St_{crit}, required for instability versus h_c and m, both at $a = h_v = h_b = 0$. Note that St_{crit} can only be defined for parameter values where the $\langle\widetilde{\boldsymbol{v}}\cdot\widetilde{\boldsymbol{b}}\rangle$-dynamo is unstable; the grey region on (*b*) indicates values of (m, h_c) for which there is no instability at any value of St. The colourbar is limited to the values (0, 15) for visibility, although St_{crit} reaches much larger values near the stability boundary.

signature of the small-scale dynamo that survives the quasilinear treatment. We leave this as an open question for future work, but highlight the stabilising effect of cross-helicity as a potential clue that may lead to the desired physical insight if pursued.

6. Summary

This paper aims to advance the existing understanding of self-organization in MHD turbulence by studying mean-field formation as a modulational instability of the underlying turbulence.

In the first part (§§ 2 and 3), we propose a wave-kinetics-based extension to mean-field theory, which we term MFWK. The MFWK is different from previous mean-field approaches in that (i) it does not assume scale separation between the mean fields and turbulence, and (ii) it self-consistently applies the mean-field treatment to the full MHD equations rather than the induction equation alone. We also introduce the modulational-instability formulation of mean-field formation, in which the equations of MFWK are linearised around statistically homogeneous turbulent equilibria.

In the second part of the paper (§§ 4 and 5), we apply the MFWK formalism to obtain two main results pertaining to the turbulent dynamo.

The first of these results is an analytical expression for the non-local response kernel relating the turbulent EMF to the mean magnetic and velocity fields for generic MHD turbulence (§ 4). To the best of our knowledge, this is the first time such an expression has been derived, as opposed to inferred through DNS. Our result is in agreement with DNS and previous analytical findings in the relevant limits, with the important exception of the dependence of the EMF on the mean flow. The disagreement between our calculation of this effect and the previous result

https://doi.org/10.1017/S0022377825100561 Published online by Cambridge University Press

(Rädler & Brandenburg 2010) highlights the importance of a self-consistent treatment of the flow.

The second main result is our prediction of a novel mean-field dynamo effect that is driven by correlations between the turbulent flow and current, $\langle \widetilde{\boldsymbol{v}} \cdot \widetilde{\boldsymbol{j}} \rangle$ (§ 5). We emphasise that such an effect cannot be captured with the usual kinematic and scale-separated approach. Although the $\langle \widetilde{\boldsymbol{v}} \cdot \widetilde{\boldsymbol{j}} \rangle$-dynamo is generally less robust than the well-known α^2-dynamo, it has the important distinction that it is not quenched by current helicity, and is, in fact, enabled rather than suppressed by magnetic fluctuations. Whether this effect survives beyond the QLA, and whether the flow–current correlations required for its onset are relevant to astrophysical environments or other environments of interest remains to be seen.

Acknowledgments

The authors thank A. Bhattacharjee for helpful comments.

Editor Steve Tobias thanks the referees for their advice in evaluating this article.

Funding

This research was supported by the U.S. Department of Energy through contract no. DE-AC02-09CH11466.

Declaration of interests

The authors report no conflict of interest.

Appendix A. Modulational instability

The MI (Zakharov & Ostrovsky 2009) is an instability of a homogeneous finite-amplitude wave that results in spontaneous symmetry breaking, namely, appearance of unstable periodic modulations of the wave amplitude. The MI is usually illustrated on the example of a nonlinear Schrödinger equation (NLSE), which arises in the context of nonlinear optics, Bose–Einstein condensates, and water waves. Although the derivation of the MI for the NLSE is commonly known (Dewar, Kruer & Manheimer 1972), we present it here for completeness, to facilitate understanding of the big picture behind the MI in the dynamo context.

The NLSE can be written in dimensionless form as

$$\mathrm{i}\partial_t \psi + \frac{1}{2}\partial_x^2 \psi = \sigma |\psi|^2 \psi, \tag{A.1}$$

where $\psi(t, x)$ is a complex field and σ is a constant. This equation has a homogeneous-wave solution

$$\psi_0(t) = A \exp(-\mathrm{i}\sigma |A|^2 t). \tag{A.2}$$

Let us consider the dynamics of such a wave if its amplitude is perturbed as follows:

$$\psi(t, x) = [1 + \eta(t, x)]\psi_0(t), \tag{A.3}$$

where $\eta \ll 1$ is a small complex function that represents an inhomogeneous perturbation to the wave amplitude. Assuming the notation

$$\hat{D} \doteq \mathrm{i}\partial_t + \frac{1}{2}\partial_x^2, \tag{A.4}$$

https://doi.org/10.1017/S0022377825100561 Published online by Cambridge University Press

we can rewrite (A.1) as follows:

$$\begin{aligned} 0 &= \hat{D}\psi - \sigma|\psi|^2\psi \\ &= \hat{D}\psi_0 + \psi_0\hat{D}\eta + \eta \mathrm{i}\partial_t\psi_0 - \sigma\left[\psi_0^*(1+\eta^*)\right]\left[\psi_0^2(1+\eta)^2\right] \\ &\approx \hat{D}\psi_0 + \psi_0(\hat{D} + \sigma|A|^2)\eta - \sigma\psi_0|A|^2(1+2\eta+\eta^*) \\ &\approx \psi_0(\hat{D}\eta - \sigma|A|^2(\eta+\eta^*)], \end{aligned} \tag{A.5}$$

where we have neglected terms quadratic in η.

This leads to the following equation for η:

$$\mathrm{i}\partial_t\eta + \frac{1}{2}\partial_x^2\eta = \sigma|A|^2(\eta+\eta^*), \tag{A.6}$$

which can be written as two real equations for $\eta_r \doteq \mathrm{Re}\ \eta$ and $\eta_i \doteq \mathrm{Im}\ \eta$,

$$\partial_t\eta_r + \frac{1}{2}\partial_x^2\eta_i = 0, \tag{A.7a}$$

$$\partial_t\eta_i - \frac{1}{2}\partial_x^2\eta_r + 2\sigma|A|^2\eta_r = 0. \tag{A.7b}$$

Seeking solutions of the form $\eta_r,\ \eta_i \sim \exp(-\mathrm{i}\Omega t + \mathrm{i}Kx)$ yields the following dispersion relation:

$$\Omega^2 = \frac{K^2}{2}\left(\frac{K^2}{2} + 2\sigma|A|^2\right). \tag{A.8}$$

It is seen from (A.8) that the primary wave (A.2) is modulationally unstable if $\sigma < 0$, specifically, for $K^2 < 4|\sigma||A|^2$. The maximum growth rate of this instability is reached at $K^2 = -2\sigma|A|^2$ and is given by $\Gamma = -\sigma|A|^2$.

If a monochromatic wave (A.2) is replaced with a broad wave spectrum, the average intensity of the corresponding oscillations exhibits a similar instability. The wave-kinetic calculation of its rate, which is also similar in spirit to our dynamo calculation in this paper, can be found, for example, in Hall *et al.* (2002). The dispersion relation of this MI reduces to (A.8) in the limit when the spectrum width is negligible, i.e. the spectrum is delta-shaped. Another arguably instructive comparison of an NLSE-based model and wave kinetics can be found in Zhou, Zhu & Dodin (2019), which addresses this problem in the context of drift-wave turbulence.

Appendix B. Review of the Wigner–Weyl transform

Here we provide a minimal, low-brow review of the Wigner–Weyl transform and list some useful properties and identities that are used throughout this work. For a more in-depth discussion, see, for example, Tracy *et al.* (2014) or Case (2008).

We will write our formulae for the specific case of operators $\hat{A}$ acting on the Hilbert space of functions $f(\boldsymbol{x})$ defined on a three-dimensional configuration space $\boldsymbol{x} \doteq (x_1, x_2, x_3)$. The formalism is, of course, more general, but here we prioritise ease of application to the specific problems considered in this paper over generality. We will also limit our consideration to scalar operators and scalar functions, as matrix-valued operators and functions can be treated element-wise with the scalar formulae.

https://doi.org/10.1017/S0022377825100561 Published online by Cambridge University Press

The Wigner–Weyl transform, or simply the Wigner transform, maps an operator $\hat{A}$ onto a function A on the 2×3-dimensional phase space $(\boldsymbol{x}, \boldsymbol{k})$,

$$A(\boldsymbol{x}, \boldsymbol{k}) = \int \mathrm{d}\boldsymbol{s}\, \mathrm{e}^{-\mathrm{i}\boldsymbol{k}\cdot\boldsymbol{s}} \langle \boldsymbol{x} + \boldsymbol{s}/2 | \hat{A} | \boldsymbol{x} - \boldsymbol{s}/2 \rangle. \tag{B.1}$$

Here, the kets $|\boldsymbol{x}\rangle$ are the eigenstates of the position operator $\hat{\boldsymbol{x}}$, normalised such that $\langle \boldsymbol{x}' | \hat{\boldsymbol{x}} | \boldsymbol{x} \rangle = \boldsymbol{x}\delta(\boldsymbol{x} - \boldsymbol{x}')$. This projection is known as the the Weyl image or symbol of $\hat{A}$.

The inverse Wigner–Weyl transform, also known as the Weyl transform, is defined as

$$\hat{A} = \frac{1}{(2\pi)^3} \int \mathrm{d}\boldsymbol{x} \int \mathrm{d}\boldsymbol{k} \int \mathrm{d}\boldsymbol{s}\, \mathrm{e}^{-\mathrm{i}\boldsymbol{k}\cdot\boldsymbol{s}} A(\boldsymbol{x}, \boldsymbol{k}) |\boldsymbol{x} - \boldsymbol{s}/2\rangle \langle \boldsymbol{x} + \boldsymbol{s}/2|. \tag{B.2}$$

It follows that the matrix elements of $\hat{A}$ in the coordinate representation, $\mathcal{A}(\boldsymbol{x}, \boldsymbol{x}') \doteq \langle \boldsymbol{x} | \hat{A} | \boldsymbol{x}' \rangle$, are connected with A via

$$\mathcal{A}(\boldsymbol{x}, \boldsymbol{x}') = \frac{1}{(2\pi)^3} \int \mathrm{d}\boldsymbol{k}\, \mathrm{e}^{-\mathrm{i}\boldsymbol{k}\cdot(\boldsymbol{x}-\boldsymbol{x}')} A\Big(\frac{\boldsymbol{x} + \boldsymbol{x}'}{2}, \boldsymbol{k}\Big), \tag{B.3}$$

and in particular,

$$\mathcal{A}(\boldsymbol{x}, \boldsymbol{x}) = \frac{1}{(2\pi)^3} \int \mathrm{d}\boldsymbol{k}\, A(\boldsymbol{x}, \boldsymbol{k}). \tag{B.4}$$

The identity, position and momentum operators have intuitive mappings,

$$\hat{1} \Leftrightarrow 1, \qquad \hat{\boldsymbol{x}} \Leftrightarrow \boldsymbol{x}, \qquad \hat{\boldsymbol{k}} \Leftrightarrow \boldsymbol{k}, \tag{B.5}$$

where we use $\Leftrightarrow$ to denote the Wigner–Weyl correspondence between operators and their symbols. Also, pure functions of the position and momentum operators map on to the same functions of the corresponding phase-space coordinate,

$$f(\hat{\boldsymbol{x}}) \Leftrightarrow f(\boldsymbol{x}), \qquad g(\hat{\boldsymbol{k}}) \Leftrightarrow g(\boldsymbol{k}) \tag{B.6}$$

for any functions f and g.

More generally, the product of operators $\hat{C} = \hat{A}\hat{B}$ maps in the following way:

$$\hat{A}\hat{B} \Leftrightarrow A(\boldsymbol{x}, \boldsymbol{k}) \star B(\boldsymbol{x}, \boldsymbol{k}), \tag{B.7}$$

where $\star$ is the Moyal star product. This product is defined as

$$A(\boldsymbol{x}, \boldsymbol{k}) \star B(\boldsymbol{x}, \boldsymbol{k}) \doteq A(\boldsymbol{x}, \boldsymbol{k}) \mathrm{e}^{\mathrm{i}\hat{\mathcal{L}}/2} B(\boldsymbol{x}, \boldsymbol{k}), \tag{B.8}$$

where $\mathcal{L}$ is the Janus operator,

$$\hat{\mathcal{L}} \doteq \overleftarrow{\partial_{\boldsymbol{x}}} \cdot \overrightarrow{\partial_{\boldsymbol{k}}} - \overleftarrow{\partial_{\boldsymbol{k}}} \cdot \overrightarrow{\partial_{\boldsymbol{x}}}, \tag{B.9}$$

and the arrows indicate the directions in which the derivatives act, so that $A\hat{\mathcal{L}}B = \{A, B\}$, where $\{\ldots, \ldots\}$ is the canonical Poisson bracket,

$$\{A, B\} \doteq (\partial_{\boldsymbol{x}} A) \cdot (\partial_{\boldsymbol{k}} B) - (\partial_{\boldsymbol{k}} A) \cdot (\partial_{\boldsymbol{x}} B). \tag{B.10}$$

In the main part of the paper, we make frequent use of the following identities:

$$A(\boldsymbol{k}) \star \mathrm{e}^{\mathrm{i}\boldsymbol{K}\cdot\boldsymbol{x}} = A(\boldsymbol{k} + \boldsymbol{K}/2)\mathrm{e}^{\mathrm{i}\boldsymbol{K}\cdot\boldsymbol{x}}, \qquad \mathrm{e}^{\mathrm{i}\boldsymbol{K}\cdot\boldsymbol{x}} \star A(\boldsymbol{k}) = A(\boldsymbol{k} - \boldsymbol{K}/2)\mathrm{e}^{\mathrm{i}\boldsymbol{K}\cdot\boldsymbol{x}}, \tag{B.11}$$

where $\boldsymbol{K}$ is a constant. For other potentially useful properties of the Moyal star, see, for example, Tracy *et al.* (2014).

https://doi.org/10.1017/S0022377825100561 Published online by Cambridge University Press

Appendix C. Quadratic invariants of MFWK

In this appendix, we show that the quasilinear MFWK equations (2.39) derived in § 2 conserve two key invariants of the original MHD model (2.1): energy (E) and cross-helicity (H_C), which are given by

$$E \doteq \frac{1}{2}\int \mathrm{d}\boldsymbol{x}\,|\bar{\boldsymbol{z}}^{+}|^2 + |\bar{\boldsymbol{z}}^{-}|^2 \tag{C.1}$$

and

$$H_C \doteq \frac{1}{2}\int \mathrm{d}\boldsymbol{x}\,|\bar{\boldsymbol{z}}^{+}|^2 - |\bar{\boldsymbol{z}}^{-}|^2. \tag{C.2}$$

Since the energy is given by $E = E^{+} + E^{-}$ and the cross-helicity is given by $H_C = E^{+} - E^{-}$, where

$$E^{\pm} = \overline{E}^{\pm} + \widetilde{E}^{\pm} = \frac{1}{2}\int \mathrm{d}\boldsymbol{x}\left(|\bar{\boldsymbol{z}}^{\pm}|^2 + |\widetilde{\boldsymbol{z}}^{\pm}|^2\right), \tag{C.3}$$

they are both conserved if and only if both $E^{\pm}$ are conserved separately,

$$\frac{\mathrm{d}E^{\pm}}{\mathrm{d}t} = 0. \tag{C.4}$$

Let us show that this is the case.

First of all, notice that the MFWK equations (2.39) can be rewritten in the following spectral form:

$$\partial_t \overline{\boldsymbol{w}}^{\pm}(\boldsymbol{q}) = \int \frac{\mathrm{d}\boldsymbol{q}'}{(2\pi)^3}[\boldsymbol{q}\cdot\bar{\boldsymbol{z}}^{\pm}(\boldsymbol{q}')][\boldsymbol{q}\times\bar{\boldsymbol{z}}^{\pm}(\boldsymbol{q}-\boldsymbol{q}')] + \boldsymbol{S}^{\pm}(\boldsymbol{q}), \tag{C.5a}$$

$$\begin{aligned}\mathrm{i}\partial_t \boldsymbol{W}(\boldsymbol{q},\boldsymbol{k}) = \int \frac{\mathrm{d}\boldsymbol{q}'}{(2\pi)^3}\Bigg\{&\boldsymbol{H}\left(\boldsymbol{q}', \boldsymbol{k}+\frac{\boldsymbol{q}-\boldsymbol{q}'}{2}\right)\boldsymbol{W}\left(\boldsymbol{q}-\boldsymbol{q}', \boldsymbol{k}-\frac{\boldsymbol{q}'}{2}\right)\\ &-\boldsymbol{W}\left(\boldsymbol{q}-\boldsymbol{q}', \boldsymbol{k}+\frac{\boldsymbol{q}'}{2}\right)\boldsymbol{H}^{\dagger}\left(\boldsymbol{q}', \boldsymbol{k}-\frac{\boldsymbol{q}-\boldsymbol{q}'}{2}\right)\Bigg\},\end{aligned} \tag{C.5b}$$

$$S_i^{\pm}(\boldsymbol{q}) = \epsilon_{ijk}\int \frac{\mathrm{d}\boldsymbol{k}}{(2\pi)^3} q_j (k_l + q_l/2) W_{kl}^{\pm\mp}(\boldsymbol{q},\boldsymbol{k}), \tag{C.5c}$$

$$\begin{aligned}H_{ij}^{\pm\pm}(\boldsymbol{q},\boldsymbol{k}) &= [\boldsymbol{k}\cdot\bar{\boldsymbol{z}}^{\mp}(\boldsymbol{q})]\left(\delta_{ij} - \frac{(k_i+q_i/2)q_j}{(\boldsymbol{k}+\boldsymbol{q}/2)^2}\right),\\ H_{ij}^{\pm\mp}(\boldsymbol{q},\boldsymbol{k}) &= q_j \bar{z}_i^{\pm}(\boldsymbol{q}) - [\boldsymbol{k}\cdot\bar{\boldsymbol{z}}^{\pm}(\boldsymbol{q})]\frac{(k_i+q_i/2)q_j}{(\boldsymbol{k}+\boldsymbol{q}/2)^2},\end{aligned} \tag{C.5d}$$

and, due to incompressibility, one also has

$$\left(k_l + \frac{q_l}{2}\right) W_{lm}^{\sigma_1\sigma_2}(\boldsymbol{q},\boldsymbol{k}) = \left(k_m - \frac{q_m}{2}\right) W_{lm}^{\sigma_1\sigma_2}(\boldsymbol{q},\boldsymbol{k}) = 0. \tag{C.6}$$

https://doi.org/10.1017/S0022377825100561 Published online by Cambridge University Press

Then,

$$\begin{aligned}\frac{\mathrm{d}\overline{E}^{\pm}}{\mathrm{d}t} &= \frac{1}{2}\frac{\mathrm{d}}{\mathrm{d}t}\int \mathrm{d}\boldsymbol{x}\ |\bar{\boldsymbol{z}}^{\pm}|^2 \\ &= \int \mathrm{d}\boldsymbol{x}\ \bar{\boldsymbol{z}}\cdot\partial_t\bar{\boldsymbol{z}} \\ &= \int \mathrm{d}\boldsymbol{x}\ \bar{\boldsymbol{z}}^{\pm}\cdot[-(\bar{\boldsymbol{z}}^{\mp}\cdot\boldsymbol{\nabla})\bar{\boldsymbol{z}}^{\pm} - \boldsymbol{\nabla}\overline{P} - \langle(\widetilde{\boldsymbol{z}}^{\mp}\cdot\boldsymbol{\nabla})\widetilde{\boldsymbol{z}}^{\pm}\rangle - \boldsymbol{\nabla}\langle\widetilde{P}\rangle] \\ &= \int \mathrm{d}\boldsymbol{x}\left\{\boldsymbol{\nabla}\cdot\left(\frac{1}{2}|\bar{\boldsymbol{z}}^{\pm}|^2\bar{\boldsymbol{z}}^{\mp} - (\overline{P}+\widetilde{P})\bar{\boldsymbol{z}}^{\pm}\right) - \mathrm{i}\bar{z}_l^{\pm}\int\frac{\mathrm{d}\boldsymbol{k}}{(2\pi)^3}\,k_m\star W_{lm}^{\pm\mp}\right\} \\ &= -\mathrm{i}\int\frac{\mathrm{d}\boldsymbol{k}}{(2\pi)^3}\int\frac{\mathrm{d}\boldsymbol{q}}{(2\pi)^3}\,\bar{z}_l^{\pm}(-\boldsymbol{q})\left(k_m+\frac{q_m}{2}\right)W_{lm}^{\pm\mp}(\boldsymbol{q},\boldsymbol{k}) \\ &= \mathrm{Im}\int\frac{\mathrm{d}\boldsymbol{k}}{(2\pi)^3}\int\frac{\mathrm{d}\boldsymbol{q}}{(2\pi)^3}\,\bar{z}_l^{\pm}(-\boldsymbol{q})W_{lm}^{\pm\mp}(\boldsymbol{q},\boldsymbol{k})q_m, \end{aligned} \tag{C.7}$$

and

$$\begin{aligned}\frac{\mathrm{d}\widetilde{E}^{\pm}}{\mathrm{d}t} &= \frac{\mathrm{d}}{\mathrm{d}t}\frac{1}{2}\int \mathrm{d}\boldsymbol{x}\ |\widetilde{\boldsymbol{z}}^{\pm}(\boldsymbol{x})|^2 \\ &= \frac{1}{2}\int \mathrm{d}\boldsymbol{x}\int\frac{\mathrm{d}\boldsymbol{k}}{(2\pi)^3}\,\partial_t W_{ll}^{\pm\pm}(\boldsymbol{x},\boldsymbol{k}) \\ &= \mathrm{Im}\int \mathrm{d}\boldsymbol{x}\int\frac{\mathrm{d}\boldsymbol{k}}{(2\pi)^3}\left[H_{lm}^{\pm\pm}\star W_{ml}^{\pm\pm} + H_{lm}^{\pm\mp}\star W_{ml}^{\mp\pm}\right] \\ &= \mathrm{Im}\int\frac{\mathrm{d}\boldsymbol{k}}{(2\pi)^3}\int\frac{\mathrm{d}\boldsymbol{q}}{(2\pi)^3}\Big[\,H_{lm}^{\pm\pm}(-\boldsymbol{q},\boldsymbol{k})W_{ml}^{\pm\pm}(\boldsymbol{q},\boldsymbol{k}) \\ &\qquad\qquad + H_{lm}^{\pm\mp}(-\boldsymbol{q},\boldsymbol{k})W_{ml}^{\mp\pm}(\boldsymbol{q},\boldsymbol{k})\Big] \\ &= \mathrm{Im}\int\frac{\mathrm{d}\boldsymbol{k}}{(2\pi)^3}\int\frac{\mathrm{d}\boldsymbol{q}}{(2\pi)^3}\left\{\left[[\boldsymbol{k}\cdot\bar{\boldsymbol{z}}^{\mp}(-\boldsymbol{q})]\left(\delta_{lm}+\frac{(k_l-q_l/2)q_m}{(\boldsymbol{k}-\boldsymbol{q}/2)^2}\right)\right]W_{ml}^{\pm\pm}(\boldsymbol{q},\boldsymbol{k})\right. \\ &\qquad\qquad \left. -\left[q_m\bar{z}_l^{\pm}(-\boldsymbol{q}) + [\boldsymbol{k}\cdot\bar{\boldsymbol{z}}^{\pm}(\boldsymbol{q})]\frac{(k_l-q_l/2)q_m}{(\boldsymbol{k}+\boldsymbol{q}/2)^2}\right]W_{ml}^{\mp\pm}(\boldsymbol{q},\boldsymbol{k})\right\} \\ &= -\mathrm{Im}\int\frac{\mathrm{d}\boldsymbol{k}}{(2\pi)^3}\int\frac{\mathrm{d}\boldsymbol{q}}{(2\pi)^3}\,\bar{z}_l^{\pm}(-\boldsymbol{q})W_{lm}^{\pm\mp}(\boldsymbol{q},\boldsymbol{k})q_m. \end{aligned} \tag{C.8}$$

Therefore, $\overline{E}^{\pm}+\widetilde{E}^{\pm}=\text{const}$, and energy and cross-helicity are conserved for our quasilinear system.

Appendix D. Diagonalising transformation for 2-D MHD

In this appendix, we show that the Hamiltonian for the fluctuating fields in 2-D is approximately diagonalisable in the strong magnetic field limit, $|\bar{\boldsymbol{b}}| \gg |\bar{\boldsymbol{v}}|$.

Consider 2-D dynamics in which $\boldsymbol{z}^{\pm}$ lie in the (x, y) plane and $\partial_z = 0$. In this case, the only potentially non-zero component of $\boldsymbol{w}^{\pm}$ is the z-component, $w^{\pm} \doteq (\boldsymbol{\nabla}\times\boldsymbol{z}^{\pm})_z$. Then, the vector equation (2.10) can be replaced with a scalar equation for $w^{\pm}$,

$$\partial_t w^{\pm} = -(\boldsymbol{z}^{\mp}\cdot\boldsymbol{\nabla})w^{\pm} + \boldsymbol{\nabla}\boldsymbol{z}^{\mp} : \boldsymbol{\nabla}\boldsymbol{\nabla}\hat{k}^{-2}w^{\pm}. \tag{D.1}$$

https://doi.org/10.1017/S0022377825100561 Published online by Cambridge University Press

Splitting the Elsässer vorticities in fluctuating and averaged parts ($w^{\pm} = \overline{w}^{\pm} + \widetilde{w}^{\pm}$ with $\langle \widetilde{w} \rangle = 0$), one obtains the following equation for the fluctuating fields $\widetilde{w}^{\pm}$:

$$\partial_t \widetilde{w}^{\pm} = \big(-(\bar{z}^{\mp} \cdot \nabla) + \nabla \bar{z}^{\mp} : \nabla\nabla \hat{k}^{-2} \big) \widetilde{w}^{\pm} + \big[-\big(\nabla^2 \bar{z}^{\pm} \cdot \nabla \big) - \nabla \bar{z}^{\pm} : \nabla\nabla \hat{k}^{-2} \big] \widetilde{w}^{\mp}, \tag{D.2}$$

where $\bar{z}^{\pm} \doteq \mathrm{i}\hat{k}^{-2}(\hat{k}_y \overline{w}^{\pm}, -\hat{k}_x \overline{w}^{\pm}, 0)^{\intercal}$ and the terms nonlinear in the fluctuating fields have been neglected. Equation (D.2) can be written as a vector Schrödinger equation for the field variables $\xi^{\pm} = \hat{k}^{-1} \widetilde{w}^{\pm}$,

$$\mathrm{i}\partial_t \boldsymbol{\xi} = \hat{\boldsymbol{\mathcal{H}}} \boldsymbol{\xi}, \tag{D.3}$$

where $\boldsymbol{\xi} \doteq (\xi^{+}, \xi^{-})^{\intercal}$ and the Hamiltonian $\hat{\boldsymbol{\mathcal{H}}}$ is given by

$$\hat{\boldsymbol{\mathcal{H}}} \doteq \begin{pmatrix} \hat{\mathcal{H}}^{+} & \hat{\chi}^{+} \\ \hat{\chi}^{-} & \hat{\mathcal{H}}^{-} \end{pmatrix}, \tag{D.4}$$

where $\hat{\mathcal{H}}^{\pm}$ are Hermitian operators given by

$$\begin{aligned} \hat{\mathcal{H}}^{\pm} &\doteq \hat{k}^{-1} \big[(\bar{z}^{\pm} \cdot \hat{\boldsymbol{k}}) - i((\nabla \bar{z}^{\pm} \cdot \hat{\boldsymbol{k}}) \cdot \hat{\boldsymbol{k}}) \hat{k}^{-2} \big] \hat{k} \\ &= \hat{k}^{-1} \hat{k}_l (\bar{z}^{\mp} \cdot \hat{\boldsymbol{k}}) \hat{k}_l \hat{k}^{-1}, \end{aligned} \tag{D.5}$$

and we have also introduced the following operators:

$$\begin{aligned} \hat{\chi}^{\pm} &\doteq \hat{k}^{-1} \big[i((\nabla \bar{z}^{\pm} \cdot \hat{\boldsymbol{k}}) \cdot \hat{\boldsymbol{k}}) \hat{k}^{-2} + (\nabla^2 \bar{z}^{\pm} \cdot \hat{\boldsymbol{k}}) \hat{k}^{-2} \big] \hat{k} \\ &= \mathrm{i}\hat{k}^{-1} \hat{k}_l (\partial_l \bar{z}^{\mp} \cdot \hat{\boldsymbol{k}}) \hat{k}^{-1}. \end{aligned} \tag{D.6}$$

Suppose we are interested in the quasiparticle dynamics up to $O(\epsilon^2)$ in the GO parameter $\epsilon \doteq l/L$. Since the off-diagonal elements of the Hamiltonian $\hat{\chi}^{\pm}$ are $O(\epsilon)$, one cannot treat the Elsässer vorticities $\widetilde{w}^{\pm}$ as decoupled scalar waves. Let us therefore consider the transformed variable $\boldsymbol{\psi} \doteq \hat{\boldsymbol{U}} \boldsymbol{\xi}$, where the operator $\hat{\boldsymbol{U}}$ is taken to be of the form

$$\hat{\boldsymbol{U}} = \begin{pmatrix} 1 & \hat{a} \\ \hat{b} & 1 \end{pmatrix}, \tag{D.7}$$

which has the inverse

$$\hat{\boldsymbol{U}}^{-1} = \begin{pmatrix} \hat{g}_1 & -\hat{g}_1 \hat{a} \\ -\hat{g}_2 \hat{b} & \hat{g}_2 \end{pmatrix}, \tag{D.8}$$

where

$$\hat{g}^1 \doteq (1 - \hat{a}\hat{b})^{-1}, \qquad \hat{g}_2 \doteq (1 - \hat{b}\hat{a})^{-1}. \tag{D.9}$$

If $\partial_t \hat{\boldsymbol{U}}$ is negligible, (D.3) can be rewritten as

$$\mathrm{i}\partial_t \boldsymbol{\psi} = \hat{\boldsymbol{H}} \boldsymbol{\psi} \tag{D.10}$$

with the transformed Hamiltonian

$$\begin{aligned} \hat{\boldsymbol{H}} &\doteq \hat{\boldsymbol{U}} \hat{\boldsymbol{\mathcal{H}}} \hat{\boldsymbol{U}}^{-1} \\ &= \begin{pmatrix} \hat{g}_1 (\hat{\mathcal{H}}^{+} + \hat{\chi}^{+}\hat{b} - \hat{a}\hat{\chi}^{--}\hat{a}\hat{\mathcal{H}}^{-}\hat{b}) & \hat{g}_1 (\hat{\mathcal{H}}^{+}\hat{a} + \hat{\chi}^{+} - \hat{a}\hat{\chi}^{-}\hat{a} - \hat{a}\hat{\mathcal{H}}^{-}) \\ \hat{g}_2 (-\hat{b}\hat{\mathcal{H}}^{+} - \hat{b}\hat{\chi}^{+}\hat{b} + \hat{\chi}^{-} + \hat{\mathcal{H}}^{-}\hat{b}) & \hat{g}_2 (-\hat{b}\hat{\mathcal{H}}^{+}\hat{a} - \hat{b}\hat{\chi}^{+} + \hat{\chi}^{-}\hat{a} + \hat{\mathcal{H}}^{-}) \end{pmatrix}. \end{aligned} \tag{D.11}$$

https://doi.org/10.1017/S0022377825100561 Published online by Cambridge University Press

To diagonalise $\hat{\boldsymbol{H}}$, the operators $\hat{a}$ and $\hat{b}$ must satisfy

$$\hat{\mathcal{H}}^{+}\hat{a} + \hat{\chi}^{+} - \hat{a}\hat{\chi}^{-}\hat{a} - \hat{a}\hat{\mathcal{H}}^{-} = 0, \tag{D.12a}$$

$$-\hat{b}\hat{\mathcal{H}}^{+} - \hat{b}\hat{\chi}^{+}\hat{b} + \hat{\chi}^{-} + \hat{\mathcal{H}}^{-}\hat{b} = 0, \tag{D.12b}$$

which also simplifies the diagonal elements,

$$\begin{aligned}\hat{\mathrm{H}}_{11} &= \hat{g}_1[\hat{\mathcal{H}}^{+} + \hat{\chi}^{+}\hat{b} - \hat{a}\hat{\chi}^{--}\hat{a}(\hat{b}\hat{\mathcal{H}}^{+} + \hat{b}\hat{\chi}^{+}\hat{b} - \hat{\chi}^{-})] \\ &= \hat{\mathcal{H}}^{+} + \hat{\chi}^{+}\hat{b}, \\ \hat{\mathrm{H}}_{22} &= \hat{g}_2[-\hat{b}(-\hat{\chi}^{+} + \hat{a}\hat{\chi}^{-}\hat{a} + \hat{a}\hat{\mathcal{H}}^{-}) - \hat{b}\hat{\chi}^{+} + \hat{\chi}^{-}\hat{a} + \hat{\mathcal{H}}^{-}] \\ &= \hat{\mathcal{H}}^{-} + \hat{\chi}^{-}\hat{a},\end{aligned} \tag{D.13}$$

such that

$$\hat{\boldsymbol{H}} = \begin{pmatrix} \hat{\mathcal{H}}^{+} + \hat{\chi}^{+}\hat{b} & 0 \\ 0 & \hat{\mathcal{H}}^{-} + \hat{\chi}^{-}\hat{a} \end{pmatrix} \tag{D.14}$$

for $\hat{a}$ and $\hat{b}$ satisfying (D.12).

In the strong magnetic field limit, $|\bar{\boldsymbol{v}}|/|\bar{\boldsymbol{b}}| \sim O(\epsilon)$, (D.12) can be solved approximately. To leading order in ϵ, (D.12) become

$$\hat{a}(\hat{\mathcal{H}}^{+} - \hat{\mathcal{H}}^{-}) + \hat{\chi}^{+} = 0, \tag{D.15a}$$

$$\hat{b}(\hat{\mathcal{H}}^{--}\hat{\mathcal{H}}^{+}) + \hat{\chi}^{-} = 0, \tag{D.15b}$$

which yield the approximate solutions

$$\hat{a} \approx -\frac{1}{2}\hat{\chi}^{+}\hat{\mathcal{H}}_b^{-1}, \qquad \hat{b} \approx \frac{1}{2}\hat{\chi}^{-}\hat{\mathcal{H}}_b^{-1}, \tag{D.16}$$

where $\hat{\mathcal{H}}_b \doteq (\hat{\mathcal{H}}^{+} - \hat{\mathcal{H}}^{-})/2$. Since $\hat{\chi}^{+}$ and $\hat{\chi}^{-}$ commute within the accuracy of the approximation, we finally have

$$\hat{\boldsymbol{H}} = \begin{pmatrix} \hat{\mathcal{H}}^{+} - \hat{\sigma} & 0 \\ 0 & \hat{\mathcal{H}}^{-} + \hat{\sigma} \end{pmatrix} + O(\epsilon^2), \tag{D.17}$$

where

$$\hat{\sigma} \doteq \frac{1}{2}\hat{\chi}^{+}\hat{\chi}^{-}\hat{\mathcal{H}}_b^{-1}. \tag{D.18}$$

In this approximation, ψ^{+} and ψ^{-} evolve independently and are governed by the Hamiltonians $\hat{\mathcal{H}}^{+} - \hat{\sigma}$ and $\hat{\mathcal{H}}^{-} + \hat{\sigma}$, respectively.

Appendix E. Correlation waves

As can be seen in the many plots of modulational frequency versus wavenumber $\Omega(K)$ throughout § 5, the generic modulational response to a high-K mean-field perturbation takes the form of a sound-like travelling wave, i.e. a wave with linear $\Omega(K)$. Although instabilities driven by the various helicities may modify or dominate over this oscillatory tendency at smaller values of K, it can be seen that the real

https://doi.org/10.1017/S0022377825100561 Published online by Cambridge University Press

components of all solutions of (5.17) eventually converge to the universal sound-like solutions as $K \to \infty$. Let us therefore consider the $K \to \infty$ limit of (5.18),

$$M_S \to \mathrm{i}\Omega + \frac{\mathrm{i}}{\Omega'}\left(-\frac{1}{3}\langle\widetilde{v}^2+\widetilde{b}^2\rangle K^2 + \frac{1}{5}\langle\widetilde{w}^2+\widetilde{j}^2\rangle - \frac{1}{30}\langle\widetilde{w}^2-\widetilde{j}^2\rangle\right), \tag{E.1a}$$

$$N_S \to \frac{\mathrm{i}}{\Omega'}\left(-\frac{1}{30}\langle\widetilde{w}^2+\widetilde{j}^2\rangle + \frac{1}{5}\langle\widetilde{w}^2-\widetilde{j}^2\rangle\right), \tag{E.1b}$$

$$M_A \to \frac{\mathrm{i}}{\Omega'}\left(\frac{2}{3}\langle\widetilde{\boldsymbol{v}}\cdot\widetilde{\boldsymbol{b}}\rangle K^2 - \frac{2}{5}\langle\widetilde{\boldsymbol{w}}\cdot\widetilde{\boldsymbol{j}}\rangle\right), \tag{E.1c}$$

$$N_A \to -\frac{\mathrm{i}}{15\Omega'}\langle\widetilde{\boldsymbol{w}}\cdot\widetilde{\boldsymbol{j}}\rangle, \tag{E.1d}$$

$$m_S \to 0, \tag{E.1e}$$

$$n_S \to \frac{1}{3\Omega'}\langle\widetilde{\boldsymbol{v}}\cdot\boldsymbol{\nabla}\times\widetilde{\boldsymbol{v}}\rangle K, \tag{E.1f}$$

$$n_A \to \frac{1}{3\Omega'}\langle\widetilde{\boldsymbol{v}}\cdot\widetilde{\boldsymbol{j}}\rangle K, \tag{E.1g}$$

where

$$\begin{gathered}
\int_0^\infty \mathrm{d}k\, k^2 E_S(k) = \frac{1}{2}\langle\widetilde{w}^2+\widetilde{j}^2\rangle,\\
\int_0^\infty \mathrm{d}k\, k^2 E_C(k) = \frac{1}{2}\langle\widetilde{w}^2-\widetilde{j}^2\rangle,\\
\int_0^\infty \mathrm{d}k\, k^2 E_A(k) = \langle\widetilde{\boldsymbol{w}}\cdot\widetilde{\boldsymbol{j}}\rangle,\\
\int_0^\infty \mathrm{d}k\, k^2 H_S(k) = \langle\widetilde{\boldsymbol{w}}\cdot\boldsymbol{\nabla}\times\widetilde{\boldsymbol{w}} + \widetilde{\boldsymbol{j}}\cdot\boldsymbol{\nabla}\times\widetilde{\boldsymbol{j}}\rangle,\\
\int_0^\infty \mathrm{d}k\, k^2 H_C(k) = \langle\widetilde{\boldsymbol{w}}\cdot\boldsymbol{\nabla}\times\widetilde{\boldsymbol{w}} - \widetilde{\boldsymbol{j}}\cdot\boldsymbol{\nabla}\times\widetilde{\boldsymbol{j}}\rangle,\\
\int_0^\infty \mathrm{d}k\, k^2 H_A(k) = \langle\widetilde{\boldsymbol{w}}\cdot\boldsymbol{\nabla}\times\widetilde{\boldsymbol{j}} + \widetilde{\boldsymbol{j}}\cdot\boldsymbol{\nabla}\times\widetilde{\boldsymbol{w}}\rangle,
\end{gathered} \tag{E.2}$$

and, as before, $m_A = 0$. To the leading order in K, and taking $\Omega' = \Omega$ for simplicity, we then have

$$M_S = \mathrm{i}\Omega - \frac{\mathrm{i}}{3\Omega'}\langle\widetilde{v}^2+\widetilde{b}^2\rangle K^2, \tag{E.3}$$

$$M_A = \frac{2\mathrm{i}}{3\Omega'}\langle\widetilde{\boldsymbol{v}}\cdot\widetilde{\boldsymbol{b}}\rangle, \tag{E.4}$$

https://doi.org/10.1017/S0022377825100561 Published online by Cambridge University Press

$$\underline{\boldsymbol{\Pi}} \doteq \frac{\mathrm{i}}{\Omega}\begin{pmatrix}\left(\Omega^2 - \dfrac{\langle \widetilde{\boldsymbol{z}}^- \cdot \widetilde{\boldsymbol{z}}^- \rangle}{3}K^2\right)\mathbf{1}_2 & \mathbf{0}_2 \\ \mathbf{0}_2 & \left(\Omega^2 - \dfrac{\langle \widetilde{\boldsymbol{z}}^+ \cdot \widetilde{\boldsymbol{z}}^+ \rangle}{3}K^2\right)\mathbf{1}_2\end{pmatrix}, \tag{E.5}$$

where $\mathbf{1}_2$ is the 2×2 identity matrix and $\mathbf{0}_2$ is the 2×2 zero matrix. It can be easily seen from (E.5) that the sound-like modes take the form of $\bar{\boldsymbol{z}}^{\pm}$ polarised modes propagating with two different speeds $V_{\pm}$,

$$\Omega^2 = V_{\pm}^2 K^2, \qquad V_{\pm} \doteq \sqrt{\langle \widetilde{\boldsymbol{z}}^{\mp} \cdot \widetilde{\boldsymbol{z}}^{\mp} \rangle / 3}, \tag{E.6}$$

provided that the turbulence is imbalanced, i.e. $\langle \widetilde{\boldsymbol{z}}^+ \cdot \widetilde{\boldsymbol{z}}^+ \rangle \neq \langle \widetilde{\boldsymbol{z}}^- \cdot \widetilde{\boldsymbol{z}}^- \rangle$.

If the turbulence is balanced, i.e.($\langle \widetilde{\boldsymbol{z}}^+ \cdot \widetilde{\boldsymbol{z}}^+ \rangle = \langle \widetilde{\boldsymbol{z}}^- \cdot \widetilde{\boldsymbol{z}}^- \rangle$), and thus $V_+ = V_- \equiv V$, $\Omega^2 = V^2K^2$ can eliminate all of the leading-order ($\sim K^2$) terms in (E.5) then distinguishing the two modes requires consideration of higher-order corrections. Letting $\Omega^2 = V^2K^2 + \delta\Omega^2$, we have to keep the next highest order in K,

$$\Omega M_S \to \mathrm{i}\delta\Omega^2, \qquad \Omega n_S \to \frac{\langle \widetilde{\boldsymbol{v}} \cdot \widetilde{\boldsymbol{w}} \rangle}{3}K, \qquad \Omega n_A \to \frac{\langle \widetilde{\boldsymbol{v}} \cdot \widetilde{\boldsymbol{j}} \rangle}{3}K, \tag{E.7}$$

$$\underline{\boldsymbol{\Pi}} \doteq \frac{1}{\Omega}\begin{pmatrix} \mathrm{i}\delta\Omega^2 & 0 & 0 & \frac{\langle \widetilde{\boldsymbol{v}}\cdot\widetilde{\boldsymbol{w}}\rangle + \langle \widetilde{\boldsymbol{v}}\cdot\widetilde{\boldsymbol{j}}\rangle}{3}K \\ 0 & \mathrm{i}\delta\Omega^2 & -\frac{\langle \widetilde{\boldsymbol{v}}\cdot\widetilde{\boldsymbol{w}}\rangle + \langle \widetilde{\boldsymbol{v}}\cdot\widetilde{\boldsymbol{j}}\rangle}{3}K & 0 \\ 0 & \frac{\langle \widetilde{\boldsymbol{v}}\cdot\widetilde{\boldsymbol{w}}\rangle - \langle \widetilde{\boldsymbol{v}}\cdot\widetilde{\boldsymbol{j}}\rangle}{3}K & \mathrm{i}\delta\Omega^2 & 0 \\ -\frac{\langle \widetilde{\boldsymbol{v}}\cdot\widetilde{\boldsymbol{w}}\rangle - \langle \widetilde{\boldsymbol{v}}\cdot\widetilde{\boldsymbol{j}}\rangle}{3}K & 0 & 0 & \mathrm{i}\delta\Omega^2 \end{pmatrix}, \tag{E.8}$$

and we find from the dispersion relation that

$$\delta\Omega = \pm\frac{\sqrt{\langle \widetilde{\boldsymbol{v}} \cdot \widetilde{\boldsymbol{w}} \rangle^2 - \langle \widetilde{\boldsymbol{v}} \cdot \widetilde{\boldsymbol{j}} \rangle^2}}{3}K. \tag{E.9}$$

In other words, these solutions support a finite growth rate even as $K \to \infty$,

$$\Gamma_\infty^2 = \frac{\langle \widetilde{\boldsymbol{v}} \cdot \widetilde{\boldsymbol{j}} \rangle^2 - \langle \widetilde{\boldsymbol{v}} \cdot \widetilde{\boldsymbol{w}} \rangle^2}{2\langle \widetilde{v}^2 + \widetilde{b}^2 \rangle}. \tag{E.10}$$

The polarisations of these modes can be found from (E.8) and (E.9), but they are fairly complicated, so we will not do it here.

Finally, note that the decorrelation term can be restored in the calculations above by setting $\Omega^2 \to \Omega\Omega'$. Since $\Omega\Omega' = (\Omega + \mathrm{i}\tau_c^{-1}/2)^2 - (\tau_c^{-1}/2)^2$, we can see that the modes discussed above are damped at a rate $\tau_c^{-1}/2$.

REFERENCES

BENDRE, A. B. & SUBRAMANIAN, K. 2022 Non-locality of the turbulent electromotive force. *Mon. Not. R. Astron. Soc.* **511**, 4454–4463.

BLACKMAN, E. G. & FIELD, G. B. 2002 New dynamical mean-field dynamo theory and closure approach. *Phys. Rev. Lett.* **89**, 265007.

https://doi.org/10.1017/S0022377825100561 Published online by Cambridge University Press

BONANNO, A., BRANDENBURG, A., SORDO, D., Fabio, & MITRA, D. 2012 Breakdown of chiral symmetry during saturation of the tayler instability. *Phys. Rev. E* **86**, 016313.

BRANDENBURG, A. 2001 The inverse cascade and nonlinear alpha-effect in simulations of isotropic helical hydromagnetic turbulence. *Astrophys. J.* **550**, 824–840.

BRANDENBURG, A. 2018 Advances in mean-field dynamo theory and applications to astrophysical turbulence. *J. Plasma Phys.* **84**, 735840404.

BRANDENBURG, A., ELSTNER, D., MASADA, Y. & PIPIN, V. 2023 Turbulent processes and mean-field dynamo. *Space Sci. Rev.* **219**.

BRANDENBURG, A. & SUBRAMANIAN, K. 2005 Minimal tau approximation and simulations of the alpha effect. *Astron. Astrophys.* **439**, 835–843.

BRANDENBURG, A., RÄDLER, K.-H. & SCHRINNER, M. 2008 Scale dependence of alpha effect and turbulent diffusivity. *Astron. Astrophys.* **482**, 739–746.

CASE, W. B. 2008 Wigner functions and Weyl transforms for pedestrians. *Am. J. Phys.* **76**, 937–946.

CHARBONNEAU, P. 2014 Solar dynamo theory. *Annu. Rev. Astron. Astrophys.* **52**, 251–290.

CHATTERJEE, P., MITRA, D., BRANDENBURG, A. & RHEINHARDT, M. 2011 Spontaneous chiral symmetry breaking by hydromagnetic buoyancy. *Phys. Rev. E* **84**, 025403.

COURVOISIER, A., HUGHES, D. W. & PROCTOR, M. R. E. 2010a Self-consistent mean-field magnetohydrodynamics. *Proc. R. Soc. A* **466**, 583–601.

COURVOISIER, A., HUGHES, D. W. & PROCTOR, M. R. E. 2010b A self-consistent treatment of the electromotive force in magnetohydrodynamics for large diffusivities. *Astron. Nachrichten* **331**, 667–670.

DEWAR, R. L., KRUER, W. L. & MANHEIMER, W.M. 1972 Modulational instabilities due to trapped electrons. *Phys. Rev. Lett.* **28**, 215–217.

DODIN, I. Y. 2022 Quasilinear theory for inhomogeneous plasma. *J. Plasma Phys.* **88**, 905880407.

EBRAHIMI, F. & BLACKMAN, E. G. 2019 Minimalist large scale dynamo from shear-driven inhomogeneity.

ELPERIN, T., KLEEORIN, N. & ROGACHEVSKII, I. 2003 Generation of large-scale vorticity in a homogeneous turbulence with a mean velocity shear. *Phys. Rev. E* **68**, 016311.

ELSASSER, W. M. 1950 The hydromagnetic equations. *Phys. Rev.* **79**, 183–183.

FEDERRATH, C. 2016 Magnetic field amplification in turbulent astrophysical plasmas. *J. Plasma Phys.* **82**, 535820601.

FRISCH, U., SHE, Z. S. & SULEM, P. L. 1987 Large-scale flow driven by the anisotropic kinetic alpha effect. *Physica D* **28**, 382–392.

GRESSEL, O. & ELSTNER, D. 2020 On the spatial and temporal non-locality of dynamo mean-field effects in supersonic interstellar turbulence. *Mon. Not. R. Astron. Soc.* **494**, 1180–1188.

HALL, B., LISAK, M., ANDERSON, D., FEDELE, R. & SEMENOV, V. E. 2002 Statistical theory for incoherent light propagation in nonlinear media. *Phys. Rev. E* **65**, 035602.

HUBBARD, A. & BRANDENBURG, A. 2009 Memory effects in turbulent transport. *Astrophys. J.* **706**, 712–726.

HUGHES, D. W., MASON, J. & PROCTOR, M. R. E. 2024 Mean field responses in disordered systems: an example from nonlinear mhd. *J. Fluid Mech.* **998**, A36.

HUGHES, D. W. 2018 Mean field electrodynamics: triumphs and tribulations. *J. Plasma Phys.* **84**, 735840407.

JIN, S. & DODIN, I. Y. 2025 On reduced modelling of the modulational dynamics in magnetohydrodynamics. *J. Plasma Phys.* **91**.

JONES, C. A., THOMPSON, M. J. & TOBIAS, S. M. 2010 The solar dynamo. *Space Sci. Rev.* **152**, 591–616.

KÄPYLÄ, P. J., KORPI, M. J., OSSENDRIJVER, M. & STIX, M. 2006 Magnetoconvection and dynamo coefficients - III. α-effect and magnetic pumping in the rapid rotation regime. *Astron. Astrophys.* **455**, 401–412.

KHOMENKO, G. A., MOISEEV, S. S. & TUR, A. V. 1991 The hydrodynamical alpha-effect in a compressible medium. *J. Fluid Mech.*. **225**, 355–369.

KRAUSE, F. & RÄDLER, K. H. 1980 *Mean-Field Magnetohydrodynamics and Dynamo Theory*. Pergamon Press.

MENDONCA, J. T. 2000 *Theory of Photon Acceleration*. CRC Press.

MITRA, D., KÄPYLÄ, P. J., TAVAKOL, R. & BRANDENBURG, A. 2009 Alpha effect and diffusivity in helical turbulence with shear. *Astron. Astrophys.* **495**, 1–8.

MIZERSKI, K.A., YOKOI, N. & BRANDENBURG, A. 2023 Cross-helicity effect on α-type dynamo in non-equilibrium turbulence. *J. Plasma Phys.* **89**, 905890412.

MOFFATT, H. K. 1978 *Field Generation in Electrically Conducting Fluids*. Cambridge University Press.

MOISEEV, S. S., SAGDEEV, R. Z., TUR, A. V., KHOMENKO, G. A. & YANOVSKII, V. V. 1983 Theory of the origin of large-scale structures in hydrodynamic turbulence. *Sov. Phys. JETP* **58**.

MONDAL, T. & BHAT, P. 2023 Unified treatment of mean-field dynamo and angular-momentum transport in magnetorotational instability-driven turbulence. *Phys. Rev. E* **108**, 065201.

NAZARENKO, S. 2011 *Wave Turbulence*. 2011th edn. Springer.

ORSZAG, S. A. 1970 Analytical theories of turbulence. *J. Fluid Mech.* **41**, 363–386.

OUGHTON, S., RÄDLER, K.-H. & MATTHAEUS, W. H. 1997 General second-rank correlation tensors for homogeneous magnetohydrodynamic turbulence. *Phys. Rev. E* **56**, 2875–2888.

PIPIN, V. V. 2023 Spatio-tsemporal non-localities in a solar-like mean-field dynamo. *Mon. Not. R. Astron. Soc.* **522**, 2919–2927.

POUQUET, A., FRISCH, U. & LÉORAT, J. 1976 Strong MHD helical turbulence and the nonlinear dynamo effect. *J. Fluid Mech.*. **77**, 321–354.

RÜDIGER, G. 1980 Reynolds stresses and differential rotation. i. on recent calculations of zonal fluxes in slowly rotating stars. *Geophys. Astrophys. Fluid Dyn.* **16**, 239–261.

RÜDIGER, G. & URPIN, V. 2001 Nonlocal dynamo waves in a turbulent shear flow. *Astron. Astrophys.* **369**, 323–328.

RÄDLER, K.-H. 2007 *Mean-Field Dynamo Theory: Early Ideas and Today's Problems*, pp. 55–72. Springer Netherlands.

RÄDLER, K.-H. 2014 Mean-field dynamos: the old concept and some recent developments. *Astron. Nachrichten* **335**, 459–469.

RÄDLER, K.-H. & BRANDENBURG, A. 2010 Mean electromotive force proportional to mean flow in mhd turbulence. *Astron. Nachrichten* **331**, 14–21.

RÄDLER, K.-H., KLEEORIN, N. & ROGACHEVSKII, I. 2002 The mean electromotive force for mhd turbulence: the case of a weak mean magnetic field and slow rotation. *Geophys. Astrophys. Fluid Dyn.* **97**, 249–274.

RÄDLER, K.-H. & STEPANOV, R. 2006 Mean electromotive force due to turbulence of a conducting fluid in the presence of mean flow. *Phys. Rev. E* **73**, 056311.

RHEINHARDT, M. & BRANDENBURG, A. 2012 Modeling spatio-temporal nonlocality in mean-field dynamos. *Astron. Nachrichten* **333**, 71–77.

RHEINHARDT, M., DEVLEN, E., RÄDLER, K. H. & BRANDENBURG, A. 2014 Mean-field dynamo action from delayed transport. *Mon. Not. R. Astron. Soc.* **441**, 116–126.

RINCON, F. 2019 Dynamo theories. *J. Plasma Phys.* **85**, 205850401.

ROBERTS, P. H. & SOWARD, A. M. 1975 A unified approach to mean field electrodynamics. *Astron. Nachrichten* **296**, 49–64.

ROGACHEVSKII, I. & KLEEORIN, N. 2003 Electromotive force and large-scale magnetic dynamo in a turbulent flow with a mean shear. *Phys. Rev. E* **68**, 036301.

RUIZ, D. E. 2017 A geometric theory of waves and its applications to plasma physics, Doctoral dissertation. Princeton University.

RUIZ, D. E., GLINSKY, M. E. & DODIN, I. Y. 2019 Wave kinetic equation for inhomogeneous drift-wave turbulence beyond the quasilinear approximation. *J. Plasma Phys.* **85**, 905850101.

SCHEKOCHIHIN, A. A. & COWLEY, S.C. 2007 *Turbulence and Magnetic Fields in Astrophysical Plasmas*, pp. 85–115. Springer Netherlands.

SCHRINNER, M., RÄDLER, K.-H., SCHMITT, D., RHEINHARDT, M. & CHRISTENSEN, U. R. 2007 Mean-field concept and direct numerical simulations of rotating magnetoconvection and the geodynamo. *Geophys. Astrophys. Fluid Dyn.* **101**, 81–116.

SCHRINNER, M., RÄDLER, K.-H., SCHMITT, D., RHEINHARDT, M. & CHRISTENSEN, U. R. 2005 Mean-field view on rotating magnetoconvection and a geodynamo model. *Astron. Nachrichten* **326**, 245–249.

SHUKUROV, A. & SUBRAMANIAN, K. 2021 *the Mean-Field Dynamo*, pp. 207–258. Cambridge University Press.

SQUIRE, J. & BHATTACHARJEE, A. 2015 Electromotive force due to magnetohydrodynamic fluctuations in sheared rotating turbulence. *Phys. Rev. E* **92**, 053101.

SQUIRE, J. & BHATTACHARJEE, A. 2016 The magnetic shear-current effect: generation of large-scale magnetic fields by the small-scale dynamo. *J. Plasma Phys.* **82**, 535820201.

SUBRAMANIAN, K. 2019 From primordial seed magnetic fields to the galactic dynamo. *Galaxies* **7**, 47.

SUR, S., BRANDENBURG, A. & SUBRAMANIAN, K. 2008 Kinematic α-effect in isotropic turbulence simulations. *Mon. Not. R. Astron. Soc.: Lett.* **385**, L15–L19.

TAYLER, R. J. 1973 The adiabatic stability of stars containing magnetic fields-I.Toroidal fields. *Mon. Not. R. Astron. Soc.* **161**, 365–380.

TOBIAS, S. M. 2021 The turbulent dynamo. *J. Fluid Mech.* **912**, P1.

TRACY, E. R., BRIZARD, A. J., RICHARDSON, A. S. & KAUFMAN, A. N. 2014 *Ray Tracing and Beyond*. Cambridge University Press.

TSIOLIS, V., ZHOU, Y. & DODIN, I. Y. 2020 Structure formation in turbulence as an instability of effective quantum plasma. *Phys. Lett. A* **384**, 126377.

VAINSHTEIN, S. I. & KICHATINOV, L. L. 1983 The macroscopic magnetohydrodynamics of inhomogeneously turbulent cosmic plasmas. *Geophys. Astrophys. Fluid Dyn.* **24**, 273–298.

VAĬNSHTEĬN, S. I. & ZELDOVICH, Y. B. 1972 Origin of magnetic fields in astrophysics (turbulent "dynamo" mechanisms). *Sov. Phys. Uspekhi* **15**, 159–172.

VEDENOV, A. A. 1967 Theory of a weakly turbulent plasma. *Rev. Plasma Phys* 229–276.

WEYL, H. 1950 *The Theory of Groups and Quantum Mechanics*. Dover Publications.

YOKOI, N. 2013 Cross helicity and related dynamo. *Geophys. Astrophys. Fluid Dyn.* **107**, 114–184.

YOKOI, N. 2018 Electromotive force in strongly compressible magnetohydrodynamic turbulence. *J. Plasma Phys.* **84**, 735840501.

YOKOI, N. 2023 Unappreciated cross-helicity effects in plasma physics: anti-diffusion effects in dynamo and momentum transport. *Rev. Mod. Plasma Phys.* **7**.

YOKOI, N. & BRANDENBURG, A. 2016 Large-scale flow generation by inhomogeneous helicity. *Phys. Rev. E* **93**, 033125.

YOKOI, N. & YOSHIZAWA, A. 1993 Statistical analysis of the effects of helicity in inhomogeneous turbulence. *Phys. Fluids A* **5**, 464–477.

YOSHIZAWA, A. 1984 Statistical analysis of the deviation of the reynolds stress from its eddy-viscosity representation. *Phys. Fluids* **27**, 1377–1387.

YOSHIZAWA, A. 1990 Self-consistent turbulent dynamo modeling of reversed field pinches and planetary magnetic fields. *Phys. Fluids B* **2**, 1589–1600.

ZAKHAROV, V. E. & OSTROVSKY, L. A. 2009 Modulation instability: the beginning. *Physica D* **238**, 540–548.

ZHOU, Y., ZHU, H. & DODIN, I. Y. 2019 Formation of solitary zonal structures via the modulational instability of drift waves. *Plasma Phys. Control. Fusion* **61**, 075003.

ZHU, H. & DODIN, I. Y. 2021 Wave-kinetic approach to zonal-flow dynamics: recent advances. *Phys. Plasmas* **28**, 032303.

ZHU, H., ZHOU, Y. & DODIN, I. Y. 2019 Nonlinear saturation and oscillations of collisionless zonal flows. *New J. Phys.* **21**, 063009.